Modellsystem zur ganzheitlichen Analyse und Optimierung der Energieeffizienz der Energiewandler auf Schiffen

Von der Fakultät für Maschinenbau
der Helmut-Schmidt-Universität / Universität der Bundeswehr Hamburg
zur Erlangung des akademischen Grades eines Doktor-Ingenieurs
genehmigte

Dissertation

von

Dipl.-Ing. Malte Freund

aus Hannover

Hamburg, Oktober 2012

Holistic Analysis of Onboard Consumption and Efficiency of the Energy Systems of Ships

Doctoral Thesis

Approved by the
Department of Mechanical Engineering
of the Helmut-Schmidt-University –
University of the Federal Armed Forces Hamburg
to obtain the academic degree of Doktor Ingenieur (Dr.-Ing.)
presented by

Dipl.-Ing. Malte Freund

born in Hannover

Hamburg, October 2012

Kurzfassung

Die Schifffahrt ist das effizienteste und bei weitem wichtigste Transportmittel im internationalen Handel. Aufgrund des hohen Transportvolumens ist die Schifffahrt trotz der im Vergleich zu anderen Transportmitteln hohen Effizienz beim Gütertransport ein signifikanter Verursacher von CO_2-Emissionen. Steigende Ölpreise sowie verschärfende gesetzliche Regulierungen der Emissionen erfordern zusätzlich Untersuchungen, wie in der Schifffahrt Treibstoff eingespart werden kann. In dieser Arbeit werden die wichtigen Einflussfaktoren auf die Effizienz eines Schiffes im Betrieb analysiert, mit dem Fokus auf Einsparpotentiale im Treibstoffverbrauch und Minderung der Emissionen. Aufgrund der lange Zeit niedrigen Energiekosten in der Schifffahrt und der damit einhergegangenen Vernachlässigung der eingehenden Verbrauchsüberwachung wird ein Bedarf an systematischer Erfassung und Auswertung der Leistungs- und Treibstoffverbräuche in den verschiedenen Betriebsmodi und unter variierenden äußeren Einflussfaktoren festgestellt.

Zur Analyse der Energieeffizienz an Bord von Schiffen wird ein modellbasiertes System vorgestellt, das die Effizienz der Energiewandler im Betrieb auswertet und darstellbar macht. Dies kann sowohl mit Echtzeitdaten an Bord, mit gespeicherten Betriebsdaten an Land, als auch mit Design-Vorgaben zur Optimierung der Maschinenanlage erfolgen. Die Grundlagen und der Aufbau der Modelle zur Analyse werden dargestellt. Die erstellten Modelle enthalten sowohl Energiewandler, die Primärenergie in Nutzenergie umwandeln, wie Motoren, als auch solche zur weiteren Umwandlung der Nutzenergie, wie Generatoren. Des Weiteren werden wichtige Verbraucher am Beispiel der Kühlwasserpumpen untersucht. Während bisherige Untersuchungen überwiegend auf der Messung der Treibstoffverbräuche basierten oder diese nicht betrachteten, wird der Treibstoffverbrauch der Motoren anhand der Maschinencharakteristik und der gemessenen Leistung mit zugehörigen Umgebungsbedingungen bestimmt. Die entwickelte Methode ermöglicht darüber hinaus die exergetische Analyse und Optimierung der Maschinenanlage im Betrieb.

An Bord eines Containerschiffs wird eine Messkampagne durchgeführt und die Methode und Modelle zur Analyse der Effizienz im Betrieb erfolgreich mit den gesammelten Daten validiert. Weitere Untersuchungen der Messdaten zeigen Verbesserungen durch optimierten Betrieb der vorhandenen Maschinenanlage auf und quantifizieren Einsparungen, die mit partiellem Austausch durch effizientere Maschinen bei dem vorliegenden Lastprofil erreicht werden können.

Acknowledgments

Contents

Subscripts and Symbols

Subscript	Description
0	reference state
a	ambient
AE	Auxiliary engine
c	Carnot
c	compressed
C	Coolant
CA	Combustion air
$conv$	convective
CW	Cooling water
el	electrical
ER	Engine room
EG	Exhaust gas
F	Fuel
FO	Fuel oil
gen	Generator
in	at inlet
irr	Irreversible
iso	reference state to ISO standard conditions
JCW	Jacket cooling water
k	correction
$loss$	Loss (in a process)
LT	Low temperature
m	Mass
ME	Main engine
$mech$	Mechanical
OC	Oil cooler
out	at outlet
Q	Heat
rec	Recovered
s	Swept
SAC	Scavenge air cooler

Subscript	Description
SW	Sea water
WH	Waste heat

Symbol	Description	Unit
φ	Rel. humidity	%
φ	Power factor	-
η	Efficiency	-
λ	Friction coefficient	-
ρ	Density	kg/m^3
A	Area	m^2
be	Specific fuel consumption	g/kWh
C_F	Carbon conversion factor	kg/kg
d	Diameter	m
E	Energy	J
$\dot{E}$	Exergy flow	W
F_n	Froud number	-
g	Gravitational constant	m/s^2
h	Specific enthalpy	J/kg
H	Pump head	bar
H	Water depth	m
k	Correction coefficient ISO 3046	-
l	Length	m
LHV	Specific lower heating value	J/kg
m	Mass	kg
$\dot{m}$	Mass flow	kg/s
n	Rotational speed	min^{-1}
P	Power	W
p	Pressure	Pa
Q	Volume flow	m^3/s
$\dot{Q}$	Heat flow	W
S	Apparent power	W
S	Entropy	J/K
t	Time	s
T	Temperature	K

Symbol	Description	Unit
UHV	Specific upper heating value	J/kg
V	Volume	m^3
v	Velocity	m/s
x	Variable	
z	Height coordinate	m

Abbreviations

AE	Auxiliary engine
ANN	Artificial Neural Network
CAN	Controller Area Network
CANSAS	IMC CAN-Bus capable measurement and control module
CANSER	IMC NMEA to CAN-Bus conversion module
CCAI	Calculated Carbon Aromaticity Index
CP	Controlled pitch
DAQ	Data Acquisition Unit
DIN	Deutsches Institut für Normung
DWT	Deadweight Tonnage
EC	European Commission
ECA	Emission Control Area
EEDI	Energy Efficiency Design Index
EEMT	Energy Efficiency Monitoring Tool
EEOI	Energy Efficiency Operational Indicator
EU	European Union
FP	Fixed pitch
GDP	Gross Domestic Product
GHG	Green house gas
GL	Germanischer Lloyd
GPS	Global Positioning System
GT	Gross Tonnage
GUI	Graphical User Interface
HFO	Heavy Fuel Oil
IACS	International Association of Classification Societies
IFO	Intermediate Fuel Oil
IMO	International Maritime Organisation
ISO	International Organisation for Standardization
LFO	Light Fuel Oil
LHV	Lower heating value
LNG	Liquid Natural Gas
LPG	Liquid Petroleum Gas

VII

MCR	Maximum continuous rating
MDO	Marine Diesel Oil
ME	Main engine
MEPC	Marine Environmental Protection Committee
MFO	Marine Fuel Oil
MGO	Marine Gas Oil
MSL	Modelica Standard Library
NMEA	Marine Interface Standard and Data Protocol for Navigational Data
PMS	Power management system
PTI	Power take in
PTO	Power take out
RoRo	Roll on roll off (Vessel)
RPM	Revolutions per minute
SECA	Sulfur Emission Control Area
SEEMP	Ship Energy Efficiency Management Plan
SFC	Specific fuel consumption
SFOC	Specific fuel oil consumption
USD	United States dollar
VLCC	Very Large Crude Carrier
WHR	Waste heat recovery

1 Introduction

Shipping is the most efficient transport mode and with more than 80% of world trade by volume [UNC2010] the most important transport mode which is closely linked to the economic growth. The efficiency of transport modes as regards carbon dioxide is generally defined as the emissions versus their activity, resulting in an CO_2-indicator for each transport mode as a basis for comparison.

The efficiency of a ship depends on internal and external factors, which can be controllable or uncontrollable. For a holistic approach of ship efficiency evaluation, the external and internal effects have to be collected and evaluated regarding their controllability. The holistic approach implements various approaches to achieve insight into the dependencies of effects and guiding towards the optimum solution under the predominant constrains. For a ship in operation, Fig. 1.1 shows exemplary efficiency influencing factors. The first step is the classification of factors affecting
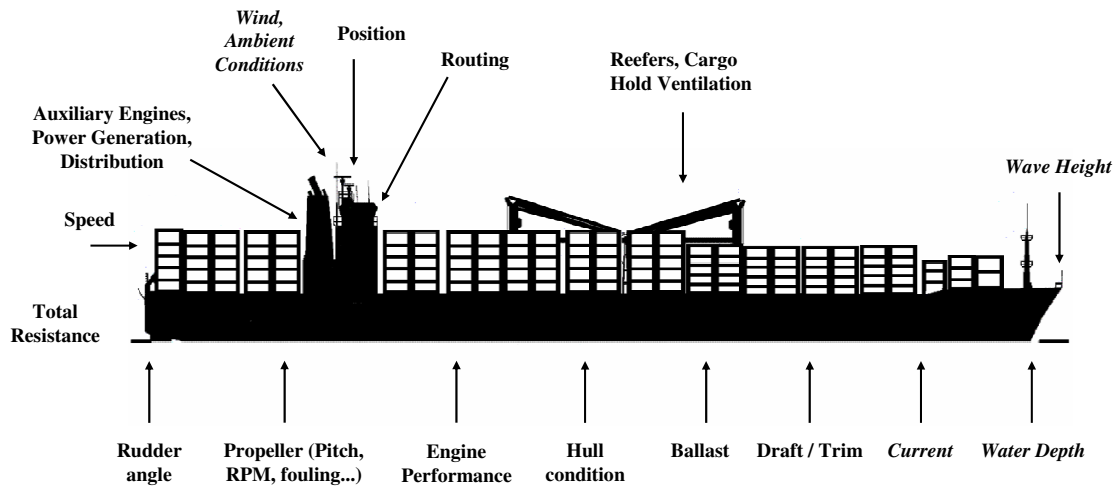
Figure 1.1. Efficiency influencing factors, internal factors in regular, *external* factors in *italics.*

efficiency into categories, for separation of promising areas for optimization from not or hardly influenceable effects. Ship efficiency is influenced by the hydrodynamics and aerodynamics of the vessel as built in the yard, the efficiency of the installed

onboard machinery and its operation within the environment and the constraints due
to weather and load condition. For the separation of the vessel from its surrounding
and the definition of internal and external, an arbitrary control volume around the
vessel can be imagined. External factors, affecting the efficiency from outside of
the control volume, include ambient conditions, wind, current, water depth, and
waves. Depending on ship type and load, these external factors have a large effect
on the efficiency of the vessel. While these are not directly controllable, they can be
indirectly influenced by choice of the route.

These influencing factors on vessel efficiency are analyzed in Chapter 2, Section 2.1. For a better understanding of the developments and evaluations, the current drivers for optimization, technical background of the systems as well as the history and state of the art are presented in the following sections, leading to the objectives of this work. In Chapter 3, the developed simulation for energy efficiency and consumption monitoring is introduced. The validation of the simulation models is described with the conducted longterm measurement campaigns on board of two container vessels. Chapter 4 describes the optimization of the efficiency based on the developed simulation models and acquired operational data. This work closes with a final result of the research in Chapter 5, where a demonstrator onboard tool is presented. This onboard tool incorporates simulation models for efficiency and consumption evaluation in real time with a transparent display of the current energetic status of the vessel and acquisition of operational data in high frequency.

2 Background and State of the Art

This chapter begins with the efficiency influencing factors on vessel operation. In the following sections, the drivers for fuel consumption reduction and various systems and technologies used on board are discussed and quantified. Concepts and products for onboard energy efficiency management and the current state of the art are introduced leading to the objectives of this work (Section 2.5).

2.1 Efficiency Influencing Factors

Efficiency influencing factors (Fig. 1.1) can be separated into uncontrollable effects and controllable effects. The former influences have to be considered but can often not be changed, while the latter can be altered to mitigate their influences. In the following paragraphs, mainly uncontrollable effects are presented. In efficiency evaluations these play an important role as an observed deviation from a theoretical vessel efficiency baseline can then be attributed to different effects (Fig. 2.1). By removing constantly changing influences of uncontrollable but measurable effects, not directly measurable but controllable effects can be detected and mitigated by onboard crew or shore-based personnel.

Uncontrollable effects

For vessels in operation, resistance and hydrodynamics can be considered mainly as uncontrollable. While for a certain degree controllable during the design phase, by defining main particulars and lines most parts of the resistance are fixed. Controllable factors for vessels in operation lie only in the exploitation of the best achievable hydrodynamics of the given hull and propeller. Calm water hydrodynamics can be influenced through trim, speed, and surface roughness. The remaining vessel's overall resistance in a seaway can be considered as external uncontrollable effect, if structural changes at the vessel are excluded from evaluation. Despite that, refits, such as changing the bulbous bow and revising the bow lines of a vessel, may prove to be economically feasible for fuel saving [HB2009].

Ship resistance is generally decomposed as the sum of calm-water resistance, seaway resistance and wind resistance. Calm-water resistance comprises friction resistance due to viscosity and the development of a boundary layer around the

Speed - Fuel Consumption Relationship
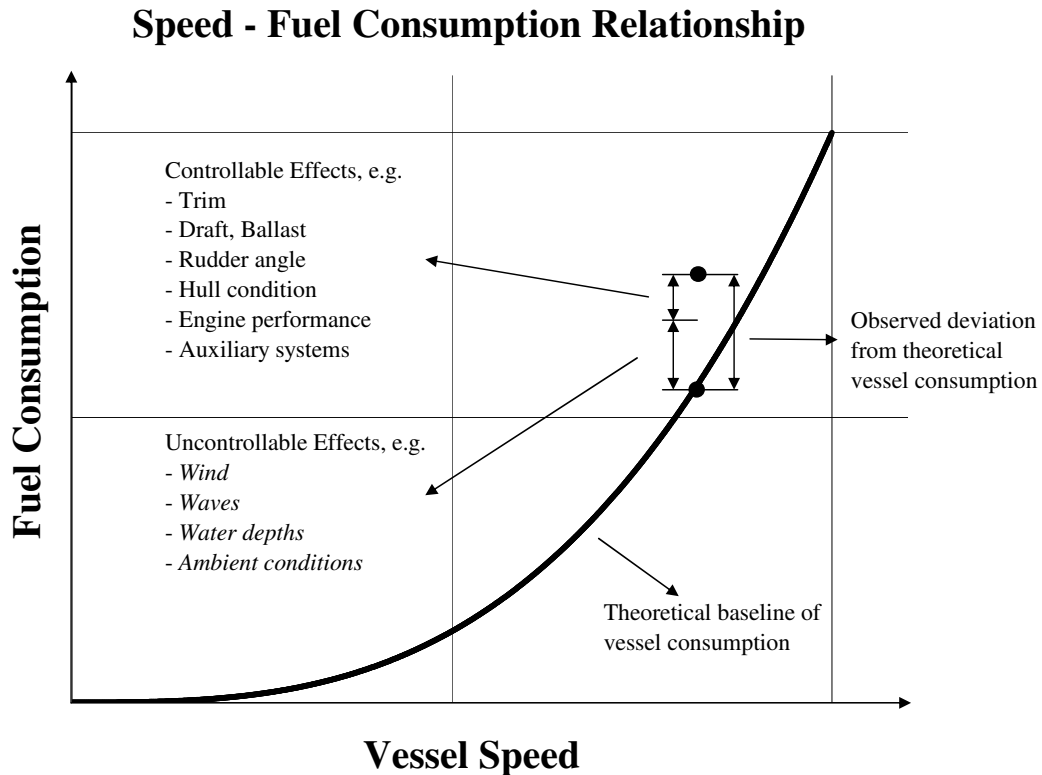
Figure 2.1. Speed vs. fuel consumption, exemplary partition of deviations from a theoretical baseline into controllable and uncontrollable effects.

vessel moving relatively to the water, viscous pressure resistance mainly due to flow separation, and wave resistance due to free-surface deformation [BER2000].

At a given hull, calm-water resistance is governed by the wetted surface and the location of the flow affecting geometrics of bow and stern, especially bulbous bow and transom. They change with the draft and trim of the vessel for wetted surface and hydrodynamic positioning, respectively. For a given displacement, each vessel has a certain trim for least resistance. This trim is often even keel at design draft, but varies at other drafts mainly depending on the position of bow and stern relative to the water surface, and the inflow of the propeller. While traditionally the trim was adjusted based on compliant hull bending moments and stresses, and captains' experience for best maneuverability and seakeeping of the vessel, nowadays tools for an optimum trim giving a minimum water resistance are available. These tools can be based on CFD calculations, towing tank tests, or sensors on the ship with operational experience evaluated by neural networks [HF2010], [MOT2006],

[ENI2009]. In general, additional displacement results in additional resistance and therefore the amount of ballast water should be reduced to the required amount, depending on bending stresses and stability of the vessel. However, in some cases it can be beneficial to take additional ballast water to trim a vessel to a more efficient position in the water.

Wave height and direction of the waves strongly affect the demand of propulsion power additionally. The added resistance in sea waves increases the required power, which is generally accounted for by the so-called *sea margin*. Depending on ship type and size, the required additional power for a certain speed, as a measure for the increased resistance, differs, with larger and slender hulls being less affected [MH2007]. Beside CFD analysis and towing tank tests, different approaches exist to determine the added wave resistance based on induced pressure, wave characteristics and vessel response, both numerical simulation and model tests [BOE1970], [ISO2002a], [BER2000], [TKB+1993].

Shallow water increases frictional and wave resistance of the vessel and alters the optimal trim of a vessel at a given velocity. Near the critical depth Froude number

$$F_{nh} \;=\; \frac{v}{\sqrt{gH}} \;=\; 1 \;, \tag{2.1}$$

v being the vessel speed and H the water depth, the resistance increases strongly. The loss of ship speed for constant propulsion power can be estimated using the diagram by Lackenby [LAC1963], Fig. 2.2, with A_m denoting the underwater cross section area amidships. For a more detailed analysis, CFD methods or towing tank tests have to be deployed.

Wind resistance affects the efficiency, especially for vessels with large lateral areas above the waterline, e.g. container vessels and ferries, and with high vessel speeds [BER2000]. Wind resistance of container vessels and general cargo vessels can be influenced by the way containers and cargo are stowed on deck, while for tankers and bulkers the wind resistance can only be reduced by an alternate design of hull and superstructure. Wind resistance is often tested in wind tunnels, while hydrodynamics are mainly optimized by CFD analysis, with typically only a final model being tested for validation in a towing tank [BER2000].

Shallow water effects and wind resistance play a role in efficiency evaluations as a measured increased resistance should be allocatable to its source. For enabling this pinpointing of effects, a distinction should be possible between allowable resistance for the given external conditions, and the additional resistance caused e.g. by trim,
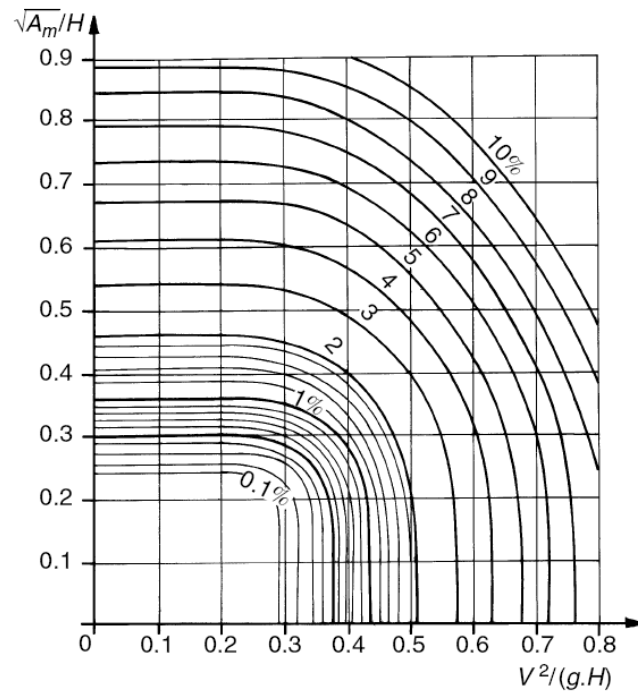
Figure 2.2. Loss of speed in shallow water, percentage of speed at constant propulsion power by *Lackenby* [LAC1963] [BER2000].

hull roughness, or other parasitic resistance.

Due to the high velocity of the propeller blade movement through the water, the surface condition of the blades is important for the friction. Increasing propeller roughness results in increasing frictional losses and therefore decreasing efficiency. Ships with frequent maneuvers in port and coastal areas with a high probability of hitting debris in the water need regular examinations of the propeller blades concerning damages, especially at the blade bow and the tips, for ensuring high propeller efficiency. Ships with long periods at berth or anchor in warm waters can also show marine fouling. The efficiency loss due to propeller deterioration is described in Section 2.3.1, Fig. 2.10.

As for the propeller, increased roughness of the hull increases the power demand for propulsion. Beside deterioration through mechanical damage and corrosion, hull fouling through algae, seaweed, shells, etc. increases the vessel's resistance. Especially vessels with long waiting or berthing periods, and vessels operating in warm waters at low speeds are subject to hull fouling, which can only be slowed down but not completely prevented by anti-fouling coatings. G. W. Swain [SWA2010]

reports an increase in power consumption of about 1% for every 15 microns increase in hull roughness of a cruise vessel. The impact of hull roughness depends strongly on hull form and operating speed. An overview of the composition of the overall resistance for different vessel types can be found in [MH2007].

Beside visual inspection, a monitoring is indirectly possible through comparison of speed through water and the produced shaft power and torque, which includes the overall hull condition and propeller condition. The monitoring enables a diver inspection or cleaning based on an indicated additional resistance, which would otherwise stay undetected and cost additional fuel oil until the next regular hull inspection.

Controllable effects

The second group of factors leading to an effective ship operation are directly controllable factors which mainly affect the efficiency within the vessel. External and internal effects unite in routing and scheduling of vessels that determine the time and position of the vessel subject to the external effects. Weather routing and scheduling can be crucial factors for propulsion power demand. Sophisticated weather routing enables the navigators to avoid regions of high additional resistance through wind and waves, which can save energy even when lengthening the actual mileage of the route (Section 2.4.4). Besides this, weather routing may also improve punctuality in the schedule, because the vessel speed can be reliably adjusted to the proposed conditions during the rest of the voyage, without the need of a higher speed at the beginning as a buffer for unexpected delays through bad weather later on. An even speed profile or better even engine load over the journey saves fuel even without weather influence, it is mainly a question of awareness and motivation of the crew.

Even larger influence on the fuel efficiency of a vessel can be found in the scheduling. By assigning departure and arrival times to a voyage, the average speed of the vessel is fixed. The propulsion power of a vessel depends in good approximation on the third power of the speed which makes the vessel's speed the paramount influence on fuel consumption. Savings through vessel operation by reducing speed, the so-called *slow steaming*, requires especially for liner operators a comprehensive analysis of savings vs. costs and consequences, but provides high savings in fuel costs without investments for vessel upgrades. In case of liner operation, lower speeds result in longer transits of each vessel. Thus, additional vessels are required in a liner trade to keep the transport volume. A detailed analysis of financial savings through reduced speed is presented for a liner fleet by Sames [SAM2007] and a 20000 TEU container

vessel by Khor et al. [KDK+2012]. Corbett et al. [CWW2009] analyze the optimal vessel speed depending on fuel prices for profit-maximizing, with the marginal abatement costs of mandated speed reductions. Due to the prevailing circumstances in shipping, especially for the container and multi purpose vessel market with high fuel costs and limited cargo at a growing world fleet, the *slow steaming* of vessels is expected to stay the general operational mode of most vessels in the near future, with newbuildings starting to being designed for the low speeds.

Engine and machinery performance are clearly internal, controllable factors for efficiency of vessel operation as they depend on maintenance and operation of the crew and the vessel operator. Especially the main engine performance, as the largest consumer, can cost valuable efficiency in form of additional losses which are accounted for by higher consumption. At the main engine, turbocharger and fuel injection pump conditions, valve and fuel injection timings, heat exchanger conditions and deposits are relevant items. The internal conversion of fuel oil into mechanical power and heat influences the efficiency, as the minimization of losses improves the efficiency. Thermodynamic optimization of the onboard machinery leads to a higher efficient energy conversion system by minimizing primary energy input through exergetic optimization [BK2009]. Where applicable, heating and cooling demand can be matched by a pinch point analysis, lowering the exergy destruction.

For variable pitch propellers (Section 2.3) the correct tuning of the propeller combinator curve and the combination of shaft generator, propulsion and diesel generators offer potential for optimization, if not adapted to current operational profile. The propeller should be operated at optimum efficiency with optimum rotational speed for best engine efficiency at given load. During low vessel speed, e.g. during maneuvering or in a restricted area, using shaft generators with main engine operating at nominal rotational speed can be less efficient than optimized rotational speed and electricity generation by diesel generators instead. Alternatively, shaft generators can be equipped with frequency converters for shaft speed-independent operation.

The rudder angle δ strongly influences the resistance of a vessel. The rudder deflects the water stream to generate a turning force on the vessel which is used as steering force. The steering force comes at the price of an increased resistance [AM1980]. During turning, also the hull resistance is increasing. As even small rudder angles strongly increase the resistance, the rudder should be used prudent at open sea e.g. by tackling rather than keeping the course against wave and wind with

a constant rudder angle. During sea passage, the rudder is usually controlled by an autopilot. At open sea outside traffic regulation, the sensitivity of the autopilot, i.e. the allowable deviation between set course and actual course, can be adjusted to limit the rudder movements. In modern autopilots, the sensitivity is self-adjusting to the current conditions and is therefore not manually adaptable by the officers. For a holistic evaluation of operation this aspect has to be kept in mind, but will not be further analyzed in this work.

On board of a vessel, except for the propulsion, most systems are electrically driven. The main consumers are pumps and fans; secondary consumers are for navigation and cargo care. The generation of electrical power on board is therefore an important part in the efficiency evaluation and accounts for about 5% to 20% of a cargo vessel's fuel consumption. Diesel engine driven generator sets typically have a bowl-shaped specific fuel consumption curve, with the lowest specific fuel consumption (and highest efficiency, respectively) between 75% and 85% maximum continuous rating (MCR), with efficiency decreasing towards full load and low loads, compare Fig. 2.3 which is based on test-bed data. This depicts that the correct operational point of diesel generator sets contributes to efficient generation of electrical power. The load results from the electrical power consumption of the vessel and the size and number of running diesel generator sets, which are controlled either automatically by a power management system (PMS) or manually by the chief engineer. The load controlled by the PMS, or the chief engineer in manual mode, is subject to required redundancy and acceptable load reserves for intermittent operating machinery and sudden increases in consumption. Additional generator sets are started when reaching the lower limit of the load reserves or generator sets are shut down when reaching the lower load limit (Section 2.4).

The focus of the presented work lies on the optimized operation of commercial freight vessels. Container vessels, multi purpose vessels, tankers and bulkers are often built with building prices as a primary focus and offer good potential for optimization. Additionally, these ship types are the main types in the world's fleet. The main consumers of electrical power on board of these ships are currently the auxiliary systems for engine operations, mainly pumps and fans, which are usually uncontrolled and run at full load, without major adaptations to the current demand and external conditions. As they are dimensioned for the highest demand possible, pumps and fans are often operated far beyond their actual demand. The *slow steaming* of vessels intensifies this difference between the design load of the systems
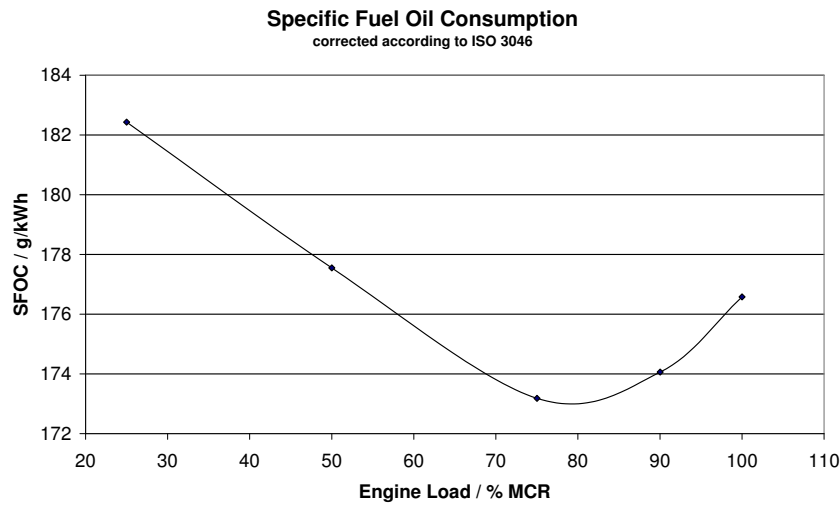
Figure 2.3. Specific fuel oil consumption of a diesel engine as function of the engine load.

and the actually required load. In slow steaming, the main engine operates only in low partial load. This results in a lower required load on the auxiliary systems, with associated significant potential savings as presented in the Chapter *Optimization*, Section 4.2.

Summary

The above mentioned internal and external effects influence the vessel efficiency. These can be mitigated by the onboard crew and the shore-based personnel. Vessel efficiency thus depends also on crew awareness for the external and internal effects and their resulting behavior. Tools for a clear presentation of available information for optimal control of the vessel can support the crew in everyday tasks.

The external and internal effects on the efficiency can be highly fluctuating or slowly aggregating. Transient processes caused by the various effects are covered in detailed analyses using complex models and sophisticated methods, like CFD calculations with free-surface modeling for added resistance in seaways. The method presented here focuses on the onboard machinery and its operation. As the power demands are collected combined with external effects and navigational data, these data provide the basis for conclusions about hydrodynamics and overall vessel operation and optimization.

2.2   Drivers for Fuel Consumption Reductions

In the following sections, key drivers for fuel consumption reduction in shipping are introduced and their potential impact on vessel operation is explained.

2.2.1   Carbon Dioxide Emissions

As climate change is now widely accepted to be anthropogenic, the United Nations Framework Convention on Climate Change (UNFCCC) is debating in yearly Conferences of the Parties (COPs) about the reduction of anthropogenic green house gases (GHG) for a post-Kyoto Protocol. The goal is set to limit the concentration of greenhouse gases in the atmosphere to 450 ppm of greenhouse gas equivalent (CO_2) which is accepted to be consistent with a 2 °C increase of global temperature. The proposed reductions in greenhouse gases include the transport sector, with shipping being a major contributor with an estimated 3.3% of the worlds GHG emissions in 2007 [BCE+2009]. Even though the final accords of the COPs in Copenhagen (COP15) and Cancun (COP16) do not include precise actions for a reduction of green house gas emissions in shipping. Plans for the inclusion of shipping into an emissions reduction scheme are under further consideration by IMO world-wide and by EU regionally.

Proposals are for example to include shipping into Marked Based Instruments, e.g. using emission trading schemes or introducing an emission levy on burned fuel. This is discussed in the IMO Marine Environment Protection Committee (MEPC), compare e.g. MEPC 54/4/2 [IMO2005] and [CGM+2006].

The emitted mass of carbon dioxide can be approximated as

$$m_{CO_2} = m_F \cdot C_F \quad , \tag{2.2}$$

where C_F is the carbon factor of the fuel, m_{CO_2} the mass of emitted CO_2, and m_F the mass of burned fuel. The equation shows that the emission is proportional to the consumption of fuel, therefore the saving of fuel is proportional to the saving of CO_2 emission. The second parameter, the carbon conversion factor, defines the carbon content of the fuel. Depending on the source, the carbon conversion factors vary within about 1.5%, which can be explained by different standardization of fuels. In Table 2.1, the carbon conversion factors defined in the MEPC Circular 681 [IMO2009a] are displayed.

By using low-carbon fuels, e.g. methane, the emitted mass of CO_2 per mass of

Table 2.1. Carbon conversion factors from MEPC Interim Guideline 681.

Type of fuel	Reference	Carbon content m/m	C_F (t_{CO2}/t_{Fuel})
1. Diesel/Gas Oil	ISO 8217 Grades DMX through DMC	0.875	3.20600
2. Light Fuel Oil (LFO)	ISO 8217 Grades RMA through RMD	0.860	3.15104
3. Heavy Fuel Oil (HFO)	ISO 8217 Grades RME through RMK	0.850	3.11440
4. Liquefied Petroleum Gas (LPG)	Propane	0.819	3.00000
	Butane	0.827	3.03000
5. Liquefied Natural Gas (LNG)	Methane	0.750	2.75000

burned fuel can be reduced even without improving efficiency of the energy conversion.

For the reduction of CO_2 emissions, it can be concluded that the two approaches are applicable:

- fuel saving

- use of low-carbon fuels .

Especially the approach of fuel saving is of large economical interest as well.

As an alternative, a carbon and green house gas neutral fuel exists which has been researched since the 1970's as renewable but transportable energy source: hydrogen. So far available only in a small scale, hydrogen is free of carbon and therefore completely CO_2 neutral if produced with renewable energies. Hydrogen can be converted into mechanical energy in gas turbines or internal combustion engines or with highest efficiency directly into electrical energy by fuel cells. Concepts for transcontinental hydrogen trade with liquid hydrogen tankers and hydrogen fueled propulsion systems are developed e.g. by Würsig [WÜR1996]. The low density and resulting low volumetric-specific energy content of liquid hydrogen results in considerably higher losses of energy for transport and distribution than is the case for current fossil-based chemical energies. The losses for transport may be expressed as the specific work for ship propulsion related to the exergy content of the transported cargo. The feasibility study showed that these losses of a 115000 m^3 liquid hydrogen tanker are by a factor of four higher than the specific losses of a 125000 m^3 LNG

tanker and by a factor of 15 higher than the specific losses of a very large crude oil carrier (VLCC) [WÜR1996]. These high losses make it economically not feasible to transport hydrogen over long distances from production facilities, e.g. large hydro power plants with electricity at low cost and with very low carbon dioxide emissions, to the consumers.

2.2.2 Sulfur Oxides and Nitrogen Oxides Emission Reductions

In 2006, the first Sulfur Emission Control Area (SECA) was established in the Baltic Sea, followed in 2007 by the North Sea and English Channel SECA. Within these SECAs, the use of high sulfur heavy fuel oil (HFO) is banned. SECAs will be enhanced to Emission Control Areas (ECAs), restricting the emission of Nitrogen Oxides (NO_x) for new-build vessels starting 2016 as well. With the tightening of regulations by lowering the limits of sulfur content in the fuel (compare Section 2.3.3.1), a change of fuels from low sulfur heavy fuel oil (LSHFO) to refined fuel oils may be required. Refined fuel oils cost currently about 1.5 times the price of HFO [BUN2012]. This results in significantly higher operating costs, with the perspective of increasing prices in near future due to the increasing demand by shipping and other reasons as laid out in Section 2.2.3. These increased costs are a strong incentive for the ship operators to improve the operation towards minimized consumption. As an additional incentive, the port tariffs are about to be related to the vessel emissions, with an nitrogen oxide surcharge already introduced in Norway.

Already in 2009, the Californian coastal waters were restricted by regional legislation to an ECA-like emission control zone. More ECAs are expected to be established worldwide, starting with the inclusion of the US and Canadian waters 200 miles off the coast in 2012 [IMO2010a].

2.2.3 Oil Production

The oil production is expected to reach its maximum at the so-called *Peak Oil* in near future, as the known reserves in easy-to-exploit oil deposits are shrinking [IEA2010]. The so-called unconventional oils will partly substitute the decline in conventional oil production. The current scenario of the World Energy Outlook 2010 is presented in Fig. 2.4, expecting crude oil production to remain constant below todays levels, with a strong decline of currently producing fields.

World oil production by type in the New Policies Scenario
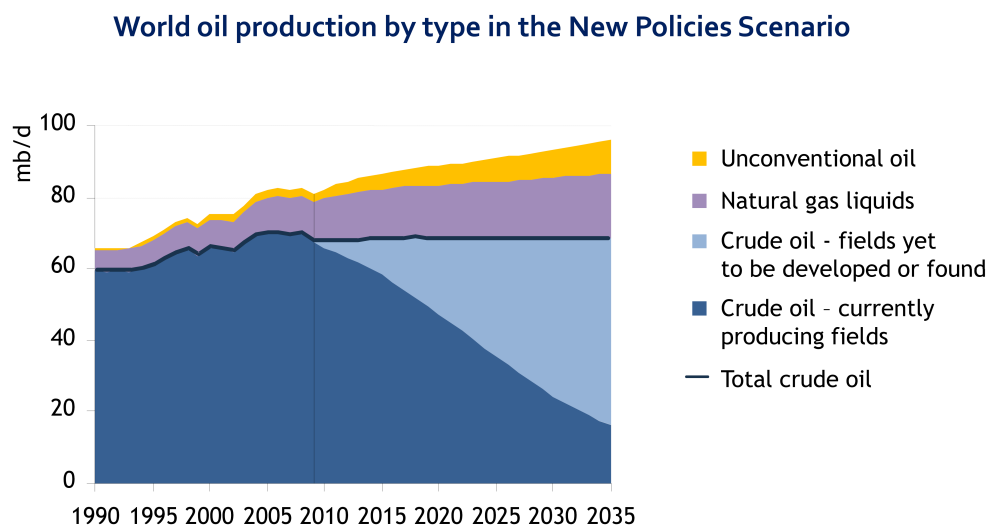
Figure 2.4. World oil production scenario 2010 [IEA2010].

This development will increase the crude oil prices, as the oil demand is expected to be still growing [IEA2010] [BCE+2009]. The scenario of new policies, which includes the implementation of current policy commitments and plans for energy savings by countries around the world, expects a steady increase in oil price, Fig. 2.5. A different case is expected for the scenario of 450 ppm GHG equivalence in the atmosphere, where the oil price is stabilized through decreased consumption, which would require a stronger decline of fossil fuel use in OECD countries than the increase of demand in newly industrialized countries and rest of the world.

These developments may lead to the diversification of ship fuels. Heavy fuel oil (HFO) gets then competition from non-oil resources, lowering the dependence on shrinking oil resources and increasing prices. Alternative fuels for shipping are especially natural gas as ship fuel, either compressed (CNG) or liquefied (LNG), which are expected to be growing strongly.

The first LNG-driven vessels are already sailing, with a high interest in their technology, as gas driven four-stroke engines reduce NO_x and SO_x emissions significantly without further exhaust gas treatment. Gas driven two-stroke engines, as dual-fuel engines with pilot-injection of HFO or MDO, reduce SO_x emissions significantly but need a further exhaust gas treatment for NO_x emission reduction. In the long-term view synthetic fuels from liquefied natural gas (GTL), biomass (BTL), and coal (CTL) are expected to be introduced into the market as well.
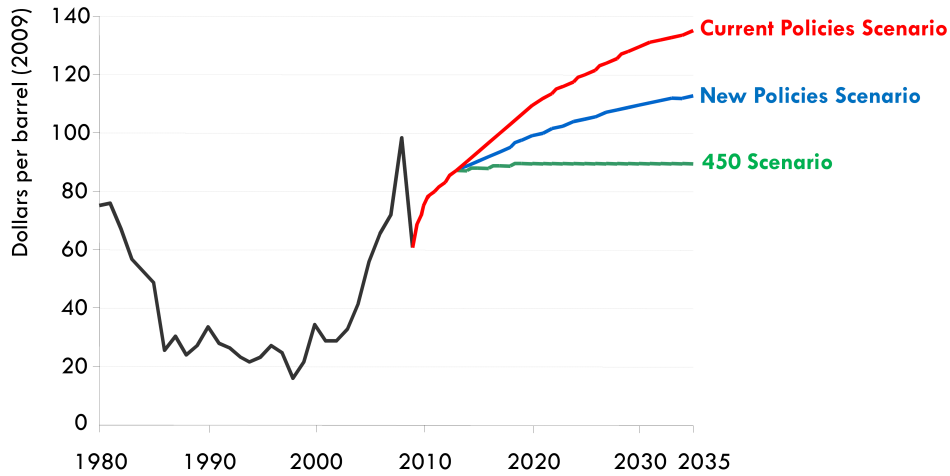
Figure 2.5. Oil price scenarios of IEA World Energy Outlook 2010 [IEA2010].

2.2.4 Fuel Oil Prices

The fuel used by the majority of commercial oceangoing vessels is residual oil, commonly called Heavy Fuel Oil (HFO), Marine Fuel Oil (MFO) or Intermediate Fuel Oil (IFO), or ISO-F-RMA to ISO-F-RML according to ISO 8217:1996 [ISO1996]. HFO consists of residuals from refinery, blended with refined oils to reach the desired specification as described in Section 2.3.3.1. Fuel oil prices are not directly bound to crude oil prices, however, graphical analysis shows that fuel oil prices clearly follow the crude oil prices as can be seen in Fig. 2.6, with slightly higher increase in prices since 2008. This may be explained by a higher demand due to an increasing world fleet and a decreasing production, as the refineries improve their processes and gain higher yields of high grade products out of the crude oil.

Figure 2.6 shows the time lines of crude oil prices (blue line) and HFO prices in Rotterdam (red dots) from 1997 to 2011 [1]. The prominent peak of crude oil and fuel oil prices in 2008 with maximum HFO prices of US $720/mt clearly marks the most important motivation for fuel saving, as the prices have tripled within only 3 years. This makes fuel oil the by far largest operational cost of vessels. When smoothing the prices for achieving an overall trend over the years without

---

[1] Sources: EIA, http://tonto.eia.doe.gov/dnav/pet/hist/wtotworldw.htm, Bunkerworld.com, OceanConnect.com
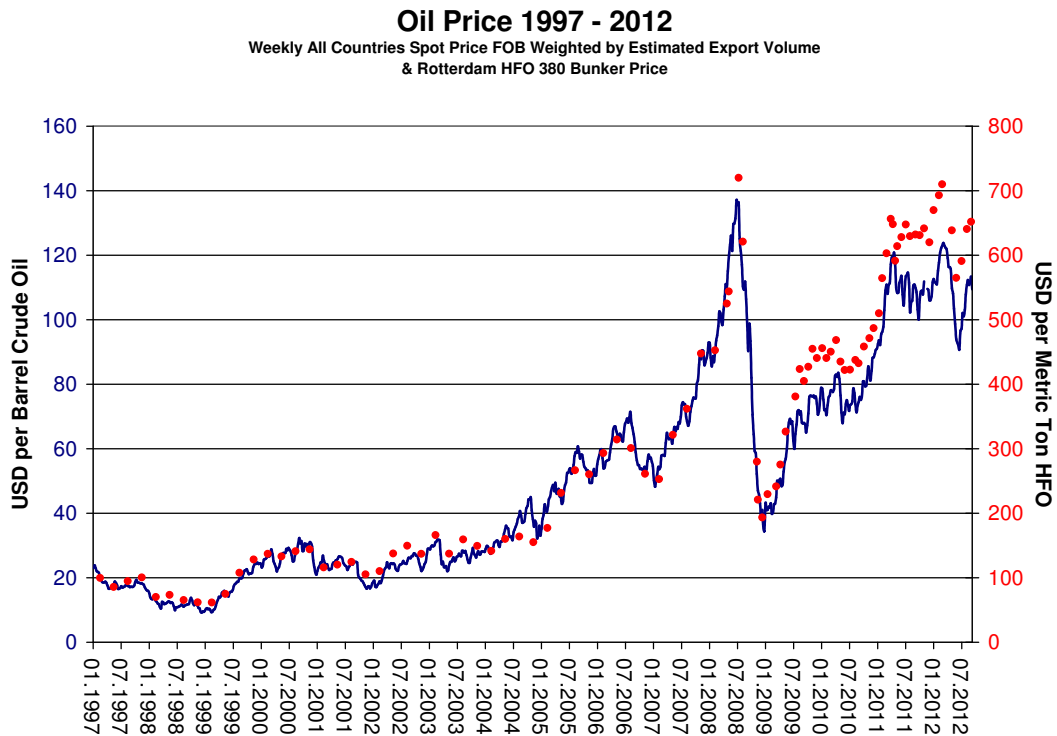
Figure 2.6. Variation of crude oil (blue line) and fuel oil (red dots) prices.

the prominent peaks, the fuel prices have approximately quadrupled within only 10 years. Current vessels, being built within this period, were therefore designed at a time when fuel costs were not as important, especially not as compared to investment cost. Due to the increase in fuel costs, the focus came back on energy saving technologies which were out of focus since the last oil crisis in the late 1970's to early 1980's, when the German research project *Ship of the Future* was started as described in Section 2.4.5. In the long period of low prices for energy ranging approximately from the mid 1980's to early 2000's, most energy saving innovations were not applied because their costs made them economically not feasible and the technology hibernated in research reports. After this, the recent increase of fuel oil prices with a perspective of persistent increase or at least stable high prices in the future can be considered a strong driver for energy saving on board of vessels. A further increase in fuel price is expected through market based instruments as a political instrument for reduction of greenhouse gas emissions.

2.2.5 Indicators for Transport Efficiency

For comparison of the efficiency of different modes of transportation, the transport efficiency in terms of emitted carbon dioxide per transported mass of cargo can be taken. The emitted carbon dioxide is a measure for the environmental impact and is equivalent to the consumed fuel multiplied with its carbon factor. This enables direct comparison of the efficiency and excludes influences through different types of propulsions and fuels used by the means of transportation. In Fig. 2.7, different types of vessels are compared to road and rail transport [BCE+2009] showing that well operated vessels are by far more efficient than road transport and generally more efficient than railway transport. For comparison, the carbon dioxide efficiency of air cargo is estimated to be around $500 - 600 \; \mathrm{g_{CO_2}}/\mathrm{t} \cdot \mathrm{km}$ [CRI2009].
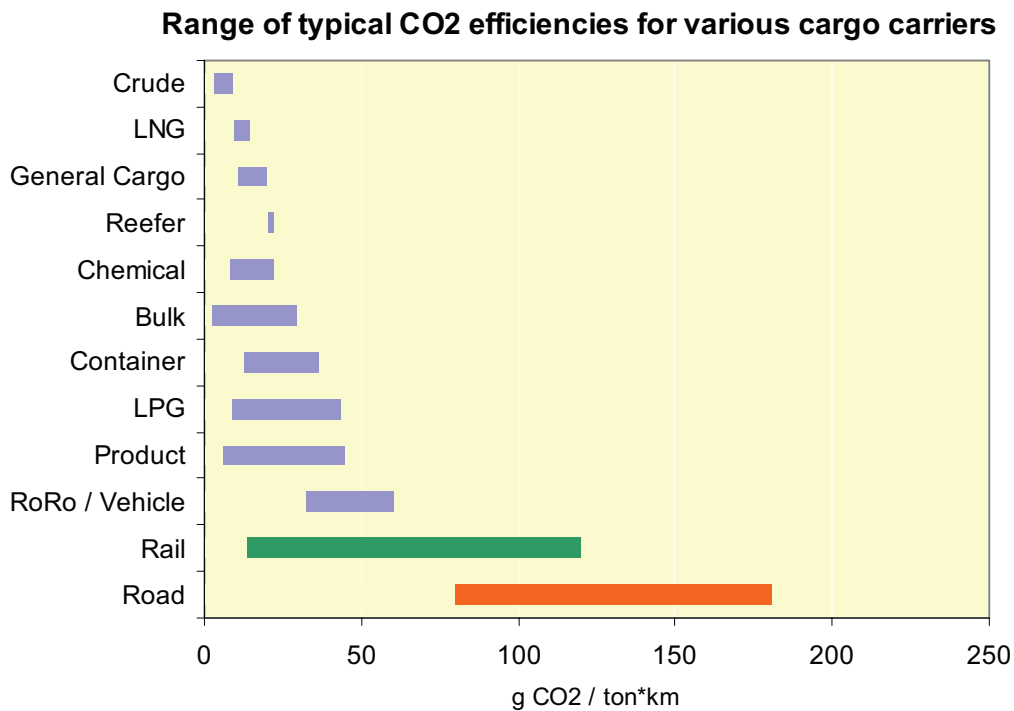

Figure 2.7. Comparison of different transport modes' efficiency [BCE+2009].

With adoption of resolution A.963(23) [IMO2004], the IMO Assembly urged the Marine Environmental Protection Committee (MEPC) to identify and develop mechanisms required for reductions of green house gas (GHG) emissions from inter-

national shipping. To achieve this, a GHG emission baseline should be established and methodologies for describing the GHG efficiency of ships in terms of an emission index and guidelines for their applications should be developed. Additionally, technical, operational and market based solutions should be evaluated.

The baseline was established as the Second IMO Green House Gas Study [BCE+2009] and at the 59th session of the MEPC, a package of interim voluntary technical and operational measures for the reduction of GHG emissions was agreed. The measures may be segregated into measures for new-built and existing vessels as well as into technical measures and market-based instruments.

2.2.5.1   Energy Efficiency Operational Indicator (EEOI)

As measure for determination of the specific CO_2 emissions and therefore transport efficiency of vessels, a defined indicator for vessels in operation was needed. The *Energy Efficiency Operational Indicator (EEOI)* was developed by the IMO MEPC and published as the Circular 684 [IMO2009b]. The EEOI defines the actual transport efficiency of a vessel. Unlike in the intermodal comparison as presented in Fig. 2.7, the indicator is defined here in terms of actual emitted carbon dioxide per actual transported ton mile,

$$EEOI = \frac{\sum\limits_{i} FC_i \cdot C_{Fi}}{\sum\limits_{i} m_{cargo_i} \cdot D_i} \quad . \tag{2.3}$$

Herein, FC_i denotes the consumed fuel in tons, C_{Fi} the related carbon factor as presented in Tab. 2.1, m_{cargo_i} the mass of transported cargo, and D_i the sailed distance in leg i. The weighted average of all voyage legs i within a certain time period, proposed to be one year, gives the vessel's EEOI for the period. This can be certified by an independent party, e.g. a classification society, as a measure of the transport efficiency in $g_{CO_2}/t \cdot nm$. This enables the direct comparison of similar vessels for their actual operational efficiency as well as benchmarking against other ships serving similar services or routes. The EEOI is designed as a voluntary instrument for all vessels, new-builds and existing fleet, which can be integrated in a *Ship Energy Efficiency Management Plan (SEEMP)* as described below.

2.2.5.2   Energy Efficiency Design Index (EEDI)

For new-build vessels, a second measure was developed. At the 59th session of the Marine Environmental Protection Committee (MEPC) of the IMO, the requirements

for an *Energy Efficiency Design Index (EEDI)* were discussed and an interim guideline circulated in August 2009 as MEPC 1/Circ 681 [IMO2009a] with a proposal for a formula that is presented in simplified form in Eq. (2.4). The EEDI should stimulate the use of efficiency enhancing innovation and technical development at a vessel's design phase and enables a comparison of vessels on building characteristics, without operational influence. The EEDI represents a theoretical efficiency of new vessels at a design point, which is defined at the design stage and verified at the sea trial before delivery.

$$EEDI = \frac{\left(\prod\limits_{j=1}^{M} f_j\right)\left(\sum\limits_{i=1}^{n_{ME}} P_{ME_i} \cdot C_{F\ ME_i} \cdot SFC_{ME_i}\right) + P_{AE} \cdot C_{F\ AE} \cdot SFC_{AE}}{f_i \cdot Capacity \cdot V_{ref} \cdot f_w}$$

(2.4)

The attained *EEDI* of a vessel is based on the emitted carbon dioxide divided by the transport work and can be applied to conventionally driven vessels. It is calculated using the main engine (ME) power P_{ME_i} in kW, defined as 75% maximum continuous rating (MCR), and auxiliary engine power (AE) at sea load P_{AE} in kW, the carbon factors of the used fuels $C_{F\ ME_i}$ and $C_{F\ AE}$ (Tab. 2.1), and the specific fuel oil consumption of main engine SFC_{ME} and auxiliary engine SFC_{AE} in g/kWh. Transport work is represented by an agreed vessel's *Capacity* multiplied by the reference speed v_{ref} in knots, which is corresponding to the P_{ME_i}. *Capacity* is defined depending on the type of the vessel as its deadweight tonnage (DWT), its gross tonnage (GT) or defined parts thereof. Correction factors f_i and f_w can account for ice class and sea conditions, respectively, but are not agreed upon yet and set to 1. Further corrections can be included for shaft generators and motors, innovative electrical energy efficient technology like waste heat recovery, and innovative mechanical energy efficient technology and propulsive aids like sails, towing kites like the Skysails system or Flettner rotors.

Individual attained EEDIs are compared to reference lines, defining if the vessel's EEDI is superior (meaning below the baseline) or inferior (above the baseline) of the average fleet at its capacity. The reference lines are regressions from the international IHS Fairplay Database (former Lloyds Register Fairplay), with IMO MEPC 62/24/Add.1 Annex 19: Resolution MEPC.203(62) Amendments to Annex VI [IMO2011] defining proposed reference lines. An exemplary reference line regression from container vessels is shown in Fig. 2.8, with vessels represented by blue dots and the regression line as the black line [MUN2011]. These baselines are to be

gradually lowered over the next 15 years, allowing only vessels with improved energy
efficient design to be build. The introduction of a mandatory EEDI for newbuildings
of the most common vessel types was agreed on at MEPC 62 in July 2011 and will
enter into force on 1 January 2013.
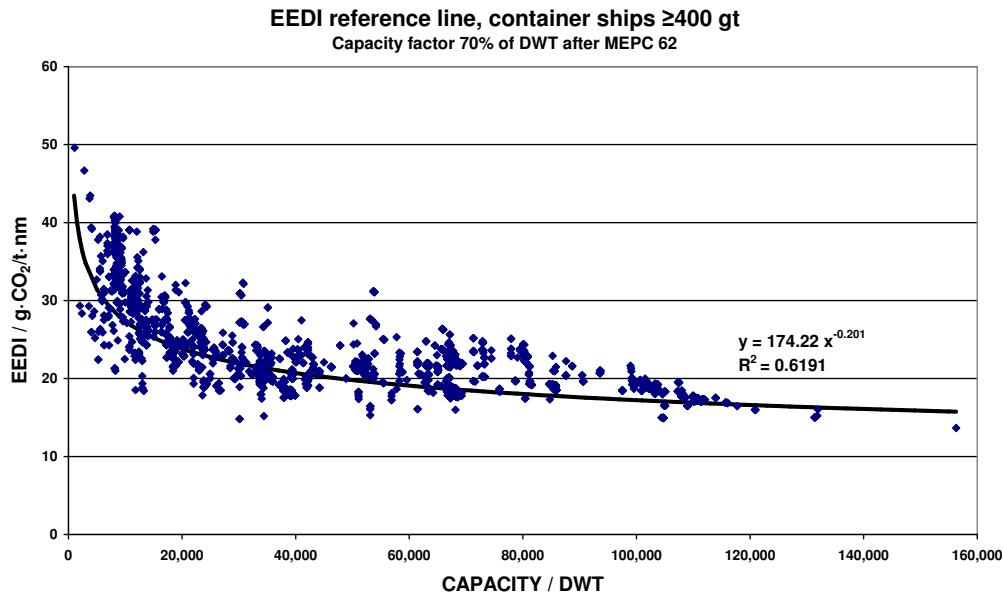
Figure 2.8. Reference line regression of container vessel EEDI [MUN2011].

2.2.5.3   Ship Energy Efficiency Management Plan (SEEMP)

The *Ship Energy Efficiency Management Plan (SEEMP)* is an agreed measure for
efficiency improvement of vessels in operation introduced by the IMO. The SEEMP
covers all parameters having an influence on fuel oil consumption and establish a
plan of best-practice initiatives to monitor the energy efficiency of vessels, e.g. with
the EEOI as measure for overall operational efficiency, and document the efforts
for improvements. Instead of a common pre-defined action plan for all vessels, the
SEEMP is defined open for energy efficiency improvement initiatives individually
customized for each ship by the ship owners or operators. These voluntary actions
can include weather routing, improved speed management for reduced waiting times
and lower speed on long passages, improved machinery operation and other best
practice initiatives for lower fuel consumption.

The monitoring of actual vessel operation, detection of saving potentials and
documentation of savings can be achieved by onboard tools with permanent acqui-

sition and storage of operational data, which's development is one aim of this work. Examples of such systems are presented in Section 2.4.4 and Ch. 5.

The SEEMP, including EEOI, and the EEDI of the vessel can be integrated in an International Energy Efficiency (IEE) Certificate as proposed by the IMO [IMO2010b].

2.3 Shipboard Systems and Technologies

From an energy system point of view, a vessel can be described as an operating power plant with consumers throughout the vessel. Power plants provide mechanical, electrical, and thermal energy for the corresponding consumers, with the propeller for vessel propulsion as the main consumer. In this section, onboard systems for propulsion, electrical power and auxiliary requirements are described in brief.

2.3.1 Main Engine and Propulsion

The main converter of energy and consumer of fuel oil aboard is the main engine for propulsion. Depending on vessel size and type, different concepts for propulsion are used. The three major types in commercial shipping can be categorized into

- 2-stroke diesel engine, gearless: Vessels >10000 GT

- 4-stroke diesel engine, high or medium speed, geared: Vessels <10000 GT, cruise vessels

- diesel-electric propulsion, 4-stroke diesel engines coupled to generators: e.g. special crafts, cruise vessels

Due to its low cost and good efficiency at the design point, most freight vessels have a configuration of one propeller directly coupled to the main engine. Freight vessels >10000 GT mainly use 2-stroke diesel engines directly connected to a fixed pitch propeller. These diesel engines are designed for running at a nominal speed of around 100 rpm and maneuvering speed down to 30 rpm.

Diesel-electric propulsion, coupling the main engines to generators and driving the propellers with electric motors, is starting to be used especially at cruise vessels and special crafts. By decoupling the propellers from the main engines, diesel-electric propulsion allows a higher flexibility in operation of the diesel engine running with optimized loads.

Propellers may be categorized into the two groups

- fixed pitch propellers (FPP)

- controllable pitch propellers (CPP)

which are graphically presented in Fig. 2.9.

Fixed pitch propellers are normally cast in one block out of copper alloy. The position of the propeller blades is fixed at a pitch that can not be adapted in operation, fixing the propeller performance curves to the prevailing weather conditions without influences by the crew. FP-propellers are generally used at vessels designed for constant operation at normal sea service, where maneuverability plays a minor role.

Controllable pitch propellers have a hydraulically activated mechanism for the control of the blades' pitch, which is integrated into the hub. CP-propellers are, due to the elaborate construction, up to 3-4 times as expensive as FP-propellers [MAN2006], require higher maintenance, and they are slightly less efficient due to the larger hub. Advantages are improved maneuverability and the potential for decoupling the vessel speed from engine speed, allowing the use of asynchron shaft generators without frequency converters or choice of optimal engine speed for given load.
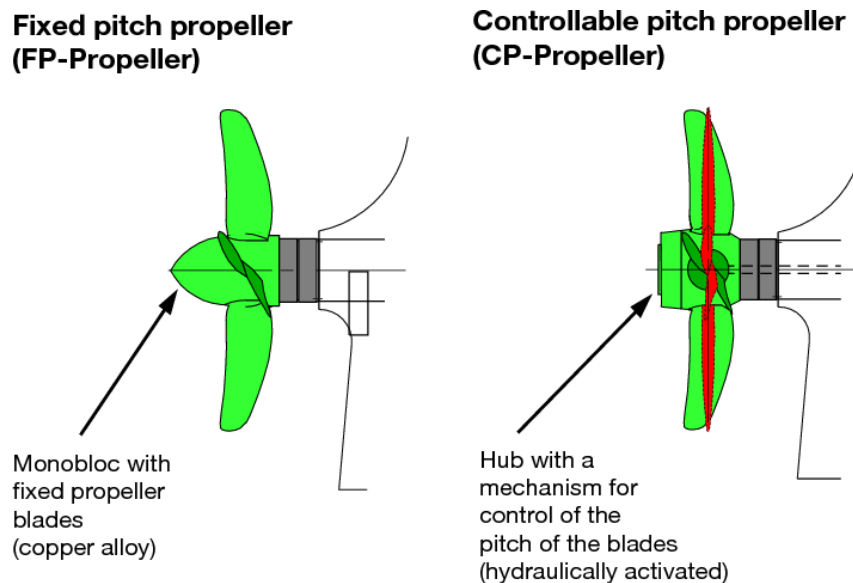
Figure 2.9. Controllable and fixed pitch propellers [MAN2006].

The high velocity of the propeller blades moving through the water results in strict requirements regarding geometry and surface finish for maximum efficiency. Already a small increase in roughness results in efficiency losses due to the increased friction. Figure 2.10 shows the efficiency loss due to increased roughness for propellers, as presented by Wärtsilä [VOE2006].
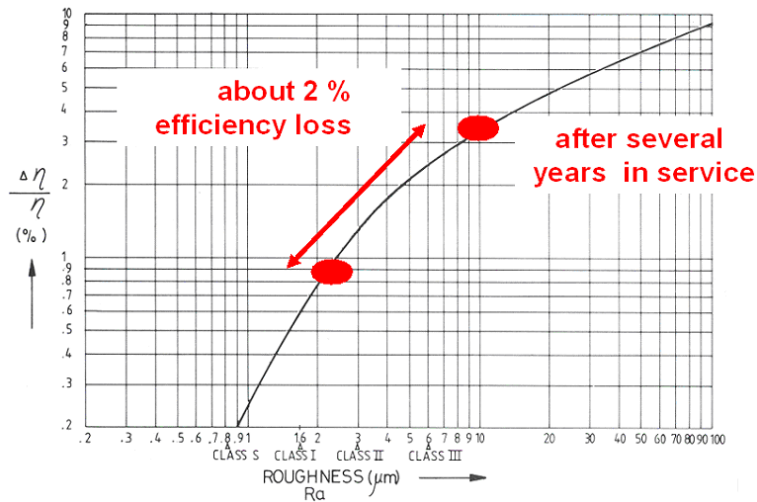
Figure 2.10. Efficiency loss of propellers due to roughness [VOE2006].

2.3.2 Auxiliary Engines and Electric Power Generation

Electrical power on board is mainly generated by diesel generators and shaft generators, less often also by waste heat recovery systems from the main engine. Diesel generator sets are units of medium or high-speed diesel engines coupled to generators, which are operated independently from the main engine. They are the most common source of electrical power on board of commercial vessels, and also the core of diesel-electric propulsion. In case of installed multiple generator sets, the generator sets are usually switched on and off approximately following the grid load. This is usually done automatically with a power management system (PMS) and a predefined minimum available load on the running generators.

Shaft generators, also called power-take-outs (PTO), can be very economical, as they are driven by the higher efficient main engine and reduce the operation time of additional diesel engines of generator sets. The fixed connection to the shaft requires a constant-speed operation of the main engine for a constant frequency, if no frequency converter is installed. During port stays, the power has to be provided by diesel generator sets or other power sources. Shaft generators can partly also be used as an power-take-in (PTI), changing the generator into an electric motor for additional shaft power or as an emergency propulsion system.

2.3.3 Auxiliary Systems for Engines and Ship Operation

For most ship types without extensive cargo care, e.g. multi purpose vessels, container vessels, tankers and bulkers, the auxiliary systems for the engines are the largest constant consumers on board. The supply of combustion air, fuel oil and lubrication, and the removal of waste heat by cooling water and air requires a significant part of the overall energy consumption.

2.3.3.1 Fuel Oil System

The majority of ocean-going freight vessels use Heavy Fuel Oil (HFO), if not banned by authorities in the region of operation. Heavy fuel oil, also known as residual fuel oil, Intermediate Fuel Oil (IFO) and Marine Fuel Oil (MFO) as introduced in Section 2.2.4, mainly consists of the residual of the refinery process, which was not cracked into more volatile, short-chained hydrocarbons. Unlike in road transportation with its purified and distilled fuels, HFO is at ambient temperature tar-like high viscose and heavily contaminated and has to be heated and separated before being used as a fuel.

Heavy fuel oil is classified according to the ISO specification ISO 8217 (2005) [ISO2005]. Common types are RMG/RMH 380 or HFO 380, with an maximum viscosity of 380 cSt at 50 °C, and RME/RMF 180 or HFO 180, with an maximum viscosity of 180 cSt at 50 °C. The quality of heavy fuel oil is determined by

- density

- kinematic viscosity in cSt at 50 °C (e.g. 180 cSt, 380 cSt)

- sulfur content (e.g. 4.5% mass/mass, 1.5% m/m)

- carbon residues

- ash

- water content ($<0.5\%$)

- cat fines (metal residues from catalytic refinery)

- cetan number and calculated carbon aromaticity index (CCAI) .

The sulfur content is limited according to IMO MARPOL Annex VI Regulation 14, which is since January 2012 3.5% m/m worldwide and 1.0% m/m for use in

sulfur emission control areas (SECA). Additional regulations apply to certain ship types and regions. The sulfur content worldwide is proposed to be further limited in 2020 to 0.5% m/m. For the SECAs, the allowed sulfur content are to be reduced to 0.1% m/m in 2015, which means effectively the use of low sulfur MDO or the installation of an exhaust gas scrubber.

Due to its high viscosity, heavy fuel oil requires a well designed fuel system with constant heating, in case of HFO 380 the temperature has to be kept above about 50 °C for being pumpable with conventional fuel oil pumps. The viscosity - temperature dependency of different fuel oils is illustrated in logarithmic graphs, Fig. 2.11 [HYU2009]. This requires heating of the whole fuel oil system, with heated storage tank, pipes, pumps, fuel oil preparation and auxiliaries.

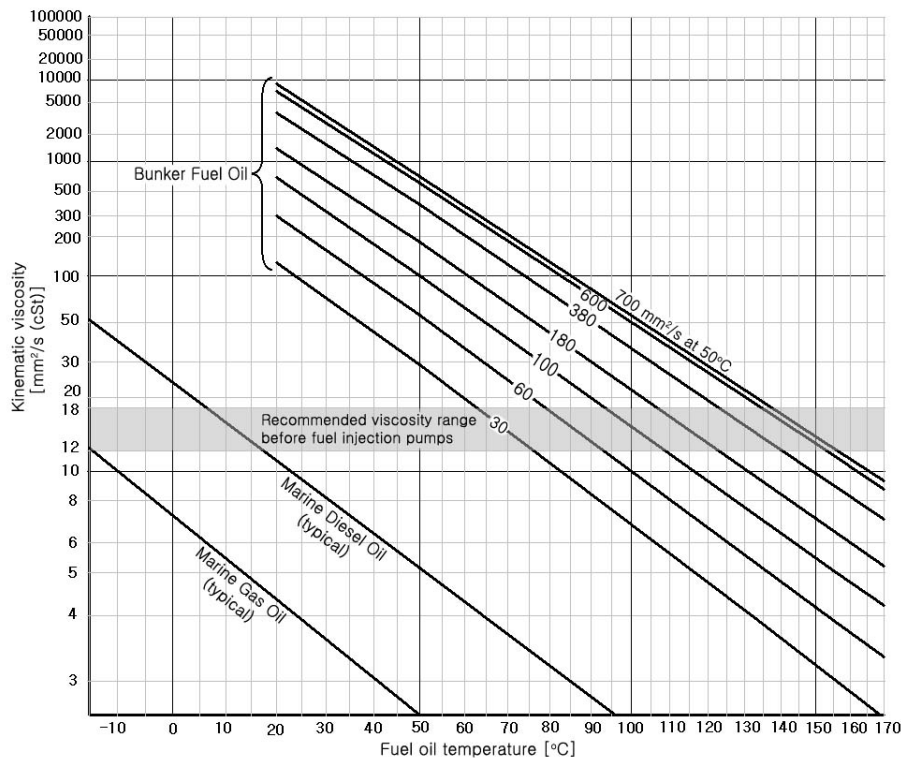**Figure 2.11.** Temperature - viscosity diagram of marine fuel oils [HYU2009].

For the separation of the burnable fuel oil from water and incombustible residues, centrifugal separators and filters are used, at separation temperatures of about 100 °C. Engines are supplied with this separated fuel oil via a fuel circulation, in which 3-6 times of the consumed fuel oil is circulating. The fuel circulation enables

faster load changes of the engines than the inertia of the fuel preparation would allow for, and avoids clogging of the fuel in low consumption. Within the fuel circulation, the pre-heater keeps an injection viscosity of 10-12 cSt [MT2007] in the circulation line by setting the injection temperature accordingly between 120 °C and 160 °C, depending on fuel quality. The pre-heater operates either with steam from the exhaust gas boiler and auxiliary boiler or electrically. A schematic of the fuel oil system is shown in Fig. 2.12 with separate systems for HFO and MDO operation [MAN2010].
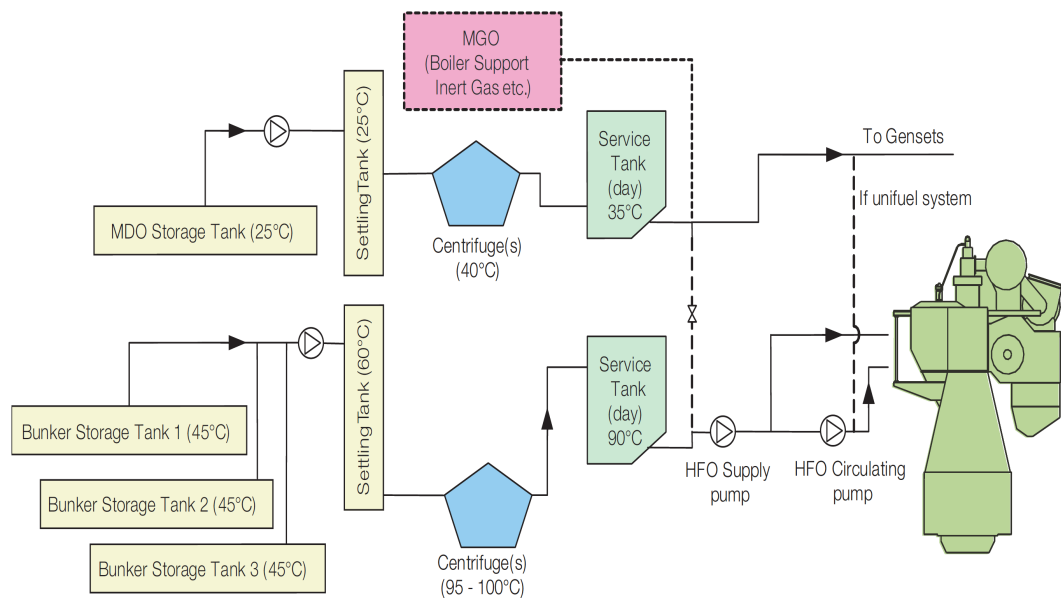
Figure 2.12. Schematic of a fuel oil system [MAN2010].

The upcoming tightening regulations result in the necessity of occasionally using low sulfur MDO instead of HFO, even though the vessel's systems are designed for HFO. In these cases another consumer has to be added in the fuel oil system. The viscosity of the fuel oil has to be kept above about 2-3 cSt [MAN2010] and therefore below certain temperatures for maintaining sufficient lubrication of the pumps. Additionally during fuel change over from HFO to MDO, the MDO flows through the fuel systems, which are still preheated from the HFO operation. Due to the high volatility of the MDO, it can gasify at the temperatures required for HFO injection. This imposes a severe risk for the engine up to main engine break down. To keep the MDO at the required temperature it is therefore cooled down

using a refrigeration system before being pumped to the engine, requiring significant electric power for the cooling unit.

For the monitoring of the efficiency of the engine and the vessel in operation, the measurement of the fuel flows in conjunction with the generated power of the engine is required. The currently available methods for fuel flow measurement and the related challenges are presented in the following paragraphs.

Fuel circulation, high temperatures and heavy vibrations impede a direct measurement of the fuel oil currently consumed by the engine. To avoid these strains, most fuel flow meters are situated behind the fuel separation, decoupled from the current consumption of the engine by the mixing tank and the circulation. Due to this decoupling, these measurements can only be used to analyze the consumption over a certain period of time, not as the current consumption at this moment.

For determination of the current consumption, two fuel flow meters have to be installed in the fuel circulation, one after the pre-heater and one after the engine fuel take-out. The difference between the two measurements is the currently injected fuel in the engine. Due to the high temperatures and the accordingly higher heat losses during the flow in the circulation, the difference in temperature can not be neglected between the two measurements. Fuel flow meters used in maritime applications are at the moment mostly measuring volume flow, e.g. from Kral AG [KRA2011], Aquametro [AQU2010] and VAF [VAF2011], compare below, where the density of the fuel oil is required for determination of mass flow. This density is depending on temperature, which can at constant pressure and temperature differences below 50 °C be approximated by

$$\rho_1 = \rho_0(1 - \beta(T_1 - T_0)) \ , \tag{2.5}$$

being ρ the density, T the temperature and β the temperature coefficient of density in state 1 with reference state 0 [N.N1971]. Due to this change in density, the measurements before and after engine have to be temperature corrected. This increases the uncertainty of the measurement, as the uncertainty in volume flow and temperature measurements are combining with uncertainties of fuel properties, and the difference of two measured absolute values is always very sensitive to errors.

Flow measurement methods can be categorized based on their underlying physical principle. The main categories used in industry are [BON2002]

- volumetric methods: rotary piston, oval gear, sliding vane, screw spindle, turbine wheel,

- differential pressure methods: Venturi nozzle, orifice,

- thermal methods: hot wire, heat capacity methods,

- coriolis method,

- run time and Doppler methods: ultrasonic and laser, and

- magnetic-inductive methods.

The physical properties of fuel oil and onboard requirements for the equipment restricts the choice of the meter. On vessels, fuel flow measurements are mainly conducted using volumetric displacement meters in different profiles and, rarely, coriolis meters. Table 2.2 gives an overview of flowmeters in maritime applications, their types and accuracies based on literature and manufacturers data.

Table 2.2. Measurement accuracies of common flowmeter types.

Flowmeter type	Source	Measured property	Accuracy	Range Q_{min}/Q_{max}
Rotary Piston	[BON2002]	Volume flow	$\pm 1.0\%$	$1 : 100$
	[AQU2010]	Volume flow	$\pm 0.4\%$ *	$\approx 1 : 25$
Oval gear	[BON2002]	Volume flow	$\pm 1.0\%$	$1 : 30$
Screw spindle	[KRA2011]	Volume flow	$\pm 0.4\%$ *	$\approx 1 : 100$
Sliding vane	[VAF2011]	Volume flow	$\pm 0.3\%$	$\approx 1 : 80$
Coriolis	[BON2002]	Mass flow	$\pm 0.2\%$	$1 : 100$
Coriolis	[VAF2011]	Mass flow	$\pm 0.1\%$	$\approx 1 : 20$
			* paired calibration	

The main engine and auxiliary engines are crucial for the vessel's safety. A stuck volumetric displacement flow meter would cause an inability to maneuver. Therefore each volumetric displacement flow meter requires a bypass in the fuel pipes for these cases, which extents the efforts in integration and space requirements on board of vessels.

2.3.3.2 Lube Oil

Operation of the main engine requires significant flows of lube oil for lubrication and cooling of bearings, pistons, and turbochargers. Its volume flow is close to the cooling fresh water flow but at higher pressure, which exemplifies that the lube oil pumps are significant consumers of electrical power. They are grouped under the

largest constant consumers on board. Lube oil returning from the engine is prepared
in separators before being pumped through micro-filters back to the engines; on
ocean-going vessels these are mainly automatic filters with automated backflushing
for cleaning. These filters have a high pressure drop. The heated lube oil is mainly
cooled against the fresh water cooling circuit of the vessels. The thermal energy of
the lube oil is only at few vessels included into a waste heat recovery system, even
though the high temperature compared to cooling water comprises a good potential.

2.3.3.3 Cooling Water

Cooling water systems on board of vessels consist usually of two or three circuits,
which can be interconnected by heat exchangers as well as mixing units. The engine
is cooled directly by a high temperature fresh water cooling circuit and a low tem-
perature fresh water cooling circuit, depending on the temperatures of the cooling
demand. These circuits are either completely separated or partially concatenated,
with a part of the low temperature cooling circuit being split into a pre-warmed
high temperature circuit. A separated cooling circuit is for cooling the fresh water
cooling circuits against the sea water. This sea water cooling circuit is separated to
limit the area exposed to the corrosive sea water especially at elevated temperature
level.

The cooling water system keeps the engine at constant temperature by removing
parts of the engine waste heat resulting from the entropy generation of irreversible
processes in the engine. When the engine is out of operation or after starting the
engine when it is still below its optimum operation temperature, the cooling water
circuit is usually used for heating the engine. In large commercial vessels, high
temperature cooling water is extensively used for heating purposes on board as well
as fresh water generation. In times of low availability of thermal power, during
port stays or maneuvering or right after engine start, the required heat for engine
preheating and other heat demand is provided by an auxiliary boiler.

The cooling water system as a vital system of the vessel is subject to strict
rules regarding its dimensioning [GER2010]. These rules state that the cooling
water system has to be able to prevent the engines' overheating in case of the
worst case scenario of tropic waters (32 °C) and an overload of 110% MCR of the
main engine(s). Systems onboard current commercial vessels are mostly constantly
operating at the design point, with temperature control via appropriate bypasses
of the heat exchangers. The bypass-control keeps the whole pumping power in
application during the main engine operation, despite the significantly lower cooling

demand due to lower travel speeds and lower sea water temperatures, especially in inner-European and transatlantic shipping. As the cooling water system is one of the main consumers of auxiliary power, this circumstance presents a significant saving potential. Instead of bypassing and throttling, the pumps can be speed controlled by frequency converters. The required pumping power to volume flow can be described by the relations

$$
\begin{aligned}
\dot{V} &\sim n \\
P_{pump} &\sim n^3 \sim \dot{V}^3
\end{aligned}
\tag{2.6}
$$

being $\dot{V}$ the volume flow, n the revolution speed of the pump and P_{pump} the required pumping power. This third-power law shows that savings in volume flow result in roughly cubed savings in pumping power, as displayed in Fig. 2.13.
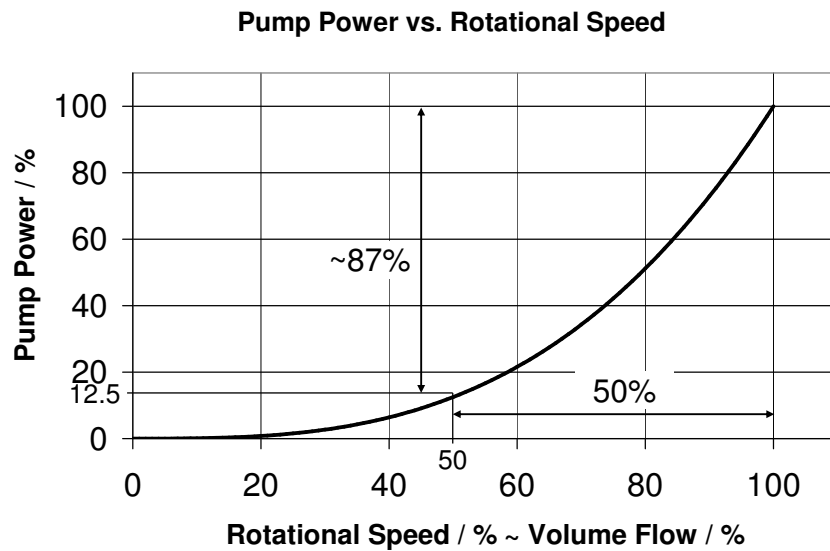
Figure 2.13. Dependency of pump power and fluid flow.

The required frequency converter for a speed control of the pumps are a standard application in shore-based power stations. The often criticized reliability issues are expected to be overcome with the latest series in frequency converters and decades of shore-based testing and installations, e.g. from KEB, Siemens or ABB.

For the monitoring of the efficiency in cooling water circuits, the determination of the cooling water mass flow and the temperatures at inlet and outlet of the heat exchangers is required. The determination of volume flow based on measured electrical power of the driving motor and the pressure increase is not possible, as the

characteristic curves of centrifugal pumps are very flat, resulting in large errors for small deviations in measured values of electrical power. Therefore, for evaluation of the mass flow in cooling circuits, more complex measurements have to be deployed, e.g. by use of volumetric displacement flow meters, ultrasonic Doppler effect measurements or the installation of measurement orifices.

2.3.3.4 Combustion and Cooling Air

Within the ship machinery, significant amounts of air are needed. Main and auxiliary engines draw their combustion air directly from the engine room, additional air is needed for cooling and air exchange in the enclosed spaces of the vessel.

As in the case with the pumps, controlled speed fans can save electric energy if the actually required air volume flow is less than the design flow of the fans. This is the case especially for engine room fans and cargo hold fans. While it is, at some ships, possible to turn off single fans for the engine room and the cargo hold room, the actual routine is often only to turn the whole set of fans on or off. Depending on ship type and size, the fans can have more than one megawatt (MW) of installed electrical power. During port stays or at low power of the main engine, the engine room fans could be speed reduced. When having reefer container in the cargo holds, container vessels have to ventilate the cargo holds. Here the control of the fans for the optimal air flow depending on ambient temperature, reefer count and load can save energy as well.

2.3.3.5 Waste Heat Recovery

Depending on the engine size and type, between 50% and 70% of the engines energy input is converted into waste heat. This waste heat is discharged from the engine within exhaust gas, cooling water, lubricating oil, and by radiation. For improvements in efficiency and saving of fuel, this heat can partly be recovered and used on board. The most common application is to utilize the heat of the exhaust gas in an exhaust gas boiler for heating purposes by either steam production or heating of thermal oil. This is used for HFO fuel preheating, cargo heating, and domestic heat. For freshwater generation, the high temperature cooling fresh water of the main engine is often used, which then evaporates seawater in an atmosphere of reduced pressure.

For large engines, an evaporator exhaust gas boiler can be used for steam production for a conventional Rankine cycle, driving a generator by a steam turbine. It

can be distinguished between single-pressure turbines and double-pressure turbines, which use a reheat cycle for higher efficiency. This increases the efficiency of the engine by up to 10%, as more of the thermal energy can be utilized. The Sankey diagram of an engine with an exhaust gas boiler for electricity generation by a steam turbine can be found in Fig. 2.14. Beside the conventional Rankine cycle using water and steam as the working fluid, research is undertaken for introducing Organic Rankine Cycles (ORC) on board of ships, which can make use of high temperature cooling fresh water as well.

Moreover, power turbines can be installed in parallel to the turbochargers. In high engine loads, a surplus of exhaust gas is diverted through this turbine and converted into mechanical power, which is then driving a generator.
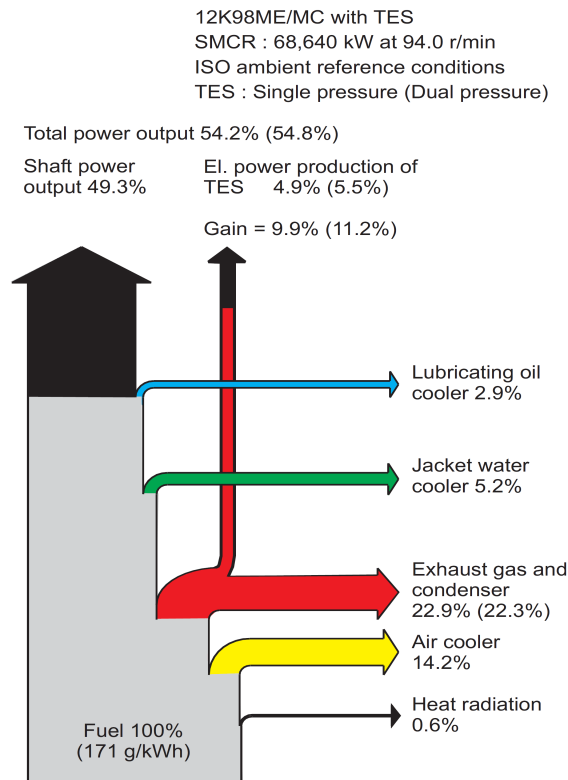

Figure 2.14. Sankey diagram of a two-stroke main engine with waste heat recovery system [MAN2005a].

Beside the main engine, vessels have increasing sizes of auxiliary engines for the various consumers aboard. Especially container vessels are equipped with up to 15 MW of auxiliary engines, in case of one of the currently largest container vessel

classes, the Maersk *PS class*, even close to 25 MW. The installed auxiliary power is therefore higher than the main engine power of most small to midsize vessels. While the main engine's exhaust heat is mostly used at least for heating purposes, the waste heat of the auxiliary engines is currently not used, even though there is a high potential.

While being in port and in times of low availability of waste heat from the main engine, currently the auxiliary boiler provides the ship with the necessary heat. Meanwhile the auxiliary engines are producing waste heat, which is not used. Therefore a potential for energy saving is the use of auxiliary engine waste heat instead of the auxiliary boiler.

A second approach of saving is made by heat management, i.e. the control of the heat use. This involves mainly shutting down of consumers in times of low heat production. Current practice of heat management is the heating of bunker tanks in use or those which are soon to be used, while other bunker tanks are not heated. An improvement could be during short port calls. If the time period is short, the bunker in the tanks will not cool down significantly in port, making it possible to turn off the heating. This lowers the heat demand in port which is currently provided by a burner-heated boiler and it would thus lower the fuel consumption and exhaust gas emission in port.

To enable a lower heat demand, additional insulation of fuel tanks, piping, and waste heat system is necessary. In some cases, the heat consuming processes could be modified for lower heat demand. Combining these methods, the present investigations indicate that the auxiliary boiler could be substituted by a waste heat recovery system on the auxiliary engines.

Reliable operation of waste heat recovery systems require a good system design fitting to the actual operational profile of the vessel. Waste heat recovery systems that are optimized to run at about 85% MCR of the main engine, as is currently generally done, can not be utilized in slow steaming. In slow steaming, vessels are operated at very low engine loads, usually with the oil fired auxiliary boiler providing the process heat as the over-dimensioned waste heat boiler can not provide this heat. A thorough investigation of the expected real operational profile for designing the waste heat recovery system may improve the operation time of the systems on board and lead to a more flexible design regarding the operateable engine loads.

2.3.3.6 Heating, Cooling and Air Conditioning

Cooling of cargo and provisions as well as air conditioning for crew and passengers are mostly achieved with compression chillers. Especially on vessels transporting refrigerated or cooled cargo in cargo holds (so called reefer vessels) and on passenger vessels, the cooling system is a significant consumer of electrical power. But even on cargo vessels air conditioning of the superstructure accounts for up to 5-10% of the electrical power consumption at sea (without counting reefer containers, LNG reliquification, and other cargo care with high energy demand) [WIL2007a]. Current compression refrigeration may be substituted in future by higher efficient absorption coolers, which could utilize waste heat from engines [WIL2007a] [WIL2007b]. Research indicates that the absorption chillers can be used in the adverse conditions on board of vessels as well. Some first test systems have already been installed on board of a general cargo vessel, a cruise vessel and offshore construction vessels.

2.3.3.7 Other Onboard Machinery

Cargo handling, port activities and maneuvering require additional machinery on board. On large commercial vessels, bow (and stern) thrusters are often the largest single consumers. Often a stand-by operation prior to actual operation of the thrusters is required for starting up a generator set, with the additional generator set running for the maneuvering time where the thruster could potentially be used.

Deck machinery for cargo handling (e.g. cranes, automatic cargo hold hatches) and mooring (mooring winches, anchor winches) are additional large consumers. The use is restricted to port or anchoring operation and therefore limited to a defined time space, where appropriate load reserves have to be available. If no load request from the systems to the power management system is available, the loads are often not predictable and therefore the load reserves are higher than required, letting the generator sets idle at low loads.

2.4 Onboard Energy Management

The following sections explain the current efficency evaluations in shipping with data handling, vessel operation and supervision, and available onboard energy management systems.

2.4.1   Current Efficiency Evaluations

A survey regarding the current efficiency evaluations in shipping was conducted under the participating ship owners within the part EU-funded research project *Flagship B1*. These owners are operating more than 300 own or chartered container vessel and tankers, also personal communication to other ship owners was included. For these vessels the owners use different measures for the evaluation of their ships' efficiency. The ships' performance is typically evaluated using the burned fuel over a defined period of time, e.g. one trade. This consumption is compared to the consumption of sister ships and to other ships on the same trade, additionally to historic data and occasionally to the predicted consumption from model tests. The weather influence as a main impact on performance is estimated based on experience and logbook data.

The actual efficiency of the ships is measured indirectly based on the specific fuel oil consumption (SFOC) of the main engine. According to technical fleet managers, performance trials are undertaken for this. These can be done in regular intervals, e.g. every quarter of a year, or at a time requested. The ship is heading for a defined time period (e.g. one hour) straight at a constant speed and power while the consumption is measured with the fuel flow meter, if installed. From the average power and the consumed fuel the SFOC of the main engine can be calculated and compared to a reference value, indicating problems of the main engine. Efficiency of the propulsion system is checked by the chief engineer via the slip-factor. By comparison of the used power at the measured speed through water, potential problems with hull and propeller are investigated. For this evaluation the weather conditions are very important but difficult to include into corrective calculations.

These performance runs have to cover a period of time which is long enough to allow for a stationary operation of the engines. For large two-stroke engines this can take more than one hour until the fuel flow is constant and the measurement is reliable. During normal operation the fuel flow measured with the flowmeter can not be taken as the actual consumption due to the storage capacity in the fuel circulation, which buffers and separates the fuel flow through the flowmeter from the fuel flow into the engine. Additionally, the accuracy of the flow meter in off-design operation is considered to be not reliable.

The condition of the main engine is considered crucial for the efficiency of the ship, since it is the main consumer of fuel. Therefore it is intended to be kept at optimum performance and is maintained regularly. In addition, the engine parameters are

regularly checked for abnormalities.

The hull and propeller conditions are also important for the overall fuel efficiency, but they are usually checked in class inspections or only once in between. Additional inspections in between are only done if the crew suspects damage or detected a significantly higher power required for a given velocity. This demonstrates that awareness of the crew for energy consumption aboard is very important, especially if monitoring is based only on these indicators at a high level, which integrate the various influencing effects into few indicators which cover a long time period.

2.4.2   Data Handling

On modern bridges, all kinds of data concerning the current status of the ship and its machinery are available. This includes but is not limited to the navigational data, weather data, power of the main engine and the auxiliary engines, the status of the machinery, and if installed the fuel consumption from electronic flow meters. Most of this data is not stored for an analysis ashore but used for maintenance and in case of a system failure. This data is analyzed if manually requested or if an alert comes up at the system.

While all of this data is available in the bridge automation system, it is usually not possible for the ship owners to save and analyze this data on their own systems. This is due to proprietary bus signals of each bridge and automation system manufacturer, which currently prohibit the data exchange between different systems like bridge automation system and owners' data analysis.

The data concerning the consumption is often summarized for the ship owner or operator in a daily report called *Noon Report*, which reports the approximate consumed fuel over the last 24 hours. It can furthermore contain navigational and weather data and the running hours of the engines. In some cases, the consumption of each engine within each operational mode (at sea, during maneuvering, in port) is noted, and the current power of the engines at the time of the report. All data are manually collected and written into the report.

The load of the auxiliary engines is controlled by the chief engineer, but it will not be recorded and the efficiency of power generation is not evaluated. The generator load depends additionally on the required available power for the operational modes from the class. At sea, the average load of the generator sets is estimated to be around 60%. When manoeuvring or sailing in restricted waters, the load is lower due to the additional stand-by generators for safety reasons.

The consumption of the boiler is logged mostly for ships with a high heat demand, whereas for ships with low demand of heating the boiler is sometimes not accounted for separately. The ambient conditions are manually journalized in the logbook. In the logbook, the position of the ship, the heading, the speed over ground and through water, and the water depth are often logged as well.

The reports from the ship are usually sent as a spreadsheet and are included into databases. Even though this may be done automatically, the data capture aboard is done mostly manually and has therefore a high error probability.

2.4.3   Vessel Operation

The essence of the evaluation and personal communication to onboard crews and shore-based inspectors is that the vessels are still operated mainly based on experience of the crew, with support from monitoring systems and automation systems. Controls are designed with the aim to maximize safety in operation and large safety margins, rather than maximizing efficiency as long as it is not interfering with safety. Diesel generators are controlled during sea passage by an automated power management system, compare Section 2.3.2, and during maneuvering and in port manually by the Chief Engineers, which imposes the largest saving potentials through improved control by enabling the turning off of unnecessary generator sets without jeopardizing the vessel's blackout prevention. Load shedding and control, beside for blackout prevention as a last measure, is virtually not existing. These indications are supported by the work of Busch [BG1998] and Napp [NG1988], who developed methodologies for predicting the electrical power demand by use of neural networks and by simulation of the onboard grid using the Monte Carlo simulation, respectively. Today, the lack of these tools seduces the crew to keep a higher number of generator sets running than necessary as a "good sleep" factor by providing a higher load reserve than needed by all possible consumers that could be turned on.

2.4.4   Onboard Energy Management Systems

Onboard tools support the crew through filtering and visualization of the energetic status as well as optimization of operation, which are essential for the efficient operation of ships, as presented above. The documentation of the available tools are often sparse, being glossy brochures and web presentations and only rarely scientific papers about the application and proven results of the tools.

In the following, currently available products of onboard and shore-based tools

are listed with a short description of their scope.

BMT SMARTpower (UK)

BMT Seatech [BMT2008] has developed the SMART product suite, which is a range of products that monitor and report on safety and performance aspects of a ship's operation. The 'power' module records ship speed, fuel consumption, shaft rpm and torque together with navigational and environmental parameters. Derived trends over time are corrected for draft, trim and environment. Current operation and corresponding time-lines are displayed. Traffic light symbols next to current values indicate deviations from pre-defined reference conditions. A reporting system for daily, voyage, or short-term performance trial reports is integrated.

Danaos Searoutes (Greece)

Danaos Searoutes [DAN2011] is a shore-based weather routing decision support tool, giving the crew a decision support for least power consumption during voyage from port of departure to port of destination through optimization of route around zones of weather with increased ship resistance (waves, wind). Danaos Searoutes is based on a hydrodynamic model of the vessel and specialized weather data, without onboard data acquisition and storage.

Decision3 (Faroe Islands)

Decision3 [DEC2011] provides a decision support tool based on training of an artificial neural network (ANN). The vessel power, speed, ambient conditions and weather as well as draft and trim data are training the network, with intelligent filtering and evaluation of the data. Aim is to display decision support for improvement based on experience of the ANN.

Eniram Dynamic Trim Assistant (DTA) (Finland)

The Eniram Dynamic Trim Assistant (DTA) [ENI2009] is a trim optimization decision support system, based on artificial neural network (ANN) and sophisticated data evaluation from dynamic trim sensors installed on board. Connection of current speed through water with trim and draft of the vessel, weather conditions (wind, wave), and the required power under these conditions. An onboard monitor displays the current performance with an indicator, how the trimming of the vessel can be improved. Time lines of trim and power are available.

FutureShip ECO-Assistant (Germany)

The FutureShip ECO-Assistant [FUT2012] is a trim assistant for decision support during trimming, based on CFD calculations of the hull resistance under different drafts and trims. It contains no onboard data acquisition and storage. The system requires no continuous operational data input, reducing the demand to a standard PC for installation of the software and can therefore be used on board as well as onshore for load planning.

Hyundai ACONIS 2000 (Korea)

The Hyundai Advanced Control & Integration System [HYU2008] offers an integration of various monitoring systems in a common user interface. These monitoring systems can include, depending on the buyers specifications, alarm and monitoring system, stand-by starter/motor control, cargo/ballast control and monitoring, power management system, PID control, hull stress monitoring, reefer container monitoring system, and ship performance.

These systems are used in ship automation with focus on ship safety. The "ship performance" monitoring option, being the system for improvement in energy efficiency and crew awareness for energy consumption, includes a trend display for speed, trim, main engine rotational speed and fuel consumption.

Kongsberg K-Chief 600 (Norway)

The Kongsberg K-Chief 600 [KON2012] is a modular marine automation system, which integrates besides alarm and monitoring systems further modules for vessel performance monitoring and decision support systems for optimized vessel operation. Engine performance can be integrated with the AVL engine performance and optimization tool AVL EPOS® and energy management with the Marorka Maren system, compare below.

Kyma Ship Performance (Norway)

The most sophisticated product of Kyma [KYM2012], the Ship Performance, integrates a shaft power measurement with a comparison to a baseline derived from sea trial and model tank tests. The system shows graphically deviations from the baselines with trending. It can generate daily and voyage fuel consumption reports, trending, and trial reports and diagnosis of vessel performance on excess fuel consumption.

LEMAG Shaftpower (Germany)

The LEMAG Shaftpower system [LEM2012] measures the shaft twist and derives torque, shaft power and RPM. The system also offers a comparison of the actual situation with a propeller curve and the inclusion of ultra-sonic flow measurement for specific fuel oil consumption evaluation [SCH2007].

Marorka Marin (Iceland)

Marorka Marin [MAR2012] incorporates the performance analyses of the machinery based on engine and machinery parameters, measurements and navigational data. Data evaluation is done using internal simulation of the machinery, including the calculation of improvement potentials through changes in operation. Marin records various machinery parameters together with navigational and environmental parameters, which can be analyzed later onboard and at shore, as well as reported as daily Noon Report or voyage report. Status of the machinery is displayed using a graphical user interface. Based on the current status and operation of the machinery, improvements of the efficiency are suggested to the user for decision support.

MICAD Marine (USA)

The MICAD Marine system [MIC2008] is a customizable onboard tool containing different modules as requested. The system estimates fuel costs based on current and proposed speed. Expected fuel costs and estimated time of arrival (ETA) at port of destination are displayed, with possibility to adjust speed and other ship parameters (e.g. propeller pitch, trim) and compare the results regarding ETA and fuel costs.

NAPA SPS Power (Finland)

NAPA [NAP2010] offers a fuel consumption optimization system based on the ship design package of NAPA. Routing and speed of the vessel are optimized for minimum fuel consumption based on hydrodynamics and calculated seakeeping of vessel from NAPA hydrodynamic modules. It offers a connection to a web-based office module that allows on-shore planning and controlling.

Propulsion Dynamics (USA)

Vessel and hull performance analysis of Propulsion Dynamics [PRO2009] is based on periodic data of the vessel performance for analysis of added resistance. No continuous data are collected but average data over long time periods, e.g. daily data, and momentary data at periodic intervals. Data analysis is performed ashore with mathematical models for calculation of the net-resistance excluding weather influences and comparison to base lines, e.g to sea trial data, for condition of hull coating and propeller.

Summary

All systems are relatively new and were developed in recent years. This explains a lack of sufficient reports about their functionality, user-friendliness and proven savings achieved in the installations. From many companies and products no reference lists are available, indicating that they may not be installed in representative numbers. Additionally, no technical information about the systems are available, e.g. which data are acquired from the machinery, how they are acquired, and how they are processed, which is expected to be highly customized on every vessel. Therefore the distinction between marketing glossy brochures and the actual system capabilities and usefulness is hardly possible without testing of the systems and the experience of seafarers using them in daily business. As the numbers of systems installed on board of vessels is expected to rise, the missing experiences and reports are expected to be published in close future.

Decision support systems for reduction of power consumption are not only a topic in shipping. In the railroad sector, the energy saving driving strategy of Deutsche Bahn *Economical Way of Driving* was successively introduced in the high-speed train ICE and other trains during the last 10 years. It consists of a computer-assisted routing system with implemented elevations and speed limits, which signals the train driver the currently used power or, in case of deceleration, produced power by the eddy-current brake. Furthermore, a comparison between schedule and actual time are displayed. In case of being on schedule, a proposal for the shutting down of propulsion power for in-time arrival at next stop with least possible power consumption are proposed, which can incorporate sections without propulsion power for the least possible braking. Overall achieved savings of the system are reported to be about 7.5% [VS1998] [LEH2007], which are partly accountable to increased awareness.

2.4.5   Results of R&D project *Ship of the Future*

The *Ship of the Future* [GER1986] already anticipated many technical trends and improvements, and the project has set the basis for the following research projects up to today. Even though the results for ship efficiency improvements had not been further applied in the following 25 years, compare below, most of the current evaluations (machinery and vessel monitoring, base line comparisons) and technical improvements (waste heat recovery, diesel engine optimization, frequency control of auxiliaries) have already been invented within the technical limitations inhering in that time. As this research project can therefore be considered the starting point and precursor of energy efficiency on board of vessels, the results of the *Ship of the Future* are described in more details.

In the oil crisis of the years 1979/1980, the first large research project for improving the ship efficiency was started. From 1980 to 1985, the project *Ship of the Future* was funded by the *German Federal Department of Research and Technology (BMFT)*. In this research project, 50 German companies, institutes, and universities headed by the *Howaldswerke-Deutsche Werft (HDW)* worked on improving the ship operation technology for higher competitiveness of shipping by increasing the level of automation, raising the standards of safety, improving machinery reliability and reducing the fuel consumption. These aims were separated into 51 technical topics for research, which were accompanied by 9 research projects of industrial sciences.

The following sections present the work packages and summarize the results related to improvements in efficiency and fuel consumption reduction.

2.4.5.1   Fuel Consumption Reduction

Concepts for reduction of fuel consumption are developed with the focus on reduction of propulsion power. Theoretical evaluations and basin tests of ship models are undertaken for optimization of hull forms for a container vessel with predefined cargo capacity and operational boundary conditions like maximum ship length and draft. The cost-effectiveness of the concepts were evaluated based on required cargo capacity, fuel costs and capital costs, and class requirements.

Inhomogeneous cargo stowing, depending on container weights, showed significant influence on the fuel consumption, but prevention of this requires more efforts and therefore higher costs in port.

Ship designs with from a capital-cost viewpoint "cheap" structural design and components are said to be possibly costly and uneconomical due to higher oper-

ational costs. The overall optimum was found to be a combination of structural design and operational means.

Optimized planning of dock times is analyzed with regard to the hull coating condition. The added resistance due to hull fouling is analyzed based on average values from daily operational data. Operational data required for the system analysis are reliable fuel flow measurement (stated to have at least $\pm 0.5\%$ accuracy), log speed for speed through water ($\pm 1\%$ accuracy), and permanently operating draft measurement sensors ($\pm 1\%$ accuracy) for a determination of the displacement. Additional input needed are weather and sea state data. By combination of these data, the deviation of resistance from a "as new" status from sea trial and first journey is calculated and trends are analyzed. The status of the hull is said to be determined weekly. Even though the resistance is depending on the operational profile and regions, the proposed method is supposed to be applicable to changing operational profiles and regions as well.

2.4.5.2 Diesel Engine Optimization

Diesel engines are recognized as the predominant ship engine, depending on the ship size and type, either as a 2-stroke or 4-stroke engine. As the main source of power and largest energy consumer, it is noted that a strong demand exists for improvements in fuel consumption, which is reflected by the research projects. The improving refinery process enables a higher share of light products from crude oil, but it results in lower grades of heavy fuel oil (HFO). This requires research for its use in ship engines without increasing fuel consumption, engine wear, and associated maintenance work.

Research is done for improving the fuel efficiency, which has been around 200 g/kWh for the large 2-stroke engines at that time, by optimization of the combustion process, improved materials and monitoring of the operation. Especially the latter is of interest here, as a diagnosis and trend system is proposed, which monitors the operation of the engine. With the least possible uumber of additional sensors, the system is monitoring the engine operation, fuel pump system, combustion chamber, and turbocharging devices. The focus is set on the early detection of malfunction, with an concurrent supervision of the engine efficiency.

The diagnosis tool compares the current condition of the engine with a mathematical model and limits in operation. Due to the accuracies in measurement, the diagnosis tool works only at engine loads above 50% maximum continous rating (MCR). A malfunction is detected in case of

- unacceptable deviations from reference values,

- exceeding of defined operational limits,

- deviations of operational data between cylinders.

For trend analysis, averages of actual values are taken once per day. 60 data sets are recurrently saved.

For 4-stroke engines, reference conditions are calculated using thermodynamic descriptions of charging, injection and combustion within the engine. 2-stroke engines are calculated using gas change cycle calculations depending on engine load according to propeller curve, scavenge air temperature and pressure, scavenge air pressure gradient, and combustion air properties. Results of the cycle calculation are approximated with polynomials or simple physical models, with reported small deviations except for the exhaust gas mass flow. The memory capacity of the available computer hardware turned out to be too limited to handle the 2-stroke program, therefore only the 4-stroke diagnosis tool was successfully tested on a test rig engine.

2.4.5.3   Auxiliary Systems

Within the project, the optimization of the auxiliary systems is emphasized, as besides the main engine the auxiliary systems are consuming a considerable amount of energy as well. The focus is set on the optimization of steam installations. In the *Ship of the Future* project, both main steam installations and auxiliary steam installations were evaluated. Main steam installations are not subject of the presented work, therefore only results of auxiliary steam installations are evaluated.

For optimized operation of the steam installations a control device is proposed, which includes the consumer side with mathematical models of their behavior. A program was developed for monitoring the efficiency of the steam installations, indicating current efficiency and indications for improvements for the operating personnel. This diagnosis tool is based on measurements of the conditions, giving increasing accuracy with increasing number of measurements points but increasing costs as well. While it could be used continuously, the authors suggest a discontinuous use. As a support tool for the operating personnel, they should choose the time of the diagnosis by experience, leaving periods of inefficient operation (e.g. maneuvering) excluded from the evaluation.

For the *Ship of the Future* idea, the whole auxiliary power demand is proposed to be reduced to the extent that it can be met by the recovered waste heat of the main

engine. All available waste heat, except for the necessary heat for bunker heating, is used for power generation in a steam cycle. For enabling this, the demand of the bunker heating should be minimized, leading to a block tank system for the bunker with minimal heat losses and the use of engine cooling water instead of steam, where it is possible.

2.4.5.4   Economic Sailing

It was noticed that economic sailing can save fuel oil even when all machinery is operating at its optimum. For supporting sailors in the choice of optimum speed through water and enabling them to recognize disturbances in operation at a glance, a display was proposed as presented in Fig. 2.15. The display shows the values of rotational speed, speed through water, fuel oil consumption and propulsion power as bar indicators, with the axis scaled in a way that under stationary conditions in calm and deep waters all bars show the same length. The bars are color-coded for quick perception if operation lies within the allowable ranges, e.g. for avoidance of excitation frequencies in propulsion or over- and under-speed of engine. In case of bad-weather conditions or shallow water influence, it is intended that the crew tries to re-equalize the graphs by changes in rotational speed to find the optimum operation under these conditions.
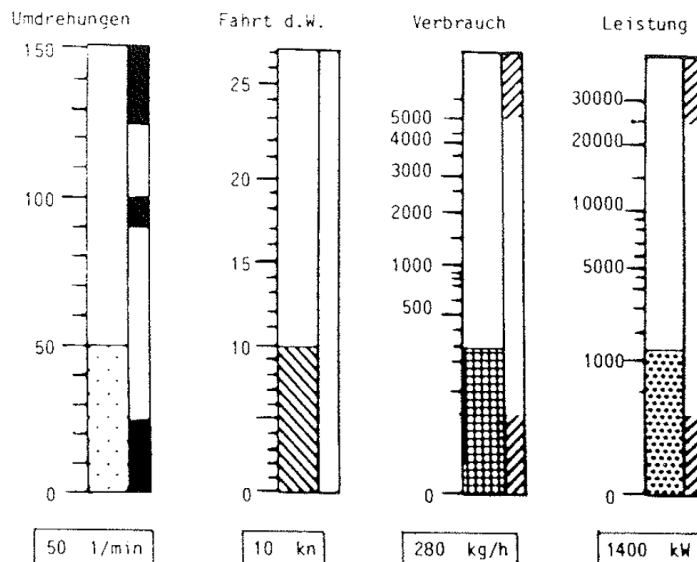

Figure 2.15. Proposed display for economic sailing in *Ship of the Future* [GER1986].

For decision support of the best course when having heavy weather, the diagram according to W.D. Moens in Fig. 2.16 is considered to be not intuitively enough readable. As a solution, a display using Cartesian coordinates shown in Fig. 2.17 is developed. The possible speed at given propulsive power is displayed as graph depending on the course, with current speed represented by the length of the bar above the ship symbol. The difference between the bar's length and the curve indicates the difference to ideal ship performance and is proposed to be removable by shifting the theoretical curve to the top of the bar.
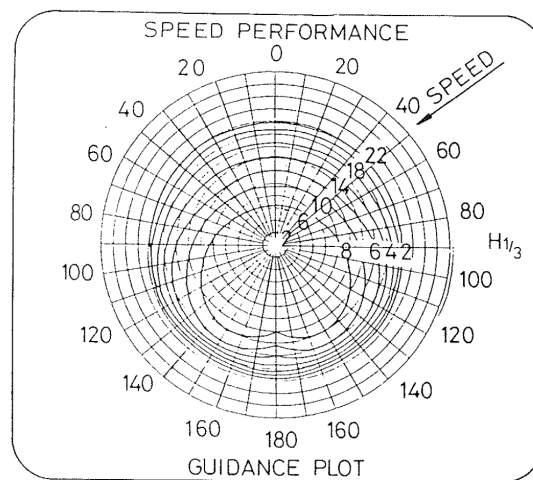

Figure 2.16. Speed performance guidance plot according to Moen, *Ship of the Future* [GER1986].

2.4.5.5   Comparison to the Presented Work

Many fuel saving techniques and operational improvements that are current state-of-the-art were already proposed or even developed in the *Ship of the Future* project. The reason for the practical non-existence of their application in shipping lies in the changes of the market conditions. After the oil crisis, the oil price dropped again, compare Fig. 2.18, making the investments in energy saving technology un-economical. The cheap oil between the mid eighties up to the early 2000's made the consumption of the vessel only a minor part of the operational costs, therefore the optimization process in ship building was focusing rather on low investment cost than on low consumption.

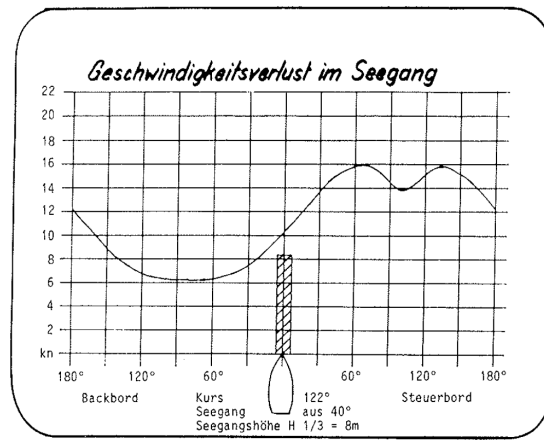An additional constraint was the limitation by available information technology.

Figure 2.17. Proposed display for course optimization in *Ship of the Future* [GER1986].
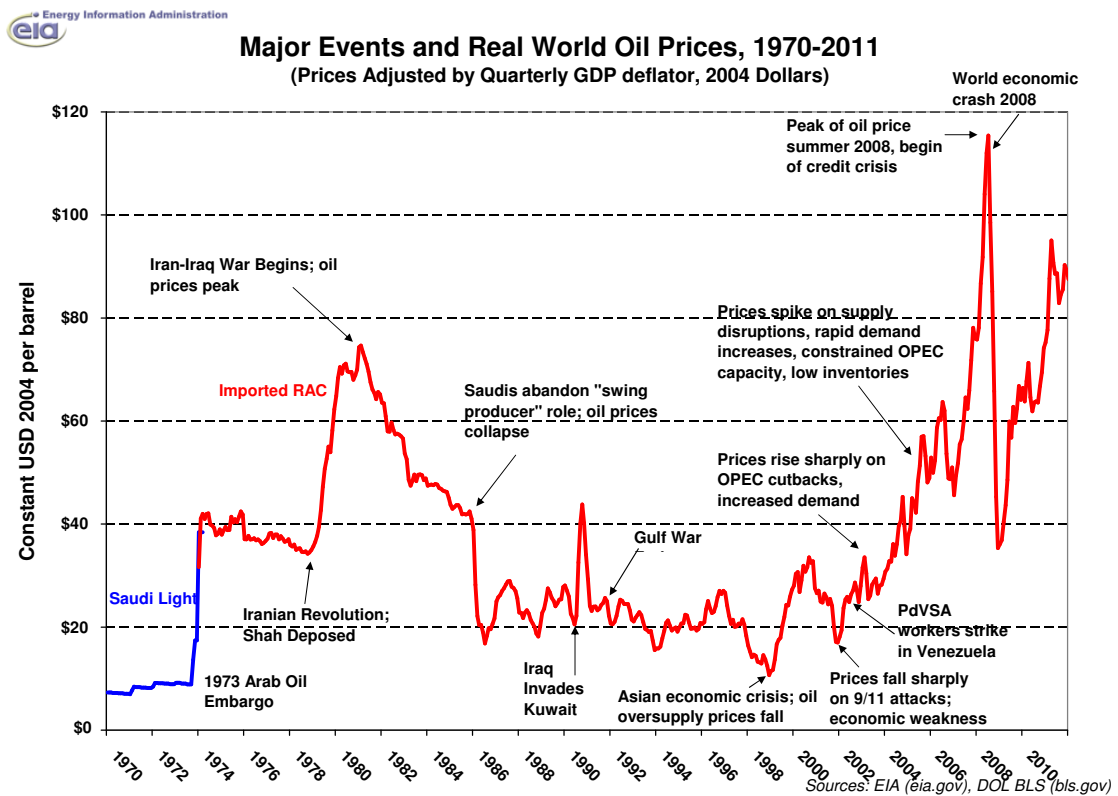

Figure 2.18. GDP corrected oil prices 1970 - 2011.

The computational capabilities in the eighties were far from what is possible today. The exponential growth of the computational capacity known as *Moore's Law* as

displayed in Fig. 2.19 [MOO1965], [WIK2010] correctly describes an 4000-fold increase since the mid-eighties, enabling nowadays real-time calculations of process parameters that were not possible during the *Ship of the Future* project.

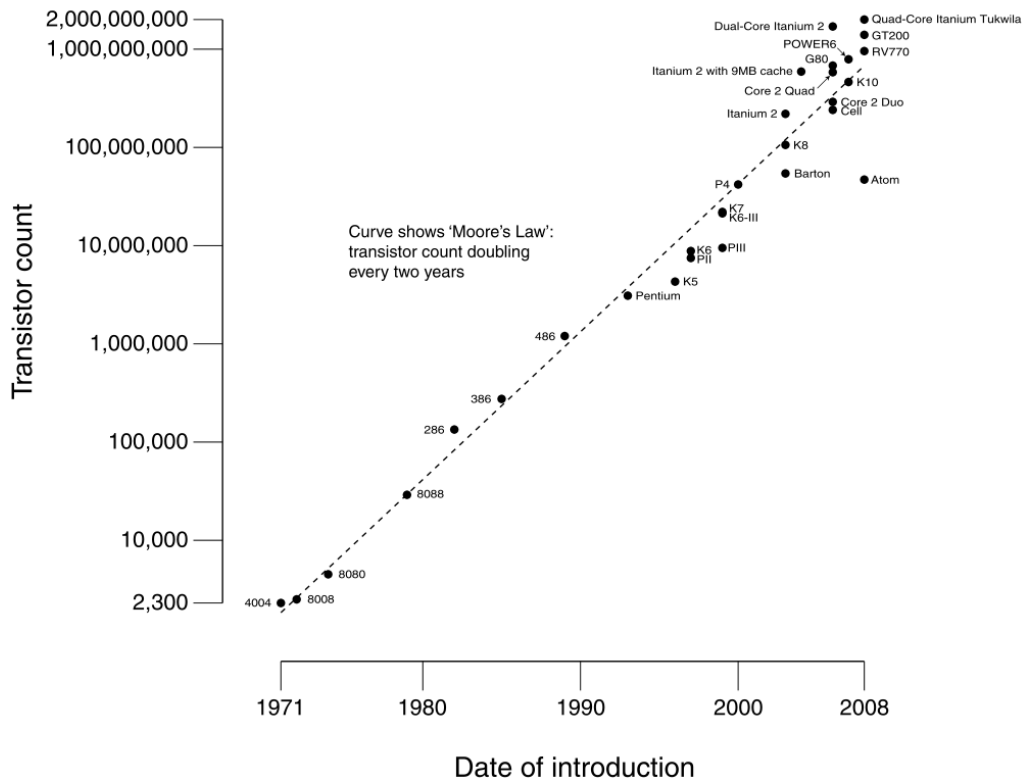## CPU Transistor Counts 1971-2008 & Moore's Law

Figure 2.19. Moore's Law - Transistor counts for integrated circuits plotted against their dates of introduction [WGS2008].

As described in the subsections above, the computation of machinery condition and comparison to reference values was initially considered but not implemented due to the lack of computational power. The proposed diagram for economic sailing (compare Fig. 2.15) was not implemented due to the mentioned limitations in computer and display technology. Even though the method of displaying the information about the current status of the vessel is different, the underlying concept of enabling the crew a decision of machinery operation based on the knowledge of the current status and the deviation from a predefined optimum at a glance can be considered comparable to ideas developed within the presented work.

These constraints were the main reasons that the promising results of *Ship of the Future* project for fuel and energy saving were not implemented in shipping and were almost lost in the following two decades. Besides some small initiatives and research projects like the European Commission co-funded research project *Flagship*, only limited focus was drawn on the efficiency of vessels in terms of fuel and energy consumption. This changed only when the concepts were being slowly reinvented in the aftermath of the all-time high of oil price in 2008 and the upcoming of stricter regulation through national and international regulatory bodies.

2.5 Objectives of this Work

Objective target of this work is the definition of a holistic approach for energy saving on board of vessels. The current state of energy flows and power consumption on board shall be evaluated with the focus on identification of saving potentials. Aim is the development of a methodology for manufacturer-independent monitoring of the energy flows on board and efficiency evaluation using simulation technology for representing the vessel's current energetic status. With a vessel life-time of 20 - 30 years, the approach shall cover not only new-builds, but also existing vessel with the inherent challenges of retrofitting equipment.

The current constrains from increasing fuel prices, tightening legislation for emissions and global discussions about reducing green house gas emission demand optimized vessel operation. Additionally, the introduction of slow steaming as a permanent state of vessel operation result in off-design operation of the vessel's auxiliary machinery.

In the research, two main barriers for improved operation of vessels identified are lack of information regarding energy efficiency on board and operational data ashore. These barriers are to be vanquished by the approach developed in the presented work. On one hand, transparent information of the crew regarding the current energetic status of the vessel allow quick revision of operational patterns for higher efficient use of machinery. Secondly, permanent data acquisition in high time resolution provides the data for shore-based analysis and optimization of operation and machinery.

In evaluation of single components under idealized conditions in laboratory, highly sophisticated physical models of components can be used. But these detailed physical simulation are too complex, time consuming and are based on often not available proprietary data of the components. Therefore the challenge is to establish a method based on available machinery data which is applicable on board with least elaborately accessible input data. This is to be obtained by simplification and abstraction to a system with required accuracy, which can be based on available data of the components and cope with inherent errors of measurements on existing vessels.

The simplification to stationary models inheres the potential for being incapable of describing the operational patterns of onboard machinery in required accuracy. This is to be evaluated based on longterm measurement data of vessel operation.

To reach the transparency in data provision on board, efficiency evaluation with the developed methodology shall be accomplished both shore-based in retrospect

based on the acquired operational data and in real time on board. The measurement, evaluation and storage enables to obtain operational profiles as well as operational patterns of machinery in general and of distinct situations and operational modes.

Current procedures for efficiency monitoring in shipping are often limited to the evaluation of the integrated value of consumed fuel over voyages from bunkering reports. These values can hardly reveal any changes in operation and impedes the possibility to look into operations for saving potentials, limiting the evaluations to baselining against a fleet, selective against machinery specifications or based on experience for certain conditions. The data for these evaluations are mainly collected manually from various sources throughout the vessel and implemented into forms on board, comprising a high susceptibility to errors.

The rarely applied onboard fuel consumption evaluation tools rely on the measurement of the fuel flow to the engines for consumption analysis. These accurate fuel-flow measuring systems providing instantaneous consumption data are costly and require additional maintenance and calibration. This applies especially if every engine is monitored individually, which is necessary for an in-depth analysis of the individual engine's operation. Due to the harsh operational environment close to the engines and the introduction of another machinery part into the critical fuel circulation, vessel operators are reluctant to install the fuel gauges of the measurement system.

The presented new methodology shall be functional without these high-tech fuel gauges. The fuel flow and current energy balances are instead to be obtained from energy system simulation, using less elaborate measurements commonly available in vessels, like engine power and rotational speed combined with ambient conditions, as input data.

As a basis for evaluation, the exergy flows in the energy system have to be analyzed, which enables to directly compare the various energy flows. The analysis, which operational pattern requires the lowest energetic input, can be conducted on the exergy basis without the influences of different fuel oil qualities and ambient conditions, and the available exergy in the different streams quantified.

These challenges are resolved with the methodology described in the following chapters. Simulation tools are presented and the developed models and components for simulation described, with their application and validation using operational data from longterm measurement data. Optimizations are proposed based on simulated machinery but actual operational data and the pilot installation of an onboard system is presented.

3 Energy Efficiency and Consumption Monitoring

This chapter presents the models developed for energy efficiency and consumption models. Starting with an introduction into the software used in this project for evaluation and simulation, the chapter leads to the underlying models and a description of their behavior.

3.1 Software

3.1.1 Modelica

Modelica is an object-oriented equation-based programming language for the modeling of complex systems using physical and mathematical models. *Modelica* is an open-source language developed since 1996 by the international *Modelica Association*, which defines and updates the language specification and maintains a standard library with components for all major applications in engineering.

Modelica is equation-based with acausal programming, which allows the implicit description of system behavior without pre-definition of data flow. This improves the versatility, as the models' input and output are not defined until the initiation of the simulation and models can be used for different directions of calculation. It incorporates multi-domain modeling for the integration of different domains. This means that electrical, mechanical, thermodynamic, hydraulic, biologic, and control application components can be modeled and connected in one overall model. *Modelica* is an object-oriented language for improved structuring of mathematical modeling, enabling definition of general classes and the inheritance of parts or their full behavior to sub-models and generics. Furthermore, the language incorporates constructs for developing and connecting components, which enables the graphical representation of the physical models for improved comprehension of complex models and the interconnection of their components. These main features and further explanations can be found in the *Principles of Object-Oriented Modeling and Simulation with Modelica 2.1* [FRI2004] by co-developer Fritzson.

Modelica is supported by commercial as well as by open-source simulation software, which provide the simulation environment with solver and graphical user interface. *Modelica* itself provides only the specification, standardization and the

tools for modeling in the library, but not the simulation environment. Examples for simulation environments are *SimulationX* by ITI as presented below, *Dymola* by Dassault Systems, *MathModelica* by MathCore and *OpenModelica* by Linköping University. The support of the language specifications depends on the integration in the simulation environment. That means that not all programs enable the use of the whole spectrum of multi-domain models and features, as can be found in the specification and the Standard Library.

The *Modelica Standard Library (MSL)* is a library containing components and models from all relevant domains of engineering. The MSL is an open source project and is provided as a free download from the *Modelica Association* webpage [MOD2012]. The components can be opened, adapted to own needs, improved or parts of its source code can be used for own components. Furthermore, integrated examples and related tutorials allow a quick start into the development of simulation models.

Models in *Modelica* can be built with differential-algebraic equations (DAE), i.e. they can be mathematically described by differential as well as algebraic equations, including partial differential equations. As the description is acausal, the solver of the simulation environment defines automatically input and output variables based on the given datasets, and no equations have to be manually solved for a variable or arranged in procedural order. Beside the continuous modeling, discrete events can be included in the simulation, e.g. a switching operation of machinery [WS2005].

Models can be exported for inclusion into hardware-in-the-loop tests, real time applications and other applications outside of the simulation environment. External source code can be implemented in *Modelica* models, which is supported in the language specification for scripts in programming languages C and Fortran. Code export and import, again, depend strongly on the capability of the simulation environment.

3.1.2   SimulationX

The software *SimulationX* from the German software company ITI GmbH [ITI2010] is a graphically-interactive programming environment for object-oriented modeling using ready-to-use proprietary libraries and *Modelica*-compatible programming with the ITI TypeDesigner. *SimulationX* version 3.x supports the *Modelica*-language and most parts of the *Modelica standard library* (MSL). Exceptions of the support are the Fluid library and therefore parts of the Thermal library and the Media library.

Simulation models can be exported into Simulink S-functions as well as a C-Code for implementation into Hardware-in-the-Loop and stand-alone applications.

Due to the restrictions in the use of the Fluid library, all fluid flows in the simulations are at the moment modeled as energy flows transferred as real values, with fluid properties being implemented as tabled data or equations in the component model.

The main window of the simulation environment is divided into different frames, compare Fig. 3.1. In the frame on the left side are the libraries, e.g. the *SimulationX* proprietary library, the MSL, and own libraries. Typically the largest frame is on the right side, which is the model frame. In this case the model frame shows a simulation model with various components and input tables. Below the model frame is the Model Explorer frame, with sub-frames for the parameters of either the simulation or single components, the simulation results, and a list of all components in the model, enabling a choice of components for editing and the model for changes in the model source code. On the bottom, the Output frame shows the output messages from file handling and simulation.

Components in the libraries are built and edited using the TypeDesigner. In the TypeDesigner, the user is guided step-by-step through the building process of a component. In the background, the TypeDesigner automatically transforms it into *Modelica*-like code, with the equations describing the behavior of the component being in *Modelica* code and e.g. the parameter definition being similar to *Modelica*.

3.1.3 Famos

Famos is a program for the analysis and the evaluation of measurement data made by IMC [IMC2010]. The program enables graphical presentation and editing functions of data in arbitrary length and resolution. Measurement data can be processed with sequences of functions, which can include all kinds of data processing for analysis like mathematical operations with different data channels, file handling, statistics and filtering. Data can be processed as time-depending data sets and XY-data sets of different channels, with optional triggering and event settings e.g. for dynamic compression, i.e. high resolution in times of high changes and low resolution for stationary periods.

Data import and export is very important for an evaluation program, but often not easy to do. *Famos* can import and export most data formats with a data assistant, which helps to define import filters. For many common data formats like Excel, binary, ASCII, comma separated, and Matlab data, the filters are already
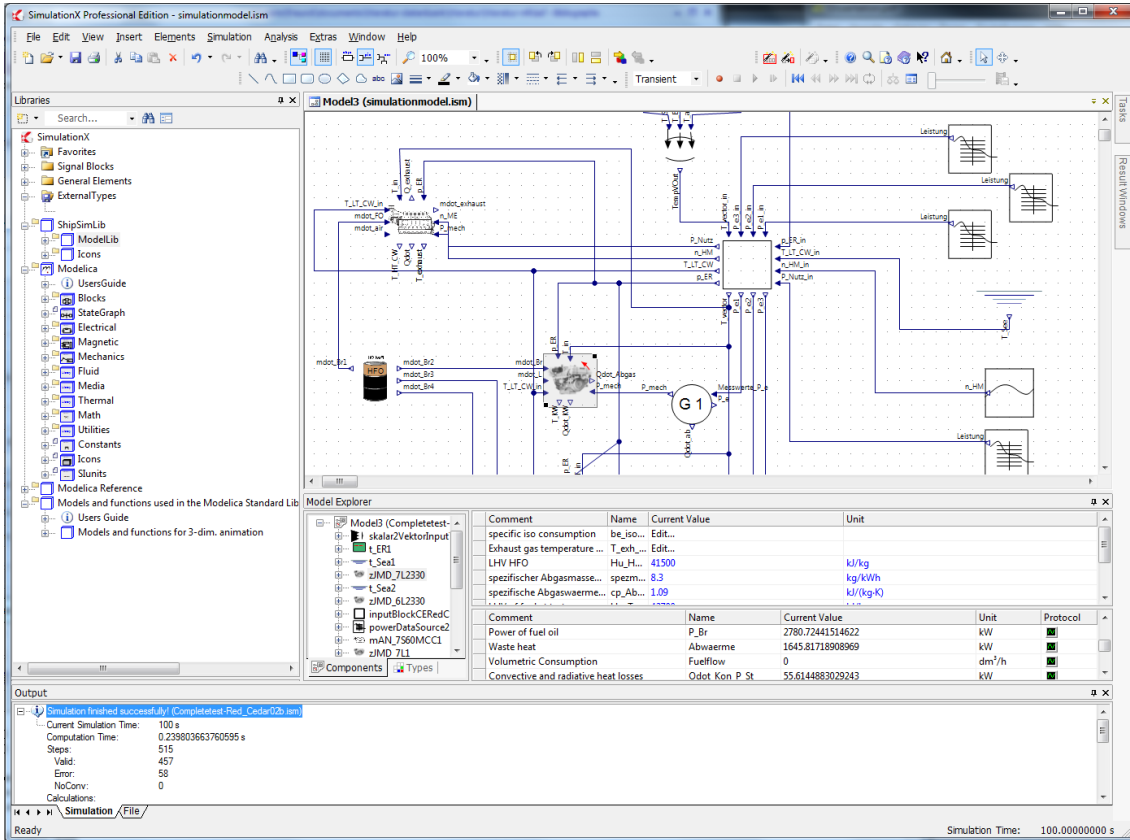
Figure 3.1. SimulationX main window.

included. In this work, especially the data exchange between *SimulationX* and *Famos* is done using these filters, reading data files including their physical units.

The binary format include time stamps, which allow the presentation of time lines with exact date and time. This is valuable for the long-term measurements onboard of vessels, as peculiar occurrences in data lines can be connected to recorded GPS positions and log book entries without special efforts.

3.2   Simulation Models for Energy Balancing

From the First Law of Thermodynamics it is known that no energy can be generated or destroyed, but only converted from one kind of energy into another [BK2009]. This conservation of energy in a system can be described with the energy balance equation

$$\frac{\mathrm{d}E}{\mathrm{d}t} \;=\; \sum \dot{Q} + \sum P + \sum \dot{m} \cdot \left(h + \frac{c^2}{2} + g \cdot z\right) \;, \tag{3.1}$$

being E the energy of the system under consideration, $\dot{Q}$ the heat flows, P the power, and $\dot{m}$ the mass flow over the system boundary, h, $c^2/2$ and $g \cdot z$ the enthalpy, kinetic and potential energy of the flowing mass, respectively. In case of a stationary system its energy is invariant over time, therefore

$$\frac{\mathrm{d}E}{\mathrm{d}t} = 0 \quad . \tag{3.2}$$

Equation (3.1) is adapted to the related problem by individual terms of energy and mass flows transported over the system boundary. Considering an undisplaceable system boundary, the power $P(t)$ transported over the boundary can be of mechanical shaft power P_s or electrical power P_{el}. Heat flows $\dot{Q}(t)$ are transported over the system boundary via conduction or convection, while additional heat may be conveyed by the mass flows' enthalpy. In case of a cooling circuit, the system boundary can be defined within the heat exchanger and around the cooling medium, allowing the transfer of heat flows. If the heat exchanger is included into the system, the heat flow is contained in the cooling medium's enthalpy as

$$\dot{Q} = \dot{m} \cdot (h_{in} - h_{out}) \quad . \tag{3.3}$$

The chemical energy content of a fuel includes the reaction enthalpy of its combustion $\Delta^{\mathrm{R}} h(T_0)$, which is defined as the enthalpy difference between the components of its stoichiometric combustion [BK2009] at the reference temperature T_0. This energy content of the fuel is known as the *Lower Heating Value (LHV)*,

$$LHV = -\Delta^{\mathrm{R}} h(T_0) \quad . \tag{3.4}$$

Using these equations of the first law of thermodynamics, the energy converting systems can be described as black box systems. Applied to an engine model, the balance results in

$$\begin{aligned} \dot{m}_{FO} \cdot \big(LHV + h_{FO}(T_{FO}) - h_{FO}(T_0)\big) + \dot{m}_{CA} \cdot \big(h_{CA}(T_{CA}) - h_{CA}(T_0)\big) \\ = P_{mech} + \dot{Q}_{WH} + \dot{m}_{EG} \cdot \big(h_{EG}(T_{EG}) - h_{EG}(T_0)\big) \quad , \end{aligned} \tag{3.5}$$

or graphically as presented in Fig. 3.2. Here, the generalized terms from Eq. (3.1) are substituted by the actual balances of fuel oil mass flow $\dot{m}_{FO}$ with its lower heating value LHV and its enthalpy $h_{FO}(T_{FO})$, the mass flow of combustion air $\dot{m}_{CA}$ with its enthalpy $h_{CA}(T_{CA})$, the mechanical power P_{mech}, the waste heat $\dot{Q}_{WH}$ and the mass flow of the exhaust gas $\dot{m}_{EG}$ with its enthalpy $h_{EG}(T_{EG})$. The enthalpies of the in- and outflowing masses are referenced to a common temperature T_0, which is the reference temperature of the fuel's lower heating value, with the related enthalpies

$h_{FO}(T_0)$, $h_{CA}(T_0)$ and $h_{EG}(T_0)$. If a waste heat boiler is applied, the equation can be extended to include the recovered waste heat $\dot{Q}_{rec}$,

$$\dot{m}_{FO} \cdot \big(LHV + h_{FO}(T_{FO}) - h_{FO}(T_0)\big) + \dot{m}_{CA} \cdot \big(h_{CA}(T_{CA}) - h_{CA}(T_0)\big)$$
$$= P_{mech} + \dot{Q}_{WH} + \dot{m}_{EG} \cdot \big(h_{EG}(T_{EG}) - h_{EG}(T_0)\big) + \dot{Q}_{rec} \quad . \tag{3.6}$$

The lower heating value LHV of the fuel is defined at a reference temperature, which is usually 25 °C [BK2009] [DIN2000]. At constant pressure, the fuels enthalpy $h_{FO}(T) - h_{FO}(T_0)$ can then be determined based on its temperature as

$$h_{FO}(T_{FO}) - h_{FO}(T_0) = \int_{T_0}^{T_{FO}} c_p(T)\mathrm{dT} \quad , \tag{3.7}$$

with the specific isobaric heat capacity $c_p(T)$, the reference temperature T_0 and the fuel's temperature T_{FO}. Idealized as ideal gases, the enthalpy of combustion air and exhaust gas can be determined as

$$h_{CA}(T_{CA}) - h_{CA}(T_0) = \int_{T_0}^{T_{CA}} c_p(T)\mathrm{dT} \quad , \tag{3.8}$$

$$h_{EG}(T_{EG}) - h_{EG}(T_0) = \int_{T_0}^{T_{EG}} c_p(T)\mathrm{dT} \quad . \tag{3.9}$$
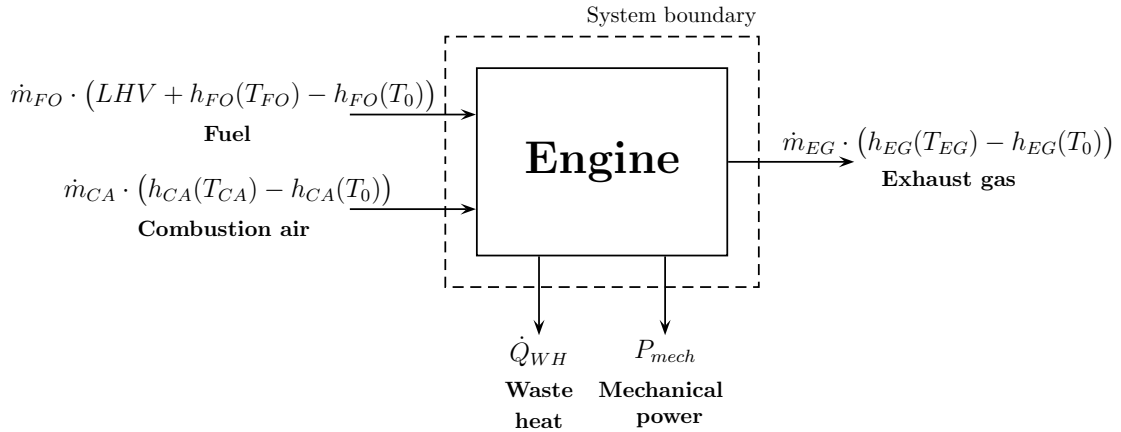
Figure 3.2. Black box model of engine with inputs and outputs.

The First Law of Thermodynamics balances the energy flows of the process, but does not determine the feasibility nor the direction of energy conversion within the

process. This is provided by the Second Law of Thermodynamics, which limits the conversion between different kinds of energy to processes, in which the entropy is increasing or at least constant in case of a reversible process,

$$\frac{\mathrm{d}S}{\mathrm{d}t} \;=\; \sum \dot{S}_Q + \sum \dot{S}_m + \dot{S}_{irr} \quad, \tag{3.10}$$

with the entropy S of the heat flow $\dot{S}_Q$, of the mass flow $\dot{S}_m$ and of the irreversible entropy

$$\dot{S}_{irr} \geq 0 \quad . \tag{3.11}$$

Therefore it is impossible to destroy entropy in a process, but it can be discharged with heat and mass flows.

The lossless conversion of kinetic and potential energy into work and vice versa is possible in case of a reversible, ideal process at $\dot{S}_{irr} = 0$. Mechanical and electrical energy can theoretically be completely converted into each other without losses, if ideal generators and electric motors are used. But it is not possible in a stationary process to convert thermal energy completely into mechanical energy [BK2009], which would be a perpetual motion machine of the second kind. This demonstrates that the convertibility of energy strongly depends on its kind and state, which requires an additional classification of the energy.

This classification of energy is obtained by introduction of the unrestricted convertible energies, which are free of entropy, and the partly convertible energies. Electrical and mechanical energy belong to the unconfined convertible energies, while thermal energy, enthalpy and inner energy of a thermodynamic system are not completely convertible into another kind of energy. Given a specified environment, unrestricted convertible energies are combined in the term *exergy*, while the restricted convertible energies are composed of the convertible exergy and inconvertible *anergy* [BK2009]. Generalized this applies for every kind of energy

$$energy \;=\; exergy + anergy \quad .$$

For the determination of energy flows and available energy for utilization in downstream processes, the availability of exergy in the different machinery can be evaluated. For thermal energy flows, the available exergy flow is depending on the ambient conditions and defined with the Carnot efficiency η_c

$$\eta_c \;=\; \left(1 - \frac{T_a}{T}\right) \quad, \tag{3.12}$$

as

$$\dot{E}_Q \;\;=\;\; \eta_c \cdot \dot{Q} \tag{3.13}$$

where $\dot{E}_Q$ denotes the exergy flow of the heat flow under consideration, T_a the ambient temperature, and T the mean thermodynamic process temperature [BK2009]. Equation (3.13) shows that it is important for waste heat recovery to tap the highest available temperature level, which leads the way to research e.g. for high-temperature cooling of diesel engines for improved waste heat recovery, compare [POS1994].

Based on the available exergy the maximum potential for recoverable energy of a waste heat flow from machinery can be determined. The energy balance of an engine presented in Eq. (3.5) can then be written as an exergy balance of the type

$$\dot{E}_{FO} + \dot{E}_{CA} \;\;=\;\; P_{mech} + \dot{E}_{WH} + \dot{E}_{EG} + \dot{E}_{loss} \;\; , \tag{3.14}$$

being $\dot{E}_{WH}$ the exergy of waste heat, $\dot{E}_{EG}$ exergy of the exhaust gas, and $\dot{E}_{loss}$ the losses of exergy in the energy conversion, resulting in anergy, defined by using the entropy production rate $\dot{S}_{irr}$

$$\dot{E}_{loss} \;\;=\;\; T_a \cdot \dot{S}_{irr} \geq 0 \;\; . \tag{3.15}$$

As the charge air is provided at ambient temperature and pressure, it contains no exergy beside its chemical exergy for combustion, which is included in the fuel's exergy, and can therefore be omitted.

Beside the exergy of power and heat flows, for balancing of an engine the exergy of the fuel oil as the input is required. A fuel in thermal and mechanical equilibrium with its environment contains an additional form of exergy, the chemical exergy. The specific exergy of a fuel e_F is composed of the upper heating value UHV of the fuel, the specific reaction entropy $\Delta^R s$ and the exergy difference between the oxidized products and the required oxygen Δe [BAE1987],

$$e_F(T_a, p_a) = UHV(T_a, p_a) + T_a \cdot \Delta^R s(T_a, p_a) + \Delta e(T_a, p_a) \;\; . \tag{3.16}$$

The exergy for chemically defined fuels can be determined using Eq. (3.16) depending on the specified environment. For chemically not defined fuels, e.g. fuel oils with their varying composition, *Baehr* [BAE1987] describes a statistical approach based on a linear dependency of exergy and lower heating value. For a defined model of the environment, the exergy of fuel oils can then be determined as [BK2009]

$$e_F = 1.075 \cdot LHV - 1.150 \;\; , \tag{3.17}$$

for the mass specific lower heating value LHV in MJ/kg and with an uncertainty of about 1% in the range of 38 MJ/kg $< LHV <$ 44 MJ/kg.

For a thermodynamic optimization of the process therefore not only the heat flows but also the related temperature levels have to be evaluated, with the aim to minimize the exergy loss in each conversion. In combination with operational data or predefined operational profiles, the simulation models described in the following sections enable the evaluation of exergy consumption and potentials for improvement. The consumed exergy for a certain process to be achieved can be compared for different machinery installations and operating modes.

The distribution of energy flows of an energy converting process can be graphically presented in Sankey diagrams. In Fig. 3.3, the energy flow (top) and the corresponding exergy flow (bottom) of a two-stroke engine at ISO conditions (defining the ambient conditions with air temperature of 298 K and air pressure of 1000 mbar [ISO2002b]) are presented based on design data [MAN2011].

With an efficiency of 49.9% of the conversion of fuel oil energy to mechanical power, the engine operates close to its best-point. The waste heat is dominated by the exhaust gas losses of 22.7% and the scavenge air heat flow of 15.6%, while the jacket cooling heat flow and lube oil cooling heat flow are losses with 7.0% and 4.1%, respectively. The convective and radiative losses of the engine account for about 0.7%.

The distribution of exergy flows show a slightly lower efficiency of exergy input to mechanical power output, as the fuel oil's exergy is higher than the fuel oil's lower heating value, compare Eq. (3.17). The irreversible process of combustion, as the main contributor, results in an exergy loss or anergy generation of 40.2%. With its relatively high temperature, the exhaust gas flow contains 9.6% of the exergy, revealing its potential for waste heat recovery.

The cooling water show a prominent content of 26.7% of the fuel's energy. Their exergy content is significantly lower, ruled by the temperature difference between the heat flows and the present ambient conditions. The jacket cooling water with its high temperature of about 363 K and the high mass flow of scavenge air cooling water at about 313 K contain mere 1.3% and 1.0% of the exergy input, respectively. With an assumed surface temperature of 323 K, convective and radiative heat flows contain less than 0.1% of the exergy input.

Operation of machinery with frequent high load changes require transient models for consideration of accelerations and change in momentums, heating up, and cooling
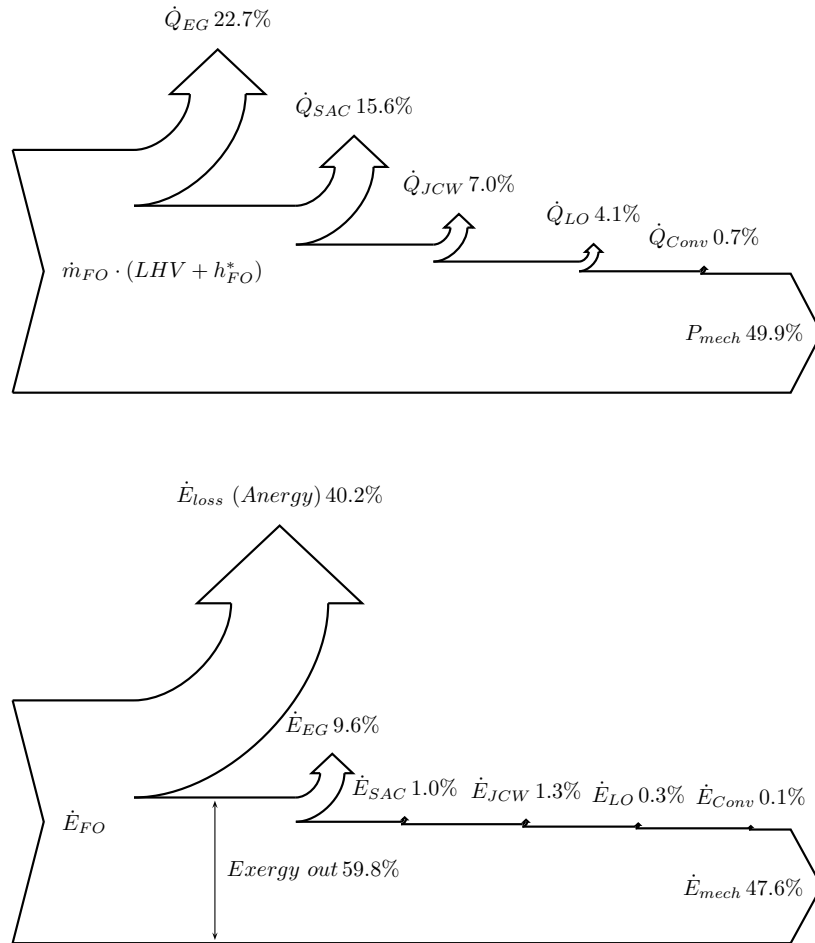
Figure 3.3. Sankey diagrams of a two-stroke main engine at ISO conditions, schemes of energy flow (top) and exergy flow (bottom) based on design data [MAN2011].

down of components. This can be modeled using detailed component specifications, e.g. finite element methods (FEM) for heat distribution in a component and consideration of related heat capacities in the geometry. The inclusion of these effects would undermine the aim to develop models for a system with acceptable accuracy but without these often proprietary manufacturer's knowledge of components and extended simulation time. To avoide the above mentioned problems, a stationary approach is chosen. Stationary operation is considered a valid simplification, as oceangoing freight vessels are operating at comparatively steady loads with only comparatively small time periods for acceleration and deceleration in maneuvering, compare Section 3.4. Moreover, models are simplified to account for all significant

losses, which are defined by the efficiencies of the energy conversions. In case of the engine models, the losses in energy conversion are partitioned into the waste heat flows of high and low temperature cooling water, exhaust gas and convection and radiation at the engine's surface. This incorporates all losses according to the test bed and manufacturers data, as described in the following sections.

In the following sections, the simulation models used in the evaluations are explained.

3.2.1 Engine Simulation Models

3.2.1.1 Main Engine Model - Characteristic Map Simulation

The modeling of the components is based on their characteristic data like performance curves, which are usually available as data sets from test bed reports and project guides. For adaptation to the operating conditions and the difference between ideal values and real operation correction terms are implemented. For main engines, differences between test bed installation and onboard installations can be found primarily in the existence of a thrust bearing, higher exhaust gas back pressure due to funnel installations like exhaust gas boilers and sub-optimal gas guidance. Also the difference between the brand new engine with optimum adjusted parameters and the used engine on board, potentially lacking some fine tuning and with already worn parts, plays a role.

The characteristics are obtained from manufacturer's data sheets, project guides, and test bed results, depending on the availability of this data. For the engines, the best source are the actual test bed data of that specific engine, as especially the large two-stroke engines are often slightly different in their tunings, resulting in different operational behavior and therefore in their consumption. Downside of this is the sometimes limited number of measurement points. Engines are adapted to the proposed resistance curve of the vessel, which is the theoretical load curve of a propeller. This load curve is measured at least at 25% maximum continuous rating (MCR), 50% MCR, 75% MCR and 100% MCR at the respective rotational speed of the engine on the test rig. Depending on test cycle and owner's or yard's specification, additional measurements are taken. These are often 10% MCR for constant speed engines, 85% MCR for best-point operation and 110% MCR as an overload test.

In case of a vessel with controllable pitch (CP) propeller and constant rotational shaft speed for use of a shaft generator, the measurements are taken at the dimensioned constant shaft speed, otherwise the shaft speed is following at CP propellers the combinator curve or at fixed pitch (FP) propellers the engine load curve. The cube dependency of the shaft power to the shaft speed is defined by the theoretical resistance curve of the vessel and the resulting propeller curve.

The collected data allow for the calculation of the consumption at the engine load curve, but does not yet represent the characteristic map of the engine with a variation of power demand at a given shaft speed. Vessels equipped with FP propeller and CP propellers in combinator mode are following the engine load curve

with deviations caused by changes in ship resistance. This depicts the demand for a characteristic map at least around the engine load curve, allowing the simulation model to interpolate around it. As there are typically no complete characteristic maps of the engines available in public, the development of the characteristic map in the vicinity of the engine load curve is done based on the known characteristic data from test bed and manufacturer's performance reports. The characteristic curve is obtained by interpolation between the single data points and then extrapolated to a characteristic map based on the differences between the adjacent points and the theoretical behavior of the engine. While the extrapolated points next to the original points from test rig are used for interpolation in the simulation, the points further aside of the curve exist only for smoothing of the inter- or extrapolation around the original point. The requirements for these values away from operational points are therefore limited to be in the right order of magnitude.

In Fig. 3.4, main engine power is plotted against rotational speed as grey dots, which are actual operational data from a measurement campaign of about 6 months, compare Section 3.4. The power is displayed as measured and not corrected to ISO conditions. Additionally, the engine load curve is plotted as a third order polynomial, being the upper blue curve, and the same load curve but excluding a sea margin of 15% as the lower pink curve. The sea margin is added to the engine load curve as a safety margin for extra resistance caused by weather conditions [MAN2006]. The two curves clearly mark the approximate operational range of the engine in the more stationary, higher power range, even though the gray data points are no testing data from manufacturer or yard but acquired on board during normal commercial shipping.

Unlike in engine applications applying changeable gears, e.g. in automobiles, or with constant speed, e.g. for generator engines, the fixed connection to the fixed pitch propeller dictates an operation within a narrow band, approximately following a third-order polynomial of the rotational speed. The layout field and load range of the engine is presented in Fig. 3.5 in conjunction with the same operational data from onboard measurement of about 6 months as displayed in Fig. 3.4. The layout field of the engine, in which the contract MCR can be positioned individually, is framed by the points R1 to R4. Herein, point R1 defines the design point of 100% MCR at 100% rpm. The line connecting R1 to R3 represents constant maximum mean effective pressure and torque. The green lines 1, 3 and 5 enframe the field, in which the engine can be continuously operated. The green line 5 is the admissible torque limit, which is limited by lack of scavenge air. Line 1 defines the torque limit between
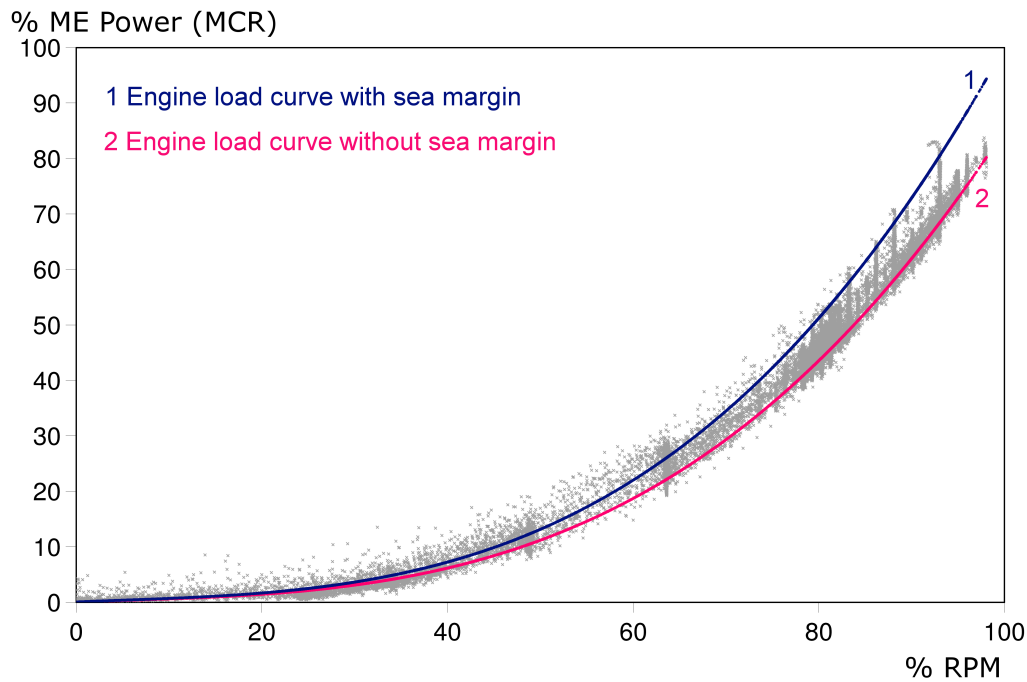
Figure 3.4. Measured main engine power vs. rotational speed and engine load curves with (upper curve, blue) and without (lower curve, pink) sea margin.

95% and 100% MCR and rpm, line 3 defines the engine's speed limit. The red lines are overload limits only to be reached in transient operation. Here, line 6 defines the maximium torque limit in transient conditions, line 2 the overload limit and line 4 the overspeed limit only allowed at by manufacturers accompanied sea trials.

The measured operational data of the vessel lie very well within these limits and follow the narrow band between the load curves induced by the propeller. This depicts that the chosen approach for developing the characteristic map can be considered valid, as the engine operates close to the load curve with the available test bed data and the extrapolation of the characteristic curve into a characteristic map is primarily required for smoothing of the interpolation.

In Fig. 3.6, the characteristic map of the ISO corrected specific fuel oil consumption (SFOC) *be* in g/kWh is plotted as background. The operational profile of the engine takes exclusively place within and close to the narrow band between the engine load curves described above. The actual operational data are therefore close to the test bed data on the theoretical engine load curve, displayed in Fig. 3.6 as red dots.
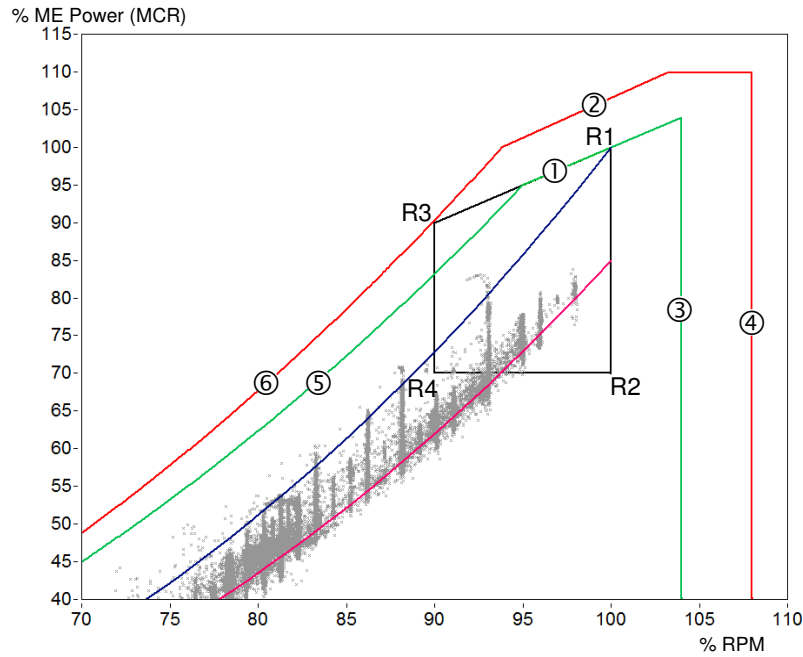
Figure 3.5. Layout field (black enframed) and load range of the engine in conjunction with measured main engine power vs. rotational speed (gray dots) and engine load curves with (blue) and without (pink) sea margin.

With the shaft power P_{mech} and the rotational speed n as measured input values, the theoretical consumption under ISO conditions can then be determined from an interpolation in the diagram and the mass flow of fuel oil $\dot{m}_{FO}$ calculated as

$$\dot{m}_{FO} = be(P_{mech}, n) \cdot P \quad , \tag{3.18}$$

with the correction to the ambient conditions as presented in Section 3.2.1.2 below.

The first law of thermodynamics demands for a common basic temperature for the enthalpy of all temperature related energy flows, which are in these case the fuel flow and the waste heat flows of exhaust gas and cooling water. This base temperature is defined as the sea water temperature, as it is the lowest available sink temperature. The energy content of the fuel oil is typically referenced to 25 °C, but its temperature dependency is considered negligible, as the variations of enthalpy within the temperature range of 0 °C to 50 °C are small according to Baehr and Kabelac [BK2009], thus they are not further regarded for in other publications, e.g. in the evaluations of Postel [POS1994].
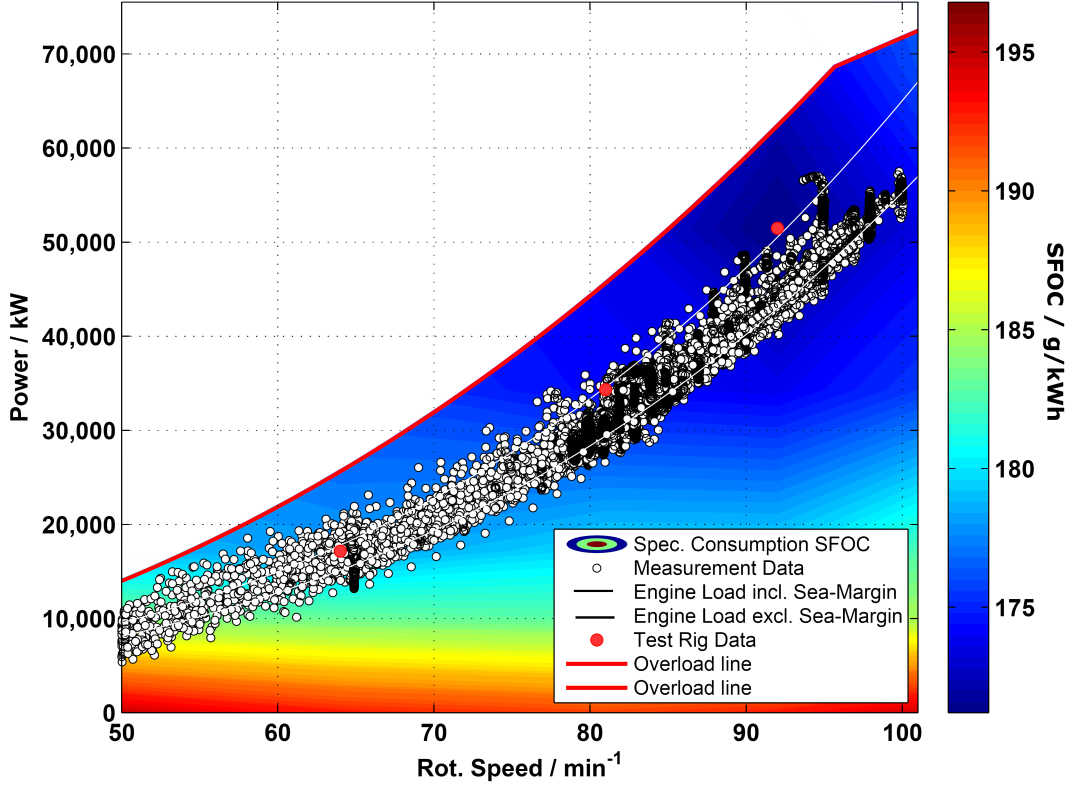
Figure 3.6. Characteristic map of SFOC in g/kWh with measured main engine power vs. rotational speed, engine load curves with (upper curve) and without (lower curve) sea margin, and engine test bed data (red dots).

The engine power is modeled as the conversion of chemical energy of the fuel into mechanical energy and heat energy,

$$\dot{m}_{FO} \cdot LHV + \dot{m}_{CA} \cdot h_{CA} \quad = \quad P_{mech} + \dot{Q}_{WH} + \dot{m}_{EG} \cdot h_{EG} \tag{3.19}$$

where $\dot{m}_{FO} \cdot LHV$ defines the chemical power of fuel oil, $\dot{m}_{CA}$ the mass flow of combustion air with its enthalpy h_{CA}, P_{mech} the produced mechanical power, $\dot{m}_{EG} \cdot h_{EG}$ the energy content of the exhaust gas, and $\dot{Q}_{WH}$ the heat flow of the engine. Efficiency of the engine producing mechanical energy can be defined as the ratio of produced mechanical energy to consumed fuel energy:

$$\eta \quad = \quad \frac{P_{mech}}{\dot{m}_{FO} \cdot LHV} \ . \tag{3.20}$$

Typically for engine specification and test rig data is that the efficiency is only indirectly given by the specific consumption *be* in g/kWh. If the specific consumption

is known, engine efficiency is described as

$$\eta \;=\; \frac{1}{LHV \cdot be} \tag{3.21}$$

with the lower heating value LHV of the consumed fuel oil.

The specific fuel oil consumption measured at the test bed prior to consigning of the engine can be considered the optimum consumption of the vessel. Under operation in the vessel, these values are most certainly not reached again. This can be attributed to the wear of parts and other factors that impair the engine's performance, and to differences between the test bed installation and the installation in the vessel, compare above.

To incorporate these factors on the consumption as well as deviations in measurement, an artifice is introduced into the calculation, which changes the overall efficiency of the engine (Eq. (3.21)) with the correction term η_k to

$$\eta \;=\; \frac{1}{LHV \cdot be} + \eta_k \;\; . \tag{3.22}$$

It is expected that the difference between nominal consumption and actual consumption is smallest around the optimum operation point, where the engine runs at design point and the highest efficiency is reached. As a measure to implement this, the corrective term is added to the theoretical efficiency instead of percentage-wise constant shifting of the efficiency curve through a multiplicative factor. Typical values from the tested two-stroke engines were in the range of -0.01 to -0.03, meaning a decrease of the efficiency by one to three percentage points.

This correction term has to be determined iteratively in the first phase of an onboard evaluation based on the difference between calculated and reported consumption. In further periods, this term has only to be changed if changes in the machinery or in the acquisition of measurement data had occurred, e.g. further impair of the engine through operational wear or change of offset in power measurement. While the correction term is defined for the first evaluations as constant value, it can be substituted by a function, e.g. $\eta_k = f(P_{ME})$ or $\eta_k = f(n_{ME})$ if further analyses reveal an improvement through a certain definition of the correctional term.

With the specific consumption be as a function of P_{mech} and n_{ME} in characteristic diagrams, engine efficiency can therefore be modeled as a function of

$$\eta \;=\; f(P_{mech}, n_{ME}, T_a, p_a, T_{CW_{in}}, \eta_k, LHV) \;\; . \tag{3.23}$$

As the focus of the presented model is set on the energy conversion of fuel into mechanical power, the exhaust gas energy, waste heat energy in cooling water and

radiation, and the combustion air are integrated at first into the term $P_{EG\ WH\ CA}$. This simplifies Eq. (3.6) to

$$\dot{m}_{FO} \cdot (LHV + h_{FO}^*) \quad = \quad P_{mech} + P_{EG\ WH\ CA} + \dot{Q}_{rec} \quad . \tag{3.24}$$

For the determination of the different heat flows we regard here the enthalpy of the exhaust gas as heat, which is a thermodynamically incorrect simplification. Energy of the fuel that is not converted into mechanical energy is considered energy of waste heat and exhaust gas enthalpy combined in the term $P_{EG\ WH\ CA}$, which has to be removed from the engine. $P_{EG\ WH\ CA}$ is here defined as

$$P_{EG\ WH\ CA} \quad = \quad \dot{Q}_{EG_{SW}} + \dot{Q}_{JCW} + \dot{Q}_{SAC} + \dot{Q}_{OC} + \dot{Q}_{conv} \ , \tag{3.25}$$

which is the sum of the heat flows of exhaust gas relative to sea-water temperature $\dot{Q}_{EG_{SW}}$, engine cooling water $\dot{Q}_{JCW}$, scavenge air cooler $\dot{Q}_{SAC}$, oil cooler $\dot{Q}_{OC}$, and convective losses of the engine $\dot{Q}_{conv}$. In the present evaluation, these heat flows can not directly be measured. Therefore manufacturers´ data are used for quantification, which are available from project guides of the engines (e.g. [MAN2009]) and the test rig reports. The individual heat flows are separated with the fractioning being implemented as interpolated curves,

$$\dot{Q}_{EG_{SW}} \quad = \quad f(\dot{Q}_{WH}, P_{mech}) \tag{3.26}$$

and

$$\begin{aligned} \dot{Q}_{JCW} = f(\dot{Q}_{WH}, P_{mech}) \ , &\qquad \dot{Q}_{SAC} = f(\dot{Q}_{WH}, P_{mech}) \ , \\ \dot{Q}_{OC} = f(\dot{Q}_{WH}, P_{mech}) \ , &\qquad \dot{Q}_{conv} = const \quad . \end{aligned} \tag{3.27}$$

An exemplary distribution of waste heat depending on engine load for a two-stroke engine is presented in Fig. 3.7 [MAN2011].

The available waste heat from exhaust gas in the operation is limited by a minimum temperature after boiler for prevention of low temperature corrosion, which results mainly from condensation of sulfur oxides to sulfuric acid. This temperature is implemented in the model as a parameter, with the predefined value of 160 °C as the minimum temperature described in [BRO1988] and [RUL2005]. For further analysis of the available waste heat, the additional heat flows corresponding to this minimum temperature $\dot{Q}_{EG_{Tmin}}$ and to the ambient temperature $\dot{Q}_{EG_a}$ are available as model outputs.

The required amount of combustion air is calculated from the exhaust gas mass flow $\dot{m}_{EG}$ and fuel oil mass flow $\dot{m}_{FO}$

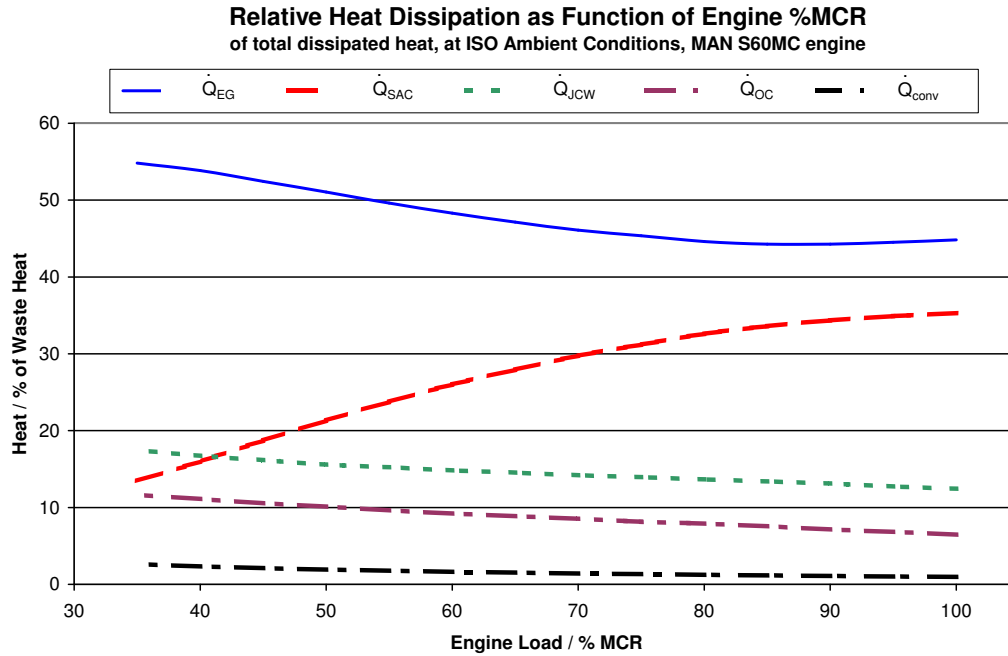$$\dot{m}_{CA} \quad = \quad \dot{m}_{EG} - \dot{m}_{FO} \ , \tag{3.28}$$

Figure 3.7. Distribution of waste heat depending on engine load [MAN2011].

being $\dot{m}_{EG} = f(P)$ a function of the engine load based on manufacturer data and $\dot{m}_{FO} = f(P, n)$ as described above by Eq. (3.18) and Eq. (3.20). The mass flow of combustion air is required for a complete balance of exergy flows and can be an input into the evaluation of the required fan power for engine room ventilation.

The graphical representation of the component within the simulation environment is presented in Fig. 3.8. The connectors for input and output data streams are displayed.

The exergies of the heat flows are available through combination with their respective temperature levels. The temperatures are available from measurements or from manufacturers data and test bed reports. In case of the cooling water, the engine outlet temperatures are bypass-controlled by engine automation system, with only minor variations over engine load.

The principle schematic of the calculation is presented as work flow scheme in Fig. 3.9.
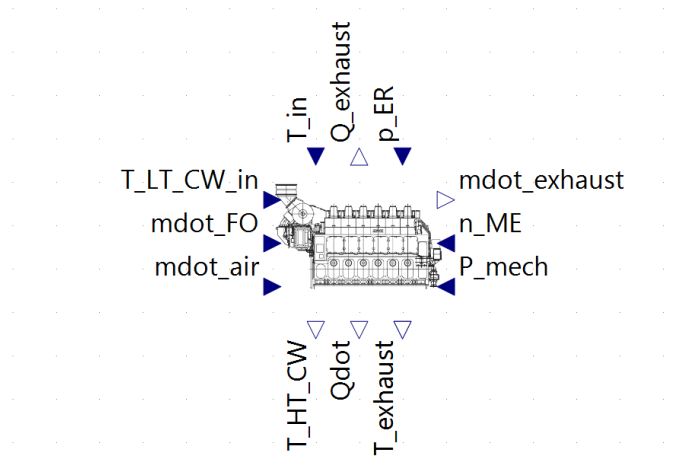
Figure 3.8. Main engine component, showing connectors for input and output data streams.

3.2.1.2 ISO Corrections for Operational Conditions

Ambient conditions are having an influence on the performance of the engine. The provision of true consistent conditions in operation is not possible, which makes a direct comparison of the produced power and consumed fuel almost impossible. For enabling this comparison of engine performances these influences have to be accounted for. In the engine models this is considered, as the conditions are continuously corrected according to ISO 3046-1:2002. In every time step, the performance and consumption are accordingly adapted to the changing ambient conditions.

The ISO standard ISO 3046-1:2002 "Reciprocating internal combustion engines - Performance - Part 1: Declarations of power, fuel and lubricating oil consumptions, and test methods - Additional requirements for engines for general use" [ISO2002c] defines reference conditions for the operation of reciprocal internal combustion engines and the influence of deviations on the engines performance, in case of the present evaluation especially the deviation in consumption depending on the ambient conditions. Reference conditions are defined as

Ambient air pressure:	1000 mbar
Ambient air temperature:	298 K
Relative air humidity:	30%
Charge air coolant temperature:	298 K
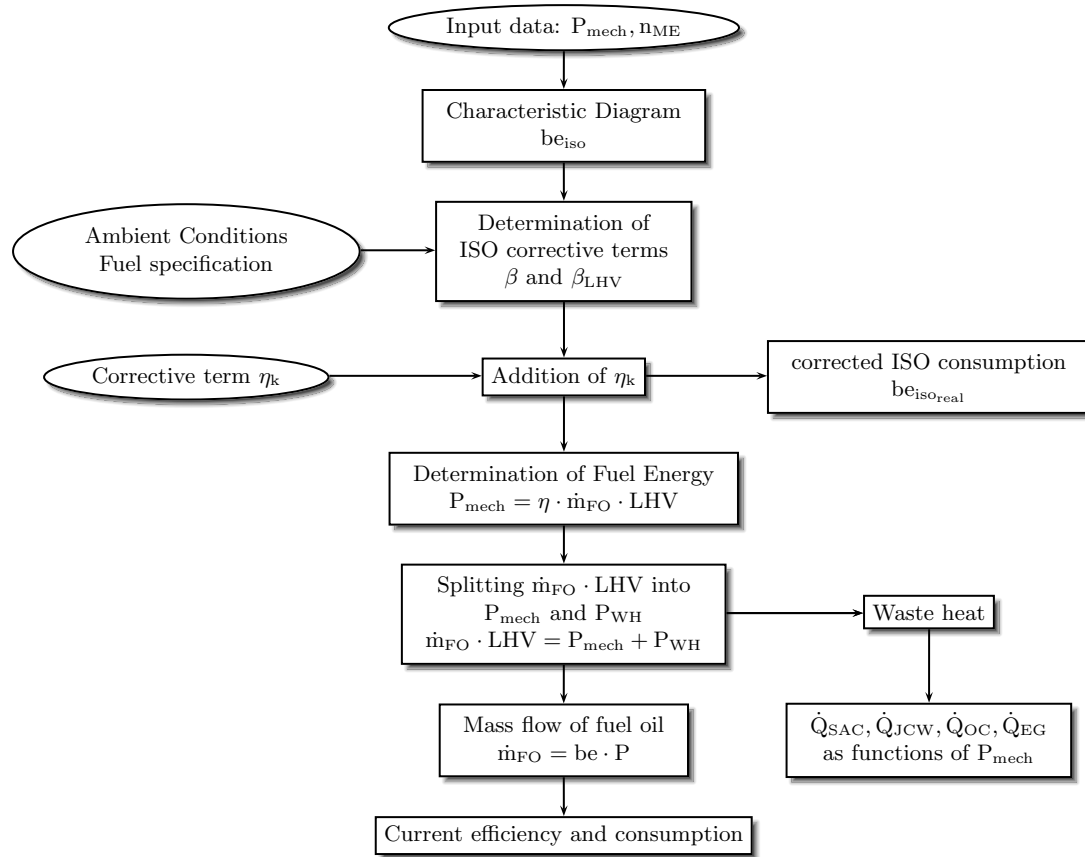
Figure 3.9. Schematic work flow of the ME simulation model.

but can be adjusted by the engine manufacturers or regulatory body and classification society bodies according to their requirements. For the power adjustment, the *International Association of Classification Societies (IACS)* requires for marine diesel engines unrestricted service at tropical conditions

Ambient air pressure:	1000 mbar
Ambient air temperature:	318 K
Relative air humidity:	60%
Sea or raw water temperature (charge air coolant inlet):	305 K

ISO standard 3046-1 defines for each engine type corresponding correction methods. For turbocharged engines with charge air coolers, relative air humidity is not considered. The correction terms for low speed two stroke engines are not defined by

the standard but have to be specified by engine manufacturers for their individual engine design.

The specific consumption be is corrected to the ambient conditions by introduction of a dimensionless correction factor,

$$be \;=\; \beta \cdot be_{iso} \tag{3.29}$$

being be_{iso} the specific consumption at reference conditions and correction factor β defined by

$$\beta \;=\; \frac{k}{\alpha} \tag{3.30}$$

where

$$k \;=\; \left(\frac{p_a}{p_{a,0}}\right)^{m} \cdot \left(\frac{T_{a,0}}{T_a}\right)^{n} \cdot \left(\frac{T_{C,0}}{T_C}\right)^{s} \tag{3.31}$$

and

$$\alpha = k - 0.7 \cdot (1 - k) \cdot \left(\frac{1}{\eta_{mech}} - 1\right) \tag{3.32}$$

being η_{mech} the mechanical efficiency of the engine. The exponents m, n, and s are defined in the ISO standard for each engine type. For turbo-charged charge air cooled four-stroke compression ignition engines, being the standard medium speed four-stroke diesel engines used for maritime propulsion, the exponents are $m = 0.7$, $n = 1.2$, and $s = 1$. Factor β can then be calculated or obtained from ISO tables as a function of k and η_m.

For low speed two-stroke engines this method is not applicable, as the manufacturers define distinct corrections for their engines based on their individual design. Additional efficiency influencing factors like scavenge air temperature and cooling water temperature are introduced for correction, in cases even varying with engine load. The correction methods and the related factors for correction are described in the engine's project guide. For MAN 2-stroke engines [MAN2009], the change in specific fuel oil consumption (SFOC) is given as a table like the one presented in Tab. 3.1 .

Transformed into an equation by correlation, the correction term to ISO condition β can be written as

$$\begin{aligned} \beta = \Big(& (25\ ^\circ\mathrm{C} - T_{LT\ CW\ in}) * 0.0006 + (25\ ^\circ\mathrm{C} - T_{ER}) * 0.0002 \\ & + (p_{ER} - 1000\ \mathrm{mbar}) * 0.00002 + (1 - \frac{LHV}{LHV_{ISO}})\Big) \, . \end{aligned} \tag{3.33}$$

Table 3.1. Changes of SFOC for correction ISO conditions [MAN2009].

Paramter	Condition Change	SFOC change
Scav.air coolant temperature	per 10 °C rise	+0.60%
Blower inlet temperature	per 10 °C rise	+0.20%
Blower inlet pressure	per 10 mbar rise	-0.02%
Fuel oil lower calorific value	rise 1% (42700 kJ/kg)	-1.00%

This equation differs strongly depending on the manufacturer and the engine type. A higher consumption of +5% in operation is permitted for the declared specific fuel oil consumption of an engine at a declared power, leading to a common underdeclaration of close to 5% in manufacturers brochures.

3.2.1.3   Main Engine Model - Diesel Cycle Simulation

A different approach for the simulation of engine behavior is taken by the development of an engine cycle process simulation of the two-stroke engine of the test vessel (compare Section 3.4.2.1). Cycle process simulation enables one to determine energy conversion, mechanical power generation, fuel oil consumption and heat flows, without relying on manufacturers performance data from project guides. A disadvantage is the required accuracy of engine and component specifications if a high accuracy is needed, which is hardly obtainable from manufacturers for secrecy reasons.

Depending on the available data, computing power and required accuracy, different approaches can be taken. The thermodynamic, fluid dynamic and chemical processes within an engine combustion chamber are highly complex, impeding a complete calculation of gas exchange, combustion, and heat transfer with purely physical models. Instead, some processes are described using empirical models for simplification. Depending on required accuracy, available process models and computing power for solving, approaches of different complexity can be taken, with the aim to achieve the required accuracy with the least complex model. Models can be categorized by the dimensionality of the system of equations. Zero dimensional models are independent of the position, with the system varying only over time.

An example here is the *Perfect Engine* according to DIN 1940 [DIN1976], which uses the standard cycle process of the Seiliger Process. The Seiliger Process describes the cycle as an isentropic compression, followed by a first isochoric and then isobaric heat supply, an isentropic expansion and an isochoric heat release, as presented in Fig. 3.10. This process is only a rough estimation, as it is based on many assumptions like the simplification of the gas exchange. For a deeper insight into the engine process, the real cylinder process has to be modeled. In contrast to the Seiliger Cycle, the real cylinder process does not use simple cycle calculation but is based on energy balances during the different stages of the process. This requires engine design and operation specifications, which are often proprietary and can not be obtained from manufacturers for modeling. This can partly be overcome by use of measurements from engine indication and the adaptation of the model to these data.
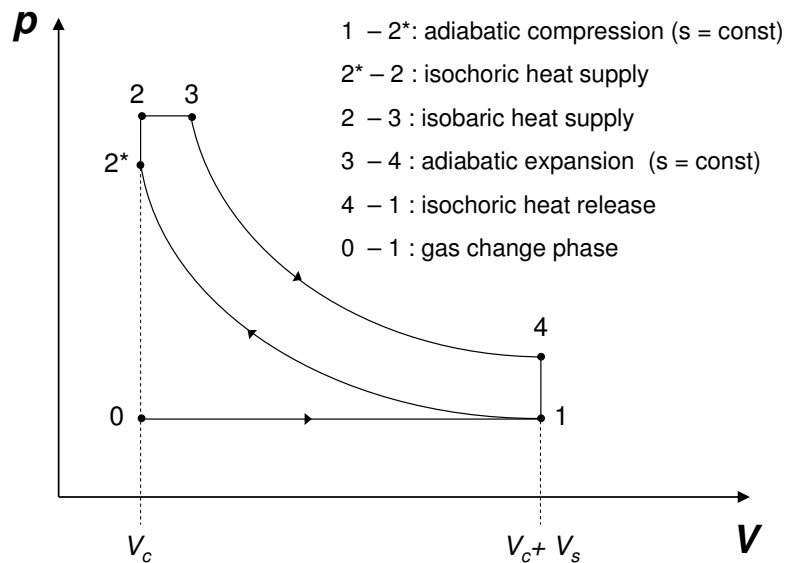
Figure 3.10. Seiliger process in a p-V-diagram.

In a trial to gain more insight into heat flows, an engine process model is developed, which satisfactorily represented the engine's behavior of the test vessel [UTH2009]. The cylinder process is simulated using a one zone model, in which the system boundary is set by cylinder liner, piston and cylinder head including the valves. The energy and mass balances of the cylinder are described as a function of inlet and outlet pressure, stoichiometry and firing pressure profile and depending on engine power and rotational speed.

The gas change phase, as a main process-influencing phase of a two-stroke engine, incorporates the inlet vent and outlet valve geometries and the resulting mass flow depending on the inlet and outlet pressures. The gas change phase is divided into the two phases of ideal displacement of the burned gas by the fresh gas, followed by the ideal mixing phase. The used uniflow scavenging via a top-mounted exhaust valve with the reduced shear flows and the comparably large stroke-to-diameter ratio lead a predominant displacement phase over the mixing phase and therefore an effective scavenging of the burned gas.

The combustion process is modeled as a double Vibe function [VB1970]. The Vibe parameter of the firing pressure profile are obtained for discrete loads from measured pressure profiles from indication measurements of the actual engine on board of the test vessel, as no information about the injection were available from manufacturer.

The heat transfer to the cooled cylinder walls as a major loss in the cylinder process is modeled using the Woschni correlation [WOS1970]. To fit the model to operational data at discrete loads, the turbulence model is iteratively adapted.

The test vessel is equipped with an engine indication system, enabling the models to be adapted to these indication data sets at discrete loads. This was necessary, as the required data for engine modeling, e.g. characteristics of the valves, could not be obtained from the manufacturer. The behavior of the engine had therefore to be iteratively adjusted to the actual behavior as measured on board.

The adaptation of the generic engine process model to represent engine performance over a wider range of loads is very sophisticated and considered not applicable for an easy-to-use simulation model for efficiency evaluation. If accurate engine process models were available from manufacturer, this approach would allow for an in-depth evaluation of the different heat flows and potentials for use of the waste heat, but the effort for establishing engine process models for each vessel again seems not to match the gained increases in data accuracy and insights into improvement potentials. For these reasons, the characteristic diagrams are used in the simulations instead of a cycle simulation.

3.2.1.4 Auxiliary Engines

Auxiliary engines generate mechanical power for driving generators. In the simulation model, the engines are modeled with a lower degree of modeling depth, as the focus is on the main engine. Auxiliary engines are often sold as combined generator set ready-made in large numbers, having no testbed data of the specific engines

available. Depending on the required accuracy in the calculation it is possible to include very detailed engine model here as well, or simplified demonstration models based on calculations of the fuel flow for a given electric load on the generator with or without ISO correction, i.e. as

$$\dot{m}_{FO\ AE} \quad = \quad f(P_{AE}) \quad . \tag{3.34}$$

Generator sets are running at a constant speed, deviating only within the tolerable deviation in grid frequency, therefore the modeling does not consider changes in rotational speed. For frequent changes in the use of AE, leading to frequent starting up and powering down of AE, the error in consumption is increasing. In normal operation the times of starting up and powering down are small compared to running time and can therefore be neglected, compare Fig. 3.25.

For auxiliary engines, the test cycle defines at least five operational points at 100% MCR, 75% MCR, 50% MCR, 25% MCR, and 10% MCR. At these points the consumption is available either as fuel flow or specific consumption. Depending on this, the consumption is modeled either as

$$\dot{m}_{FO\ AE} \quad = \quad \frac{LHV_{testrig}}{LHV} \cdot \rho_{FO} \cdot \dot{V}_{FO} \tag{3.35}$$

being $LHV_{testrig}$ the lower heating value of the fuel and $\dot{V}_{FO} = f(P_{AE})$ the tabled volume flow of fuel oil at the test rig, or as

$$\dot{m}_{FO\ AE} \quad = \quad \frac{LHV_{ISO}}{LHV} \cdot P_{AE} \cdot be_{AE} \tag{3.36}$$

being $be_{AE} = f(P_{AE})$ a tabled function of the specific consumption. Corrections for the lower heating value (LHV) of the fuel oil are for HFO operated engines in the range of $\frac{LHV_{ISO}}{LHV} = \frac{42700 \text{ kJ/kg}}{40500 \text{ kJ/kg}} = 1.054$. The fuel oil consumption at 0% load, if not available from manufacturer, is extrapolated from the consumption at 50% MCR, 25% MCR, and 10% MCR. The error caused by this extrapolation is considered small, as the auxiliary engines are operated only for very short time in these very low loads compared to operation time. Auxiliary engines typically don't operate in idle mode, which occurs only when starting up and turning off, as they are operated either connected to the grid providing electricity or turned off. For consideration of the ambient conditions, the specific fuel oil consumption be_{AE} can be implemented with a correction term according to ISO and the manufacturer's project guide.

Exhaust gas temperature of the auxiliary engine is integrated depending on the engine load as tabled data from test rig report or from manufacturer's specification. Along with the exhaust gas mass flow from the same sources, the available waste

heat of the exhaust gas and the corresponding temperature can be determined. Here, as for the main engine models explained in Section 3.2.1.1, the available heat flows are determined based on the sea water temperature for energy balances, ambient temperature, and minimum temperature for the prevention of low temperature corrosion. The heat flows are available as outputs from the simulation model for further evaluation, e.g. waste heat recovery studies, and exergetic analyses.

3.2.2   Generators

Generators on board of the vessels are usually driven by auxiliary engines (generator sets), the propeller shaft (shaft generator), or turbines (waste heat recovery steam turbine, exhaust gas power turbine). The generator models are developed to be independent of the driving system, enabling a quick adaptation to the present requirement. The generators are modeled as conversion of mechanical power to electrical power with their specific efficiency curve, defining the required mechanical power for a given electrical power,

$$P_{el} = \eta_{gen} \cdot P_{mech} \tag{3.37}$$

being $\eta_{gen} = f(P_{gen}, |S|)$ the efficiency of the generator as a function of the load. The real electrical power P_{el} can be replaced by the apparent power $|S|$ and the associated power factor $cos(\varphi)$,

$$P_{el} = |S| \cdot cos(\varphi) \tag{3.38}$$

if they are available as measurement values on board. The power factor can be determined once as an average value and set as a parameter in the model. In the present evaluations, only the real power was available and the power factor was estimated to be $cos(\varphi) = 0.8$. All losses of the generator can be considered to be converted into heat, therefore waste heat is calculated from the efficiency using the additional interrelation

$$P_{mech} = P_{el} + \dot{Q}_{gen}; \tag{3.39}$$

in which $\dot{Q}_{gen}$ defines the required cooling or available waste heat, respectively. The generator models are inheriting behavior from a generator parent model, changing the efficiency curve and parameters for adaptation to the specific generator.

3.2.3 Other Components

Additional models of components were created, which were necessary for evaluations in different contexts. Amongst others were models of switchboards for electrical energy distribution, and gears for matching the engine speed to propeller and generator speeds.

3.2.4 Components for Measurement Data Input

The provision of input data to the simulation models of engines and auxiliary systems is implemented with input components, containing the data as time lines. These data can originate from measurements on board of vessels, as described in Sections 3.4.1 and 3.4.2, or from theoretical operational profiles transformed into representative time lines of operation. The time lines are stored as splines in the components, with an output connection to allocate the time lines to the vessel equipment components.

All time depending input data are provided with such components. For engine components, these input components contain the time lines under evaluation of generated power, rotational speed, cooling water temperatures and ambient conditions.

3.2.5 Integration into a Simulation Model

The energy flows in the vessel are investigated by means of a simulation model of the single components, which are connected within the simulation environment to represent their interconnectivity and the energy flows in the real vessel. In this project, a library of components of energy converting systems aboard the test vessels was developed, which will be described in the following sections. In Fig. 3.11, a screenshot of the simulation environment *ITI SimulationX* is presented, with the library of components in the left frame and a simulation model in the right frame.

The modeling is separated into models for energy conversion from chemical energy to mechanical and electrical energy (compare above) as well as for selected important power consumers. The power conversions and their successive losses can be presented in the Sankey diagram, symbolizing the linkage of efficiencies through the different types of power provided to the consumers. The primary energy conversion aboard vessels can be defined as the energy conversion from chemical energy into mechanical energy, with the losses of conversion being accounted for as waste heat and exhaust gas enthalpy. These losses of the primary conversion can be considered as by-products and be again the inputs for processes, in this case for waste heat
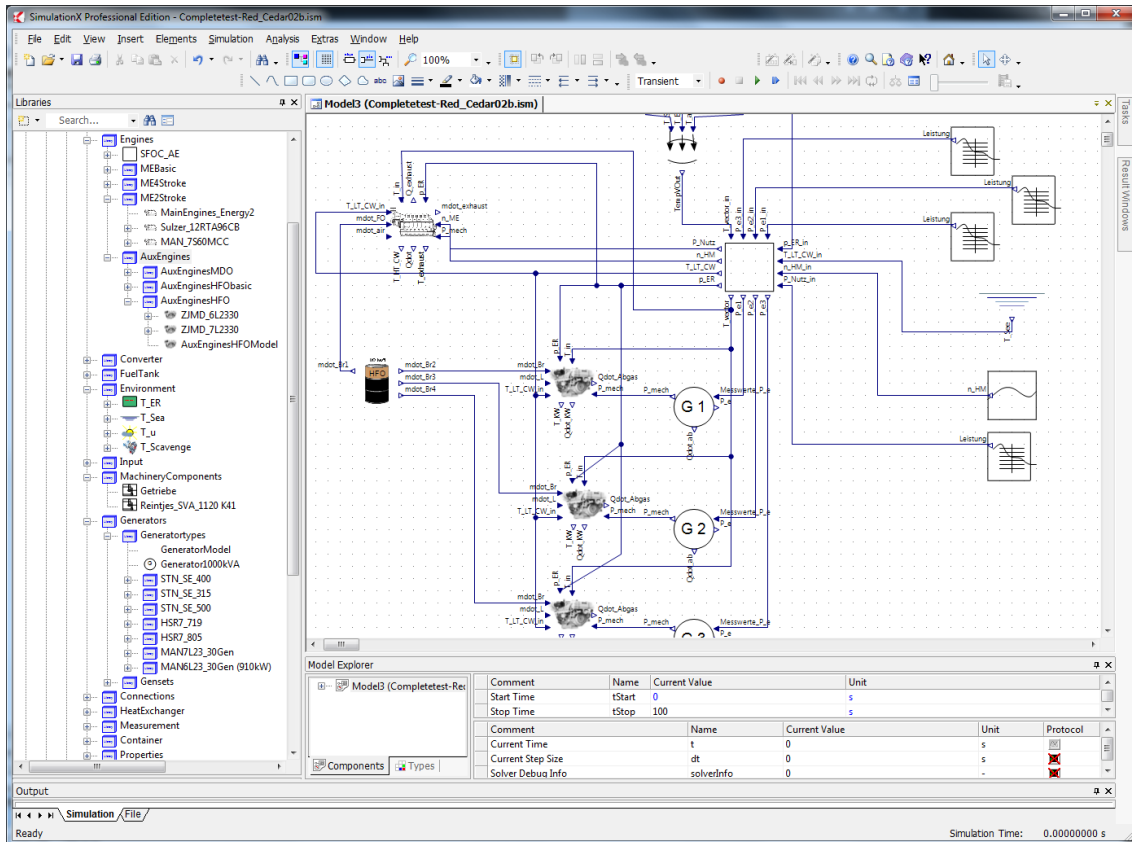
Figure 3.11. Simulation environment with the library of components (left frame) and simulation model (right frame).

recovery. Secondary conversion can be defined as the conversion from mechanical energy into electrical energy, if used for driving a generator, or propulsion energy, e.g at a propeller.

3.3   Results of the Simulation

The simulation is the basis for a solution which is suitable for industrial use. This includes the applicability to a real world measurement on board of a vessel with its inherent challenges through changing conditions, sensors without recent calibration and a limited access to process parameters. Implemented in an onboard tool with data management for the feeding and storage of data, it can be the center point of an long-term monitoring system for vessel and onboard machinery performance.

The costly high frequency and high precision fuel flow measurement for evaluation

of the consumption within the varying operations can be reduced to a less elaborate measurement of the produced power, with the time-depending variations being provided by the simulation model of the machinery. Instead of examining outflow or content of the fuel oil tanks at distinct time intervals as an integrated value as described in Section 2.4, the simulation feeding into data storage provides a detailed figure of the consumption of the energy converting systems in high frequency for instant onboard evaluation and retrospective onboard and shore-based evaluation. The provided data can then be analyzed and interpreted both automatically, compare Ch. 5, and manually for prominent points and deviations from predefined reference values.

3.4   Validation and Testing

3.4.1   Measurement Data of a Container Feeder

As a first validation of the approach of using a simulation model for calculation of fuel consumption and efficiency, data of an already completed measurement program were used. *Germanischer Lloyd* participated in 2004 in the research project *FCShip*, in which the possibility of using fuel cells in maritime applications was evaluated. The consumption of mechanical, electrical and thermal power of the container feeder "Astra" was recorded over 13 months. This 137m long vessel has a cargo capacity of 822 TEU and 150 reefer plugs for the power supply of refrigeration containers. The "Astra" is equipped with a 8400 kW four-stroke diesel main engine for propulsion, driving a controlled pitch propeller (CPP). Electrical power is provided by an shaft generator, two auxiliary diesel engines driving generators, and an emergency generator set, which can additionally be used for power generation in port. The main engine consumes heavy fuel oil (HFO), diesel generators and auxiliary boiler are consuming marine diesel oil (MDO).

The measurement points were integrated into the vessel already during construction at the yard, which enabled to include 52 measurement points for an extensive view of the energy flows in the vessel. The measurement program included produced mechanical power at the propeller shaft and electrical power of the generators, temperatures and pressures in the engine room, thermal oil temperature before and after boiler, as well as ambient conditions and the power consumption of cooling water pumps, boiler feed pump and various electrical consumers. Relevant measurement points are listed in Table 3.2 below.

Table 3.2. List of relevant measurement points of the container feeder vessel.

Description	Unit	Measurement device
Shaft torque	Nm	Strain gauges
Shaft speed	min^{-1}	Pulse sensor
Power shaft generator	W	Generator control unit
Current shaft generator	A	Ampere meter
System voltage	V	Volt meter
Temperature engine room	°C	Pt100
Pressure engine room	bar	Baro transmitter
Current boiler feed pump	A	Ampere meter
Temperature thermal oil before boiler	°C	Pt100
Temperature thermal oil after boiler	°C	Pt100

The energy converting components modeled were the four-stroke main engine, as described in Section 3.2.1.1, the shaft generator, the vessel's gears box, and its boiler. With these components, a simulation model of the vessel was developed [OEH2008].

The shortest reporting period in the vessel's logbook was one day, which sets the shortest time period for comparison of simulation results with reported data. The simulation of one-day periods resulted in differences of up to 20% between reported consumption of the engines and integrated value of the simulated consumption in that period. This can be explained by discontinuous transfer of fuel oil from bunker to fuel oil preparation and day tank, which is not always consumed at the day of its accounting in the reports. Based on this experience, which supports the previous results about the accuracy of daily reporting described in Section 2.4, only longer periods for simulation where evaluated.

A 32-day period was chosen for the validation of the HFO and MDO consumption, as in all longer periods some data from logbook or documentation were missing, which were needed for the analysis. In this period, the simulation of the fuel oil and energy consumption based on measured power and heat consumption was compared to the reported values.

The simulation model of the main engine and boiler system is presented in Fig. 3.12, being the main engine in the middle ① and shaft generator ②, boiler ⑥ and gear box ⑦ right of the main engine. Additionally, the input components for power and rotational speed ③ and ambient conditions ⑤ are presented as well as components collecting the fuel flow related output data of main engine and boiler ④. The

interrelation of the components are represented by the connectors, which symbolize data flows in the model.
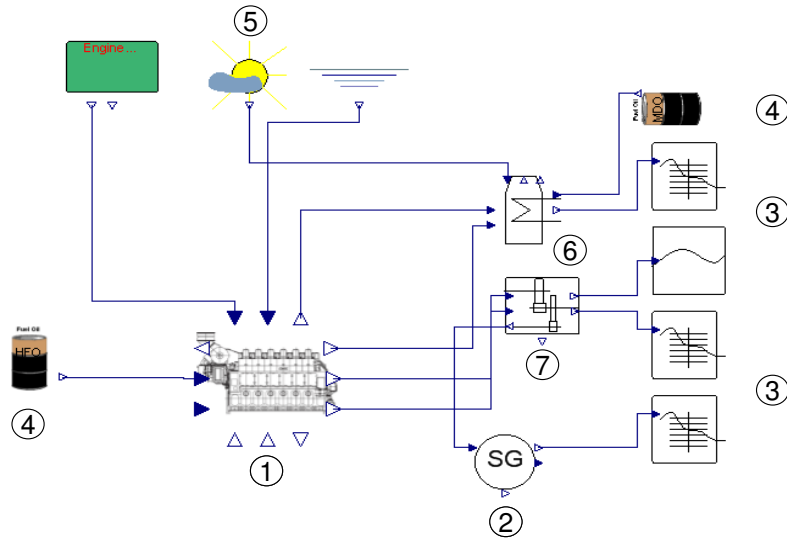
Figure 3.12. Simulation model of the container feeder main engine (1), shaft generator (2) and boiler model (6) with input tables (3,5).

The data flow for the main engine in the simulation model can be explained as following. The input data of shaft power and rotational speed ③ are fed into the gear box model ⑦, where it is combined with the power of the shaft generator ② with the related efficiencies of the gears. The resulting shaft power and rotational speed is then fed into the main engine model ①. Additionally, the ambient conditions of the engine room and the sea water temperature ⑤ are provided to the engine model. The computed mass flow of fuel oil is then fed to the tank model ④, where the momentary values of fuel mass flow are further processed and all fuel related data are provided for analysis.

As the fuel specification were not completely documented, the lower heating value (LHV) of the fuel had to be estimated based on the interrelation between lower heating value, density and sulfur content as shown in Fig. 3.13. Based on the reported HFO densities of 950 kg/m^3 to 978 kg/m^3, the lower heating value was estimated to be 41500 kJ/kg, without consideration of the sulfur content, which was not reported. Considering a sulfur content of 1.5% m/m, the LHV estimation would be overstated by 700 kJ/kg, leading in the simulation to an undervalue in fuel oil consumption of 1.7%.
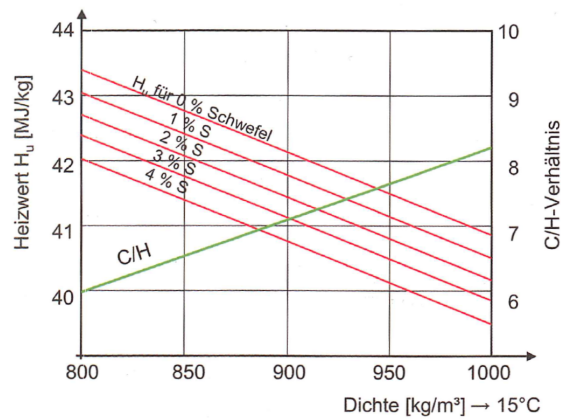
Figure 3.13. Interrelation between lower heating value, density, and sulfur content of fuel oil [MBA2006].

Validation of the MDO consumption of the diesel generators and generators were done using the measured electrical power as input into the simulation, feeding into the generator models. This is presented in Fig. 3.14, with the three auxiliary engines ① connected to the related generator ② and the input components ③ on the right, and the fuel oil component ④ on the left. These models had a lower degree of modeling depth, as in this first approach no correction for ambient conditions were included. The consumption of MDO was only reported as an integral value for both auxiliary engines and auxiliary boiler, therefore the consumption from both simulations had to be added. The accounting of the difference between calculated consumption and reported consumption to auxiliary engines or boiler was therefore not performed, as any adaptation of the model for minimization of these differences would imply a higher accuracy than the actual models have.

The validation of the simulation models with adaptation of the correction term η_k lead to the differences as presented in Tab. 3.3. The consumption model for HFO

Table 3.3. Results of the validation of the container feeder [OEH2008].

System	relative difference	absolute difference
HFO	-0.5%	3.0 t
MDO	-8.5%	2.4 t

consumption with its deviation within the measurement accuracy can be considered accurate enough for further evaluations. For the auxiliary engines in this case an
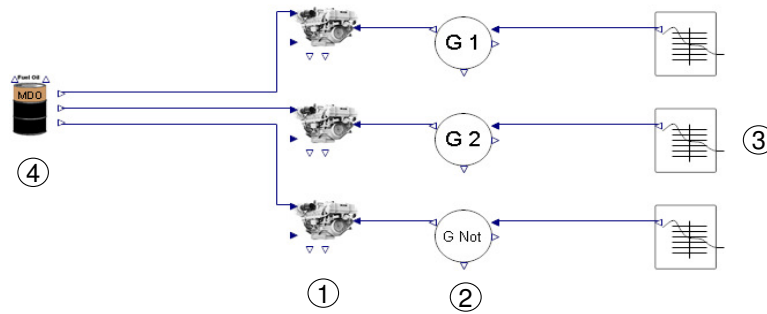
Figure 3.14. Simulation model of MDO consuming generator sets with tank (4), auxiliary engines (1), generators (2), and input data components (3).

accuracy of about 10% was achieved, which is the difference between reported and simulated consumption in the evaluated time period. This relatively high value can partly be explained by not reported boiler consumption and fuel specifications, which had to be estimated. As the auxiliary engine models are proposed for simulation of different configurations and operational profiles of machinery and not accounting for transient operations, the actual accuracy for trend analysis is presumed to be higher and considered accurate enough for the evaluations.

Beside the mentioned measurement data of a 32-day period, a generic operational profile covering 48 hours was developed for comparable conditions in simulation runs for optimizations. This enables simulations under defined conditions, allowing for the identification of influencing parameters. From the reports it is known that a typical journey of the container feeder in the Baltic region is about two days. The typical journey includes port stay in two ports with departure and arrival maneuvering, and sea passage. Based on the operational profile according to [KAE2004] the time periods are defined as presented in Tab. 3.4.

Table 3.4. Generic operational profile of container feeder [KAE2004].

Operation	Relative time [%]		Time [h]
Port	22	at departing and arriving port each	5.28 ($\times$2)
Maneuver	4	after and before berthing	0.96 ($\times$2)
Sea	74		35.52 ($\times$1)
sum	100		48

Based on this generic operational profile the influences of machinery operation and related saving potentials can be evaluated.

3.4.2 Measurement Campaign Postpanmax Container Vessel

3.4.2.1 Test vessel

A second measurement campaign had been conducted, which had been customized to the requirements of the efficiency evaluation method developed. The concept was to gain insight into the energy consumption and its operational profile, with a high time resolution for the different energy consumers for comprehension of the energy flows. Furthermore, the measurements should work with the least possible sensors and low requirements on measurement equipment. The measurement campaign was conducted within the research project *Flagship*, which was partly funded by the European Commission (EC) under the Sixth Framework Programme with the aim to improve the safety, environmental friendliness and competitiveness of European maritime transport. The description of this measurement campaign has already been worked out as part of a confidential Flagship research report. While the EC research report was not made public, confidentiality is not of concern in this part.

The measurements were conducted aboard an 8000 TEU container vessel of a research project partner. The 2005 built container vessel of the postpanmax class can carry a maximum deadweight tonnage of 100 000 t. It is propelled by a Wärtsilä Sulzer 12 cylinder engine type RTA96C, which produces up to 68640 kW at 102 rpm. The power is directly transmitted to one fixed pitch propeller and enables a maximum speed of 25 kn. General dimensions and specifications of the vessel are also shown in Tab. 3.5. The electrical power is generated by five generator sets driven by MAN L27/38 engines. The maximum electrical power that can be provided to the onboard grid is 12 MW. This high installed power is mainly needed for reefer container transport, while the average load of the ship's auxiliary engines at sea passage is only about 10-15% of the installed power. The consumption is comparable to the reported consumption of a typical post-panmax container vessel of the Danish Marine Group "Green Ship of the Future" Container Ship Concept Study [GRE2009]. The process and domestic heat is provided by two steam boilers. While the main engine is running, an exhaust gas heated boiler provides the required amount of steam. In port and at low main engines loads, an oil fired auxiliary boiler is used for steam production.

During the measurements, the vessel was operated year round in a Europe Far-East service. This liner service connects Hamburg via the Suez channel with Singapore and Chinese ports, with only a few stops in between. The actual route as acquired on board is displayed in Fig. 3.15 as an overlay of GPS data to a MS Vi-

Table 3.5. Dimensions and specifications of the test vessel.

Detail	Specification
Delivery	2005
Length	320 m
Width	42 m
Draft	14 m
Deadweight Tonnage	100 000 t
Main Engine type	Wärtsilä 12RTA96C
ME power	69 MW
Auxiliary Engine type	MAN L27/38
AE combined power	12 MW
Boilers	Two steam boilers, oil fired and exh. gas heated

sualEarth aerial view of the earth. The long-term measurement campaign enables to include operation in harbor, maneuver, restricted waters, shallow water passages, deep water passages, and open sea. Therefore, all operational modes of the vessel and the accruing power consumption are covered in high time resolution. The route enables the inclusion of all ambient conditions from northern Europe (North Sea, cold) to desert (Suez, hot and dry) and tropics (Singapore, hot and humid) in all seasons.

3.4.2.2 Measurement Campaign

The measurement campaign aboard the container vessel was set up to obtain real operational data of consumed power and the present conditions in the engine and the engine room. All data were taken simultaneously for consistent evaluations. Power, rotational speed and torque of the main engine were measured parallel to the ambient conditions temperature, pressure and humidity in the engine room and the seawater temperature as well as cooling water, scavenge air, and exhaust gas temperatures. This enables the evaluation of actual working conditions and efficiency of the engine, with the possibility to detect reasons for abnormal operation or malfunction, e.g. at turbocharger or scavenge air cooler fouling. The list of measurement points can be found in Tab. 3.6.

A missing value in the campaign is the vessel's speed through water, which was not available in the vessel's navigational data stream and therefore could not be acquired with the limited resources of the project. Instead, the rotational speed of the propeller shaft and the speed over ground have to be used for the evaluations.

Figure 3.15. Route of the post-panmax container vessel (in MS VisualEarth).

Table 3.6. List of measurement points at the test vessel.

Description	Unit	Measurement device
Shaft torque	Nm	Shaft power meter (strain gauge)
Shaft rotational speed	min^{-1}	Shaft power meter (pulse sensor)
Electrical power gensets	W	Generator control units
Sea water temperature	°C	Pt100
Engine room temperature	°C	Pt100 (weather station)
Engine room air pressure	bar	Baro transmitter
Engine room humidity	%	Capacitive sensor (weather station)
Charged air temperature	°C	Pt100
Charged air pressure	bar	Pressure transducer
Low temp. cooling water temperature	°C	Pt100
Rotational speed of turbocharger	min^{-1}	Pulse sensor
Speed over ground	kn	GPS
Course over ground	°	GPS
Heading	°	Compass
Position	Lat., lon.	GPS

Additional information is needed for the evaluation but not available as data streams, due to the lack of available signals from the components. These data are collected manually from the nautical and engine logbooks or the daily reports from board the ship, the so-called noon reports (compare Section 2.4.2), Tab. 3.7.

Table 3.7. Manually acquired information at the test vessel.

> Draft, Trim
> Wind speed
> Wind direction
> Fuel tank fillings / consumption data per leg of journey

The measurement equipment had to be installed on board during the short stopover at the container terminal in Hamburg, allowing for about 2 days of installation work. For achieving this as well as maximizing the flexibility, a modularized approach had been taken, as displayed in Fig. 3.16 and based on the experience of GL's measurement department for long-term measurement as described in [MR2005].

The main data acquisition unit (DAQ) is located in the engine control room, which is shown in Fig. 3.16 as the bottom box. The DAQ performs synchronized capture of CAN bus data. The measured data can be triggered, mathematically processed and displayed. The DAQ stores the measurement data on flash discs, which are regularly exchanged and send ashore for data evaluation. The specification can be found in Tab. 3.8.

Table 3.8. Specification of data acquisition unit (DAQ).

Parameter	busDAQ-2
CAN-nodes	2
CAN transfer protocol	High Speed 1 MBaud (ISO 11898),
	Low Speed 125 KBaud (ISO 11519)
baud rate	Max 1 Mbits/s
channels	<512 per device
LAN-interface	TCP/IP 10/100 Mbit/s, RJ 45
storage	Compact Flash

The data are fed to the DAQ by substations, using the CAN bus for interconnections, illustrated in Fig. 3.16 as blue (CAN 1) and green (CAN 2) lines. The substations are consisting of four CANSAS modules and one CANSER module. The CANSAS modules are multipurpose amplifier modules which enable the connection
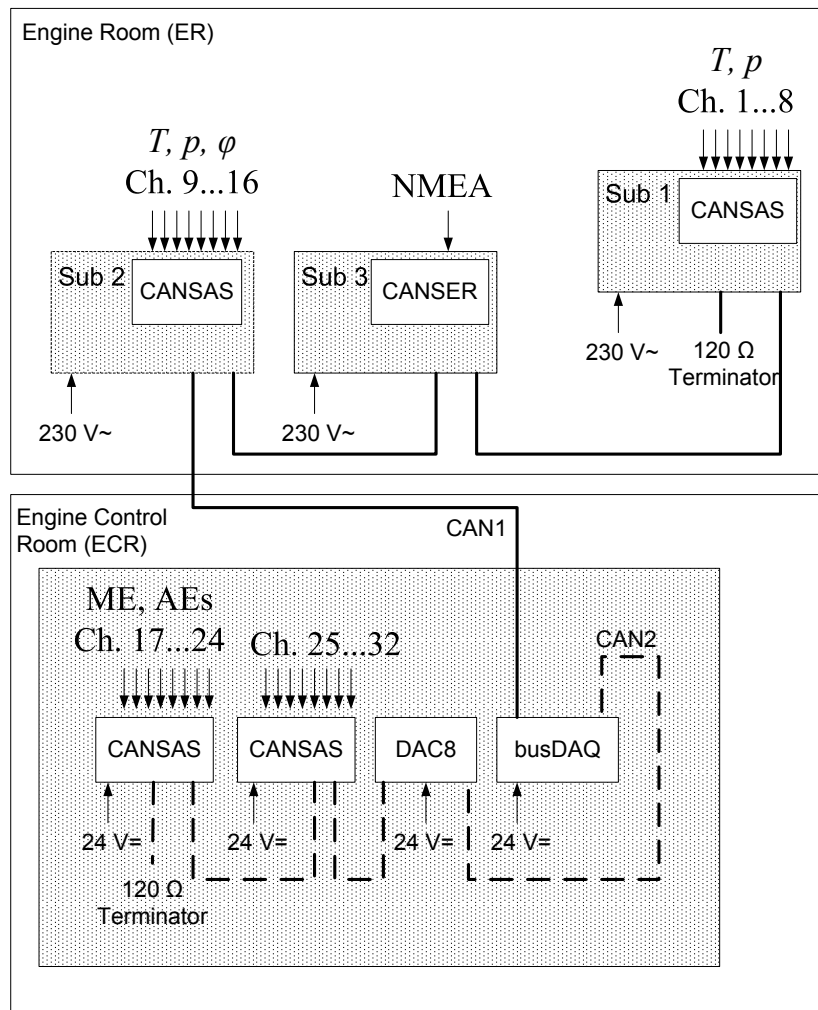
Figure 3.16. Graphic of the data acquisition.

of analog signals, PT100 and thermocouple temperature sensors, and pressure sensors to the CAN bus. The specifications can be found in Tab. 3.9.

The CANSER module connects the navigational data obtained from onboard NMEA signal at the bridge to the CAN bus. Two CANSAS modules are integrated in the same control cabinet as the data acquisition unit and collect the power of the auxiliary engines, the shaft power measurement of the main engine and the turbocharger rotational speed. These are available in the engine control room as analog signals, as described below.

The substations Sub 1, Sub 2 and Sub 3, Fig. 3.17, are located in the engine room, connected to each other and to the DAQ in the engine control room via the

Table 3.9. CANSAS module technical specification.

Parameter	value typ.	max	test conditions
inputs	8		DC, differential
measurement modes	voltage, current, resistor, thermocouples, PT100, bridge		
sampling rate / channel		1 kHz (max)	
resolution	16 Bit		
bandwidth	0 ... 200 Hz		-3 dB
voltage ranges	± 5 mV ... ± 50 V		
gain: uncertainty	0.02%	≤ 0.05%	of reading
noise	0.4 μV rms 14 nV/vHz		0.1 ... 220 Hz, (RTI)

CAN bus. Sub 1 is installed beside the scavenge air cooler of turbo charger no. 3, Sub 2 and Sub 3 are installed outside the engine control room in the vicinity of the waste heat boiler. In the pictures are the CANSAS modules (Sub 1 and Sub 2) and the CANSER module (Sub 3) as light blue boxes in the upper half of the substations visible, with the signal wiring, switches and fuses installed below. Substation Sub 1 collects the signals of the Pt100 temperature sensors of scavenge air, low temperature cooling water at scavenge air cooler, and seawater before main cooler and the signal of the pressure transducer of the scavenge air pressure.
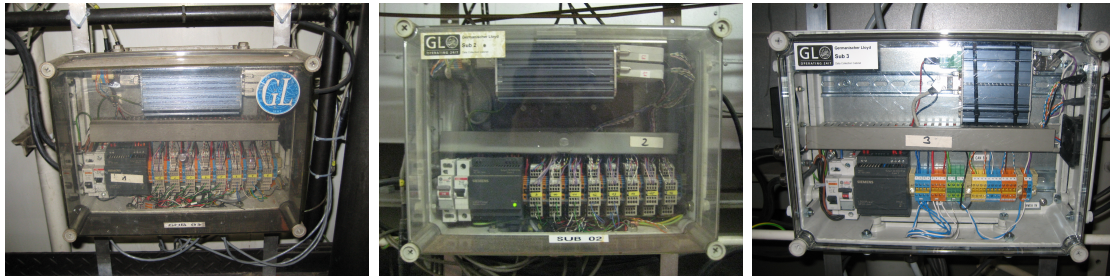
Figure 3.17. Substations Sub 1 (left), Sub 2 (middle) and Sub 3 (right).

Scavenge air temperature and pressure are measured at the same blank plug in the charge air casing, as shown in Fig. 3.18. The pressure transducer is thermally isolated against the hot casing. LT cooling water and seawater temperature (Fig. 3.19) are measured outside of the tubes, as no sensor could be introduced into the actual water flow. As the temperature is measured on the surface of the tube, in stationary operation a small but constant temperature gradient through the tube walls is assumed. The Pt100 temperature sensors are glued directly onto the tubes and

are insulated against the engine room with a 4 mm thick rubber casing and a further insulation consisting of a sheet of 3 mm polyurethane covered by an aluminum foil. The measurement error can be estimated for the case of maximum cooling water temperatures of 66 °C and engine room temperatures of 30 °C at a forced convection with 2 m/s air velocity. Under these conditions, the deviation between cooling water core temperature and measured temperature on the tube can be determined to be below 0.1 K. A measurement error of 0.1 K below the actual cooling water inlet temperature would result in a correction error of specific fuel oil consumption at the exemplary two-stroke engine as presented in Section 3.2.1.2 of about 0.06% of the consumption under ISO conditions. This is by an order of magnitude smaller than the uncertainty in power measurements.
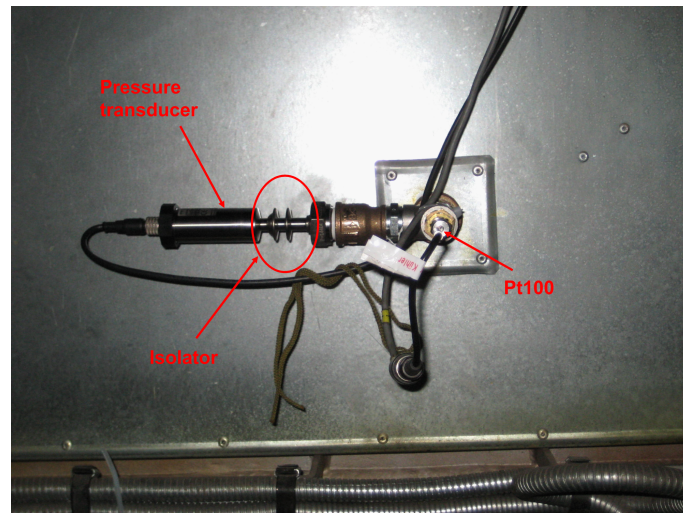
Figure 3.18. Pressure sensor and PT100 of scavenge air.

The engine room conditions are measured at two points in the engine room, using a baro transmitter and a combined temperature and humidity sensor (weather station) of Feingerätebau K. Fischer GmbH, Fig. 3.20. Air pressure is measured close to substation Sub 2 in the vicinity of the engine control room and considered equal in the whole engine room, neglecting the difference in elevation to the engine. Temperature and humidity are measured directly at turbo charger no. 3 inlet, measuring the conditions under which the engine is running. These sensors are connected to Sub 2 and transmitted as digital signal to the data acquisition and storage unit in the engine control room.

The power measurements are obtained from the permanently installed monitoring
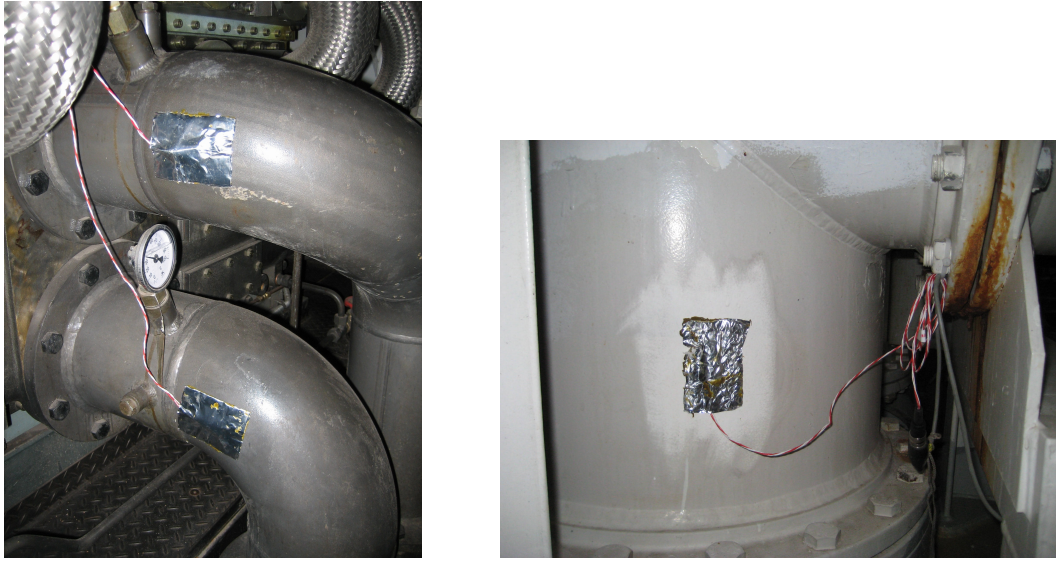
Figure 3.19. Low temperature cooling water temperatures of scavenge air cooler (left) and sea water temperature sensor (right).

Figure 3.20. Pressure sensor (left) and temperature and humidity sensor at turbo charger (right) for engine room conditions.

systems on board. Shaft power data, being rotational speed, power and torque, are collected as analog signals from the ship's shaft power meter shown in Fig. 3.21. The signals are obtained from its control unit in the engine control room. For ensuring that no interference of the measurement equipment with the control unit occurs, optocouplers are engaged, which isolates the measurement circuit from the control unit's circuit and allows only signals to be transferred from control unit to the data

acquisition unit. The optocouplers are displayed on the right side in Fig. 3.21.
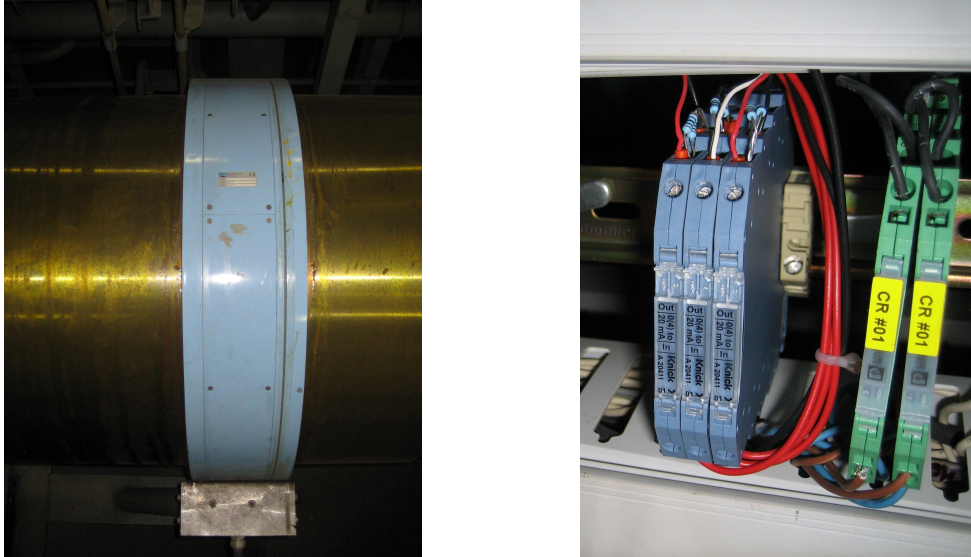
Figure 3.21. Shaft power measurement unit (left) and optocoupler as isolator for shaft power connection to DAQ (right).

The electrical power of the generator sets are obtained from the generator control units as shown in Fig. 3.22. Each generator set is controlled by a separate control unit and switch board, from which the current power can be emitted as analog output signal. These signals are processed by the CANSAS module and sent to the DAQ for storage.

Rotational frequency of the turbocharger is obtained from the turbocharger monitoring unit in the engine control room. Speed and course over ground, heading and position are obtained from the NMEA data stream of the automation system. The CANSER module converts the data stream to measurement values and sends it to the DAQ for storage.

Additional data were required for the evaluation, which could not be acquired electronically from onboard systems. These are the consumption data per journey of main engine, generator sets and boiler, the draft and trim of the ship, and the weather including wind force and direction and sea force. These data are available in the ship's log books and reports. Therefore, the ship's crew and owner supplied the daily report, called noon report, which includes weather and consumption data, as well as further reports and log book excerpts, which were manually evaluated in the context of the measurement data.

Figure 3.22. Generator control switch board.

The measurement accuracy is governed by the accuracies of the sensors and the CANSAS modules. The CANSAS modules convert the incoming analog signals from sensors and control boards into digital CAN bus data. The accuracies of the CANSAS modules can be found in Tab. 3.9. The measurement accuracy of the sensors and control boards are displayed in Tab. 3.10, in case of the shaft power meter with both the manufacturer data and the estimation based on the strain gauge accuracy.

3.4.2.3   Challenges and problems in the measurement campaign

The measurement campaign onboard was a great success, but challenges and problems occur always and can hardly be avoided. The following paragraphs describe some occurrences.

For preparation of the installation on board, a sister vessel was visited and the possibilities for installing the different sensors and obtaining the signals were checked. At the sister vessel all proposed connections and data streams were available, therefore the concept for the measurement campaign proved to be good. During the installation on board it was found out that the visited sister vessel was different in that kind, that some connections were not possible and the NMEA data stream from navigation system was differing from the stream of the sister vessel's, lacking some information. This change would have to be done in automation system and

Table 3.10. Measurement accuracies.

Measurement sensors:	Accuracies:
Shaft power meter: Kyma SPM	0.5% (manufacturer data) Estimated value: 1.48%, based on strain gauge accuracy
Electrical power generator sets: Hyundai HIMAP	1% (manufacturer data) The relative accuracy relates to full scale value (20 mA)
Pt100: RS, class B	$\mathrm{d}T = \pm(0.30\ \mathrm{K} + 0.005 \cdot |t|)$, t in °C
Weather station Feingerätebau Fischer	$\mathrm{d}T = \pm(0.10\ \mathrm{K} + 0.0017 \cdot |t|)$, t in °C $\mathrm{d}\varphi \leq \pm 2\%$ RH (at 25°C, 5 ... 95%)
Baro transmitter Feingerätebau Fischer	$\mathrm{d}p < 0.5$ mbar
Pressure transducers:	0.2% of max. value 10 bar ± 0.02 bar

considered too high effort for the measurement campaign. Due to this fact, neither the speed through water nor the water depth were available as measurement values. Instead of ship speed through water, the available signals of speed over ground and rotational speed of the propeller were taken for the evaluations. The water depth was only necessary if shallow water effects had to be excluded from results or prominent peaks in measurements were evaluated regarding the influences. In these cases, the position of the vessel from GPS was manually checked for the water depth in the region.

An originally allotted wireless local area network (WLAN) connection between the substations in the engine room and the data acquisition unit in the engine control room failed due to frequent loss of connection while sea going. The origin of the disturbing frequencies could not be located. Therefore, a cable connection was established and the WLAN connection replaced.

After a crank shaft explosion on board of the vessel it was worried that the measurement equipment was destroyed. The measurement data from the DAQ showed for all sensors around the main engine either no signals or implausible values. An onboard survey finally revealed that all cablework was destroyed by the heat, but the sensors were still working. The measurements were continuing as soon as the cablework had been exchanged.

3.4.3   Operational Data of the Container Vessel

As mentioned above, the measurement campaign had the aim to establish a database of real operational data for the development of methodologies and tools for efficiency evaluation and optimization. The campaign proved to be a very important tool for definition of the actual requirements of energy consumption aboard a large seagoing vessel. The acquired real operational profile and timelines of energy consumption allow for an insight in operation and establishing of a basis for evaluation of the saving potentials.

The test vessel is driven by a large two-stroke diesel engine, as described in Section 3.4.2.1. These engines are designed for propelling the vessel close to nominal speed. From engine manufacturers' side, no information about low-load operation below 50% MCR are given in the engine's project guides and specifications. This should be kept in mind when evaluating the histogram of the main engine's power consumption, which represents the actual operational profile. Due to various external drivers (high fuel oil price, less transported goods, new delivered ships in a saturated market) even container vessels are not operated at high speeds any more. This leads to operation with more than 50% of the sea passage time below 50% MCR, compare histogram in Fig. 3.23 below, which means outside of the manufacturer's specifications. The histogram contains a time period of about 6 months of operational data.

Besides this, it shows roughly a quarter of the time of port stays and 5% of maneuvering, while the vessel was operated less than 0.5% of the time at 80% MCR and above.
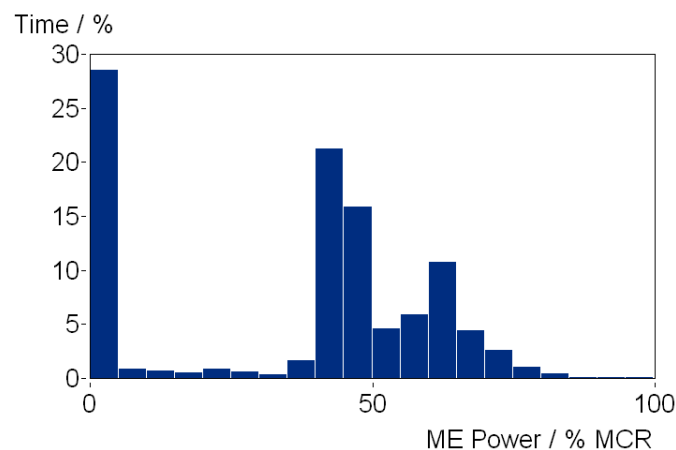
Figure 3.23. Histogram of main engine power consumption in per cent main engine MCR.

These real operational histograms are important for evaluation of the auxiliary systems and the performance of the engines in general. The data show how vessels are actually operated. This enables to establish a far more realistic basis for identification of saving potentials in operation than when assuming design operation.

The histograms are computed from timelines of the measurement channels, which are analyzed as well. In Fig. 3.24 an exemplary time line of one month is displayed, which includes port stays, maneuvering and sea passages and the fluctuation of power consumption within each of this. The noticeable power peaks are daily accelerations for cleaning of the engine. Due to the slow steaming, the engines can clog with soot and fuel remains, which are supposed to be burned away in these periods of high loads.
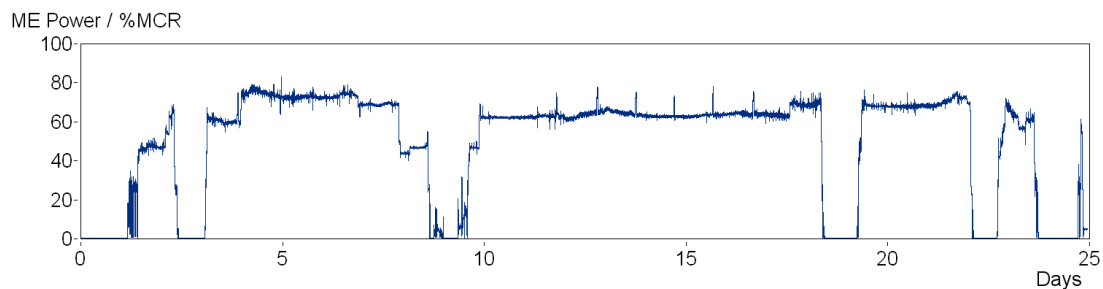
Figure 3.24. Time line of main engine power over 24 days.

The electrical power consumption is analyzed for the same time period. In Fig. 3.25 the histograms of electrical power consumption for sea passage (top) and port stays (bottom) are shown in percentage of installed auxiliary engine power. Taking into consideration that the number of reefer containers with their consumption is always changing, the consumption at sea is within a very narrow range of power, even though the main engine power varies much more (compare Ch. 4).

Timelines of the electrical power consumption can be displayed per generator set or in total. For overall optimization, the absolute value of power consumption is of greatest interest. A time line of consumed power can be found in Fig. 3.26. The high peaks in the consumption, more than tripling the consumption, are caused by the bow thrusters and can therefore only be found in maneuvering. As expected from the histograms, the power consumption is very stable during sea passage.
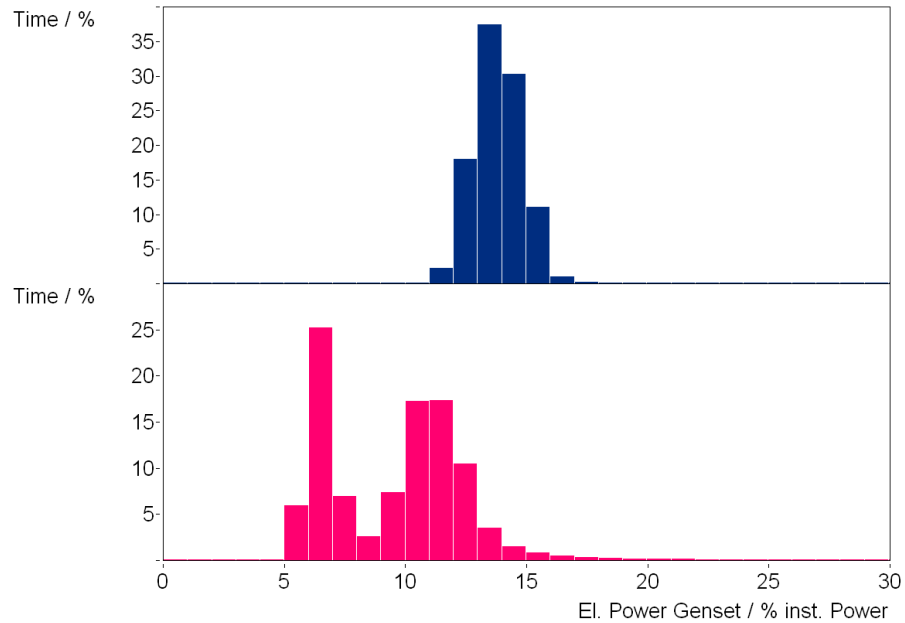
Figure 3.25. Histogram of electrical power consumption in percentage of installed power at sea passage (top) and port stays (bottom).
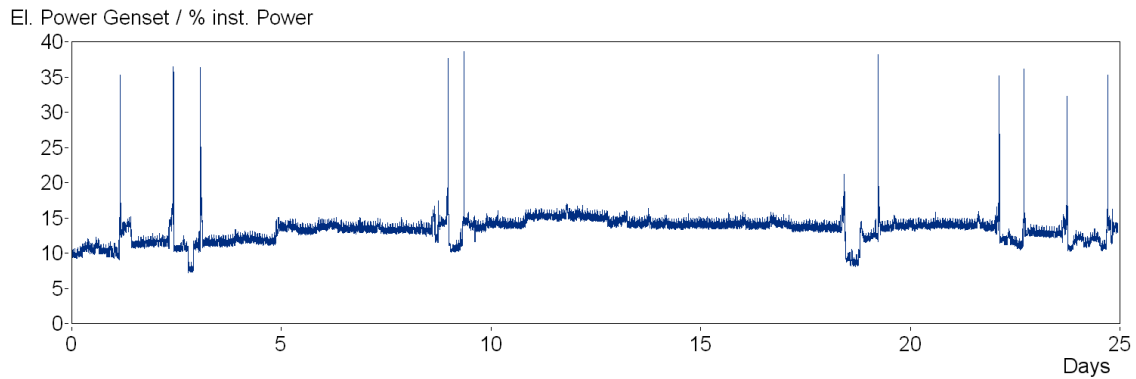
Figure 3.26. Time line of generated electric power.

3.4.3.1   Model of the energy conversion of the container vessel

The collected data of the power consumption with corresponding ambient conditions were used as input data for the simulation model of the energy conversion. In Fig. 3.27, the modeled components of the energy converting systems are shown. The energy converting components main engine ① ME, auxiliary engines ① AE and generators ② are enframed by the fuel oil evaluation component ④ and the input
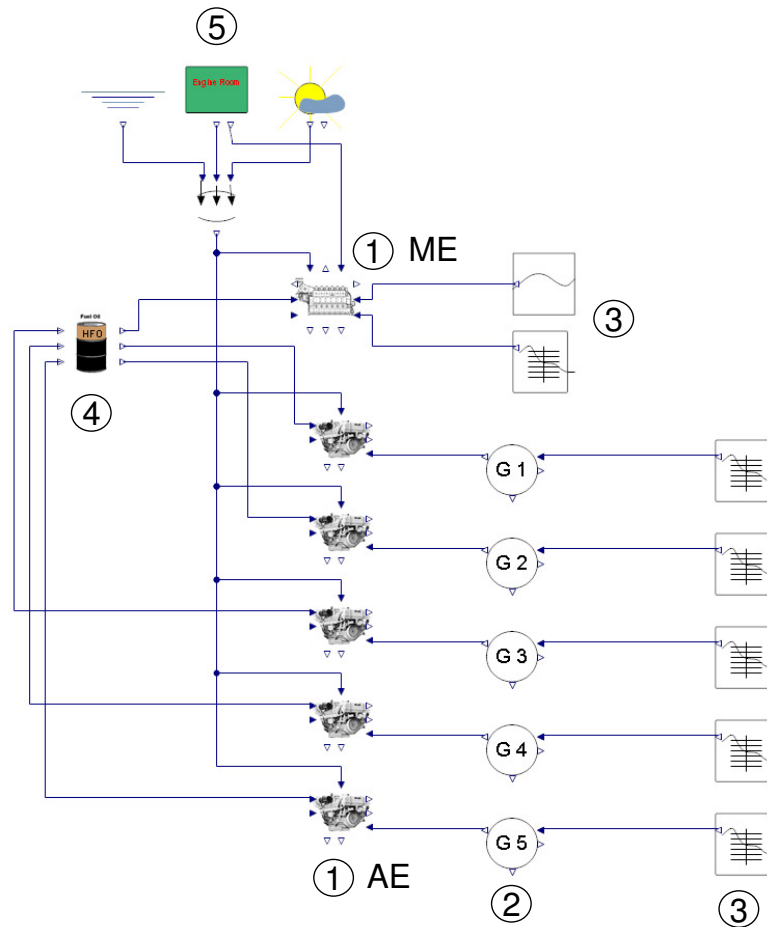
Figure 3.27. Overview of the modelled energy converting system of the test vessel.

data providing components, shown at the right for power and rotational speed ③ and at the top for ambient conditions ⑤ of the simulation model. The data streams are represented by blue lines, connecting the output of the data providing component with the input of the data computing or collecting component.

All input data components were filled with their respective data sets, which are fully synchronized throughout all data channels. Due to limitations in data handling of the simulation environment, data sets of about 4 weeks are used for the calculations of the consumption and efficiencies and the corresponding time lines. The simulated consumption data from these periods are compared to the reported consumption of the vessels engine logbook and daily noon reports. After the calibration phase of the simulation, the calculated main engine consumption at time periods about half a journey in the Far-East trade (Europe - Far-East or vice versa,

about four weeks) are very well within the expected accuracy of $\pm 2\%$ of the reported consumption, often within $\pm 1\%$.
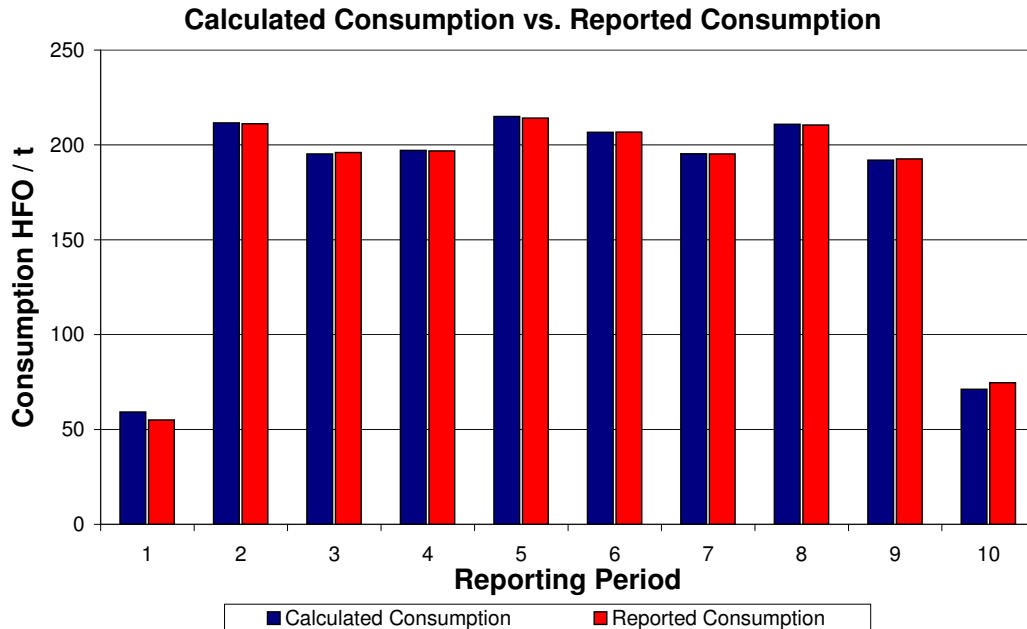
Figure 3.28. Calculated and reported consumption during one voyage leg.

The deviation of calculated consumption to reported consumption is demonstrated for one exemplary leg over 10 reporting periods, covering 8 days. The first and the last reporting periods include maneuvering and restricted waters, while the periods in between are daily reports during sea passage. As the vessel passes different time zones westbound, the reporting days are not equally 24 hours but include several days of only 23 hours.

In Fig. 3.28, the calculated consumption and the reported consumption from logbook are compared. As differences of a few tons are compared to 200 t of fuel oil, the deviation is not clearly visible.

The difference between calculated and reported consumption in tons are presented in Fig. 3.29, with the average deviation of 1 t included as reference column. In the graph indicate a positive deviation a higher calculated consumption than reported and vice versa. The deviations at first and last reporting period are peculiar. They occur in the period of passage from port to open sea. Explanations for the higher deviations are on one hand transient operation of the machinery during maneuvering and in restricted waters, which may not be adequately represented by the

Deviation of Calculated Consumption to Reported Consumption
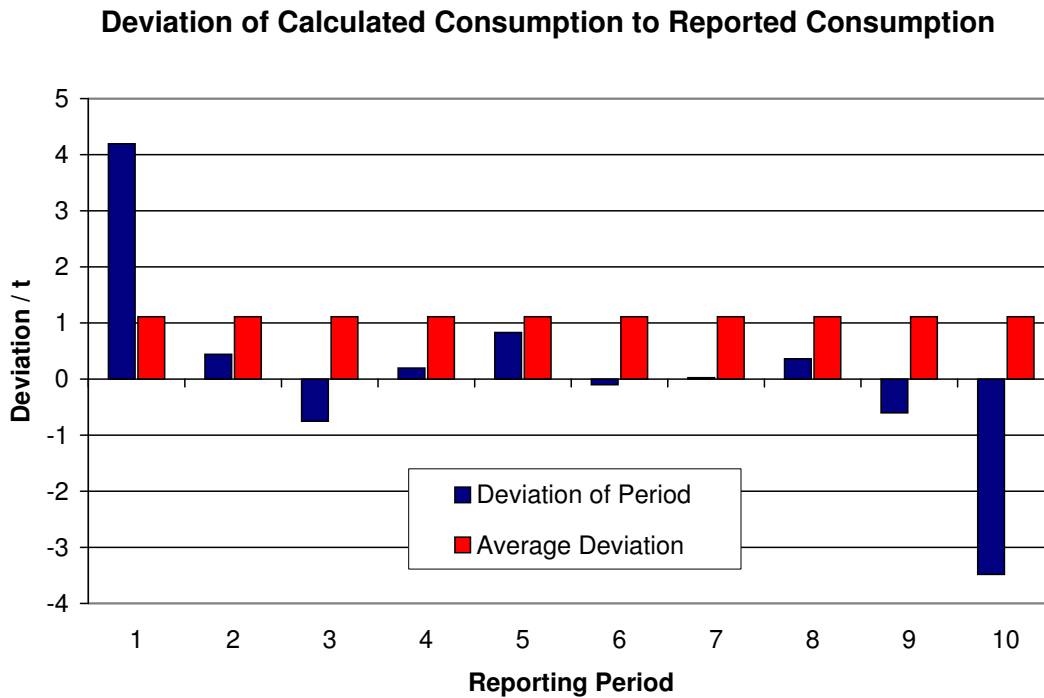
Figure 3.29. Deviation of calculated to reported consumption in tons during one voyage leg, positive deviation indicate higher calculated than reported consumption.

simulation model. A different explanation is based on the experience of reporting from superintendents and chief engineers. As the reported under-consumption at the beginning of the leg almost equals the reported over-consumption at the end of the leg, an inaccuracy in reporting on the first period may had to be balanced on the last day for equalizing the reported consumption to the left bunker.

A major influence for small daily variations are the uncertainties in reporting times, as the actual time of reporting (usually daily at noon local time) does not correspond with the time of the reading of the meters. Already a quarter of an hour difference of reading can make up to 3 t of fuel consumption.

A similar picture is given if the deviations are plotted in per cents, Fig. 3.30. The average deviation in this leg of 0.06% clearly indicate the competiveness of the methodology. Due to the relatively low consumption in reporting period 1 and 10 compared to the other periods, the percentaged deviations of the already in absolute numbers high deviations appear even larger with +7.6% and -4.7%, respectively.

Deviation of Calculated Consumption to Reported Consumption
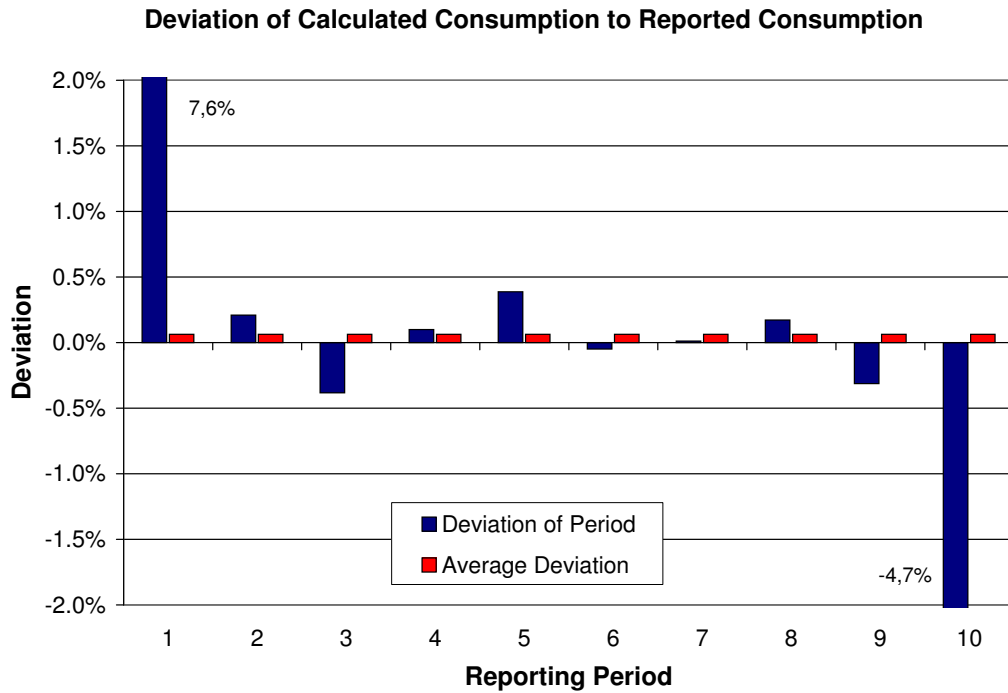
Figure 3.30. Deviation of calculated to reported consumption in per cent during one voyage leg, positive deviation indicate higher calculated than reported consumption.

3.4.3.2   Statistical analysis of simulated versus reported consumption

A statistical analysis covering 140 days with 230 reporting periods is conducted. Including all reporting periods, a standard deviation between calculated and reported values of 2.36 t consumed fuel is observed. The histogram of deviations of simulated to reported fuel consumption is presented in Fig. 3.31, clearly showing a clustering of deviations in the range of ± 2 t. Negative values indicate higher consumptions according to the logbook than simulation results. The highest deviation during the evaluated period can be found as -8 t.

In these 230 periods over all operational modes the reported consumption varies strongly. The highest consumption in a reporting periods was 237 t while the lowest were 0 t during port stays. The distribution of fuel consumptions per reporting period was:
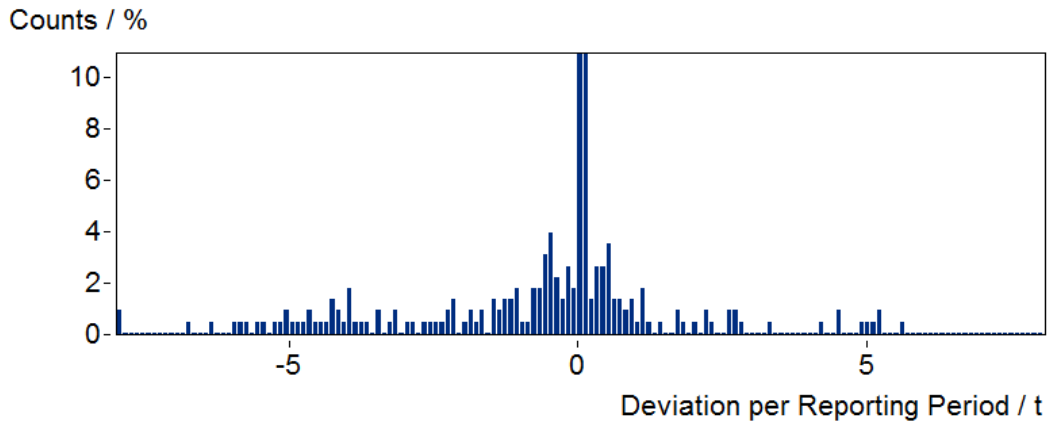
Figure 3.31. Deviation of simulated from reported fuel consumption as histogram in tons.

Consumption	Periods
0 t	10%
0-50 t	37%
50-100 t	8%
100-150 t	14%
150-200 t	21%
>200 t	10%

This wide range in consumption per period impedes an analysis of deviations in per cent of consumed fuel in that period. In Fig. 3.32 a histogram of these percentaged deviations is presented. The prominent peak of data sets at 100% deviation is caused by periods with no reported but simulated consumption. Two values, which were completely out of range, are not displayed. At simulated consumptions of 0.001 t and 0.006 t in the periods, the reported consumptions were 0.9 t and 1.3 t, respectively, which is expected to be due to different times of consumption readings and reporting or a correction between tank filling and previous readings. A time difference between reading of the fuel gauges and reporting time of just 15 minutes can result in close to 3 t difference for the engine under full load. This shows that the exact time of the reading is crucial for such a comparison. As the reporting scheme did not allow for such exact readings, time periods with higher consumptions and therefore smaller relative errors due to variations in reading times are to be compared.

An analysis of deviations in per cent is therefore done only for a subset of data, where the absolute deviation is significantly smaller than the consumption in each
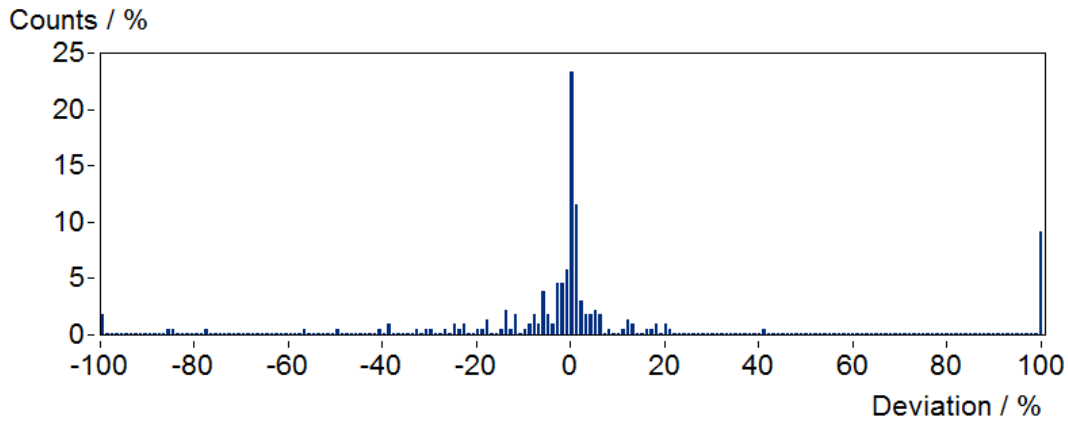
Figure 3.32. Deviation of simulated from reported fuel consumption as histogram in per cent of each period's consumed fuel.
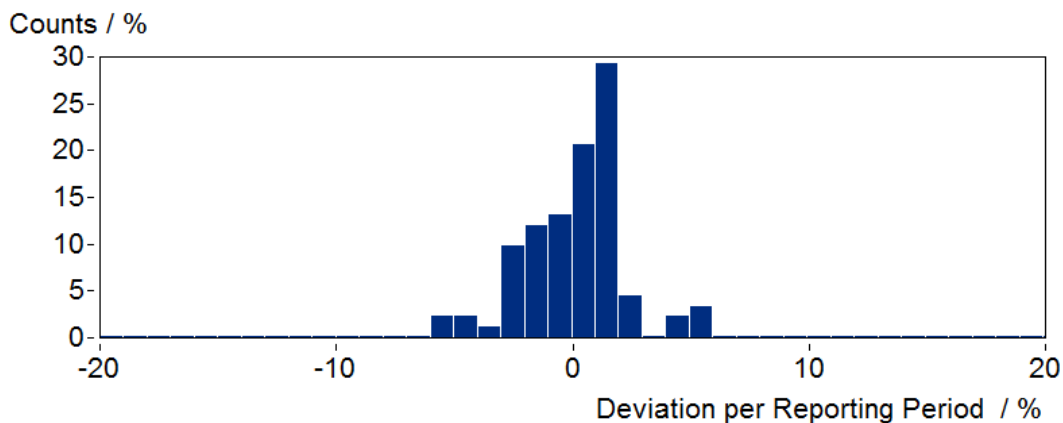
Figure 3.33. Deviation of simulated from reported fuel consumption as histogram in per cent of each period's consumed fuel, only periods with consumption >100 t.

period. Taking only reporting periods with consumption larger than 100 t, a deviation in per cent of the consumption per period can be compared and a histogram developed as displayed in Fig. 3.33. A clear distribution around the point of zero deviation indicates a good congruence of simulated with reported consumption. In these periods, an averaged relative standard deviation of 1.6% is observed, with 80% of periods in the range of ±2% and 100% within ±6%.

Beside the single reporting periods, the completed voyages from Europe to Far-East and vice versa in this time period can be evaluated. For voyages, the deviations decrease significantly, as already indicated for a voyage leg above in Section 3.4.3.1.

In Fig. 3.34, the calculated and reported consumptions of the six voyages conducted in the time period are presented. The consumption of these voyages is between 3000 t and 4000 t, with the last voyage being unfinished with a consumption of about 1000 t of heavy fuel oil.

The deviation between overall calculated and reported consumption within the whole time period is 0.70%, with a standard deviation of the voyages of 1.46%. The deviations are presented in Fig. 3.35. The highest deviation observed can be found in voyage 2, with a 2.47% higher calculated consumption compared to reported consumption from board.

Calculated Consumption vs. Reported Consumption
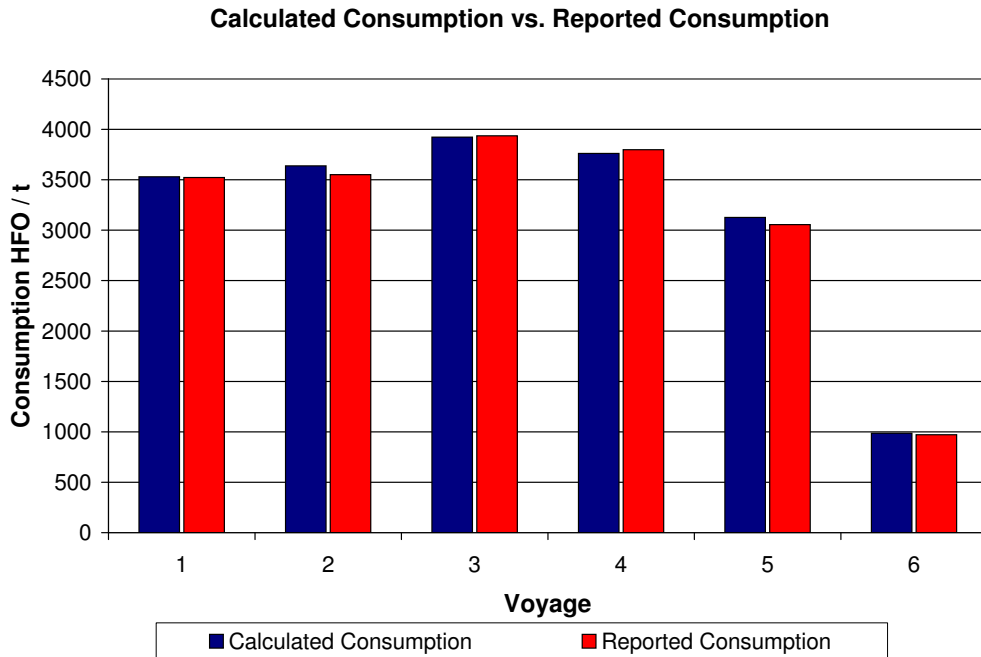
Figure 3.34. Calculated and reported consumption of complete voyages.

Deviation of Calculated Consumption to Reported Consumption
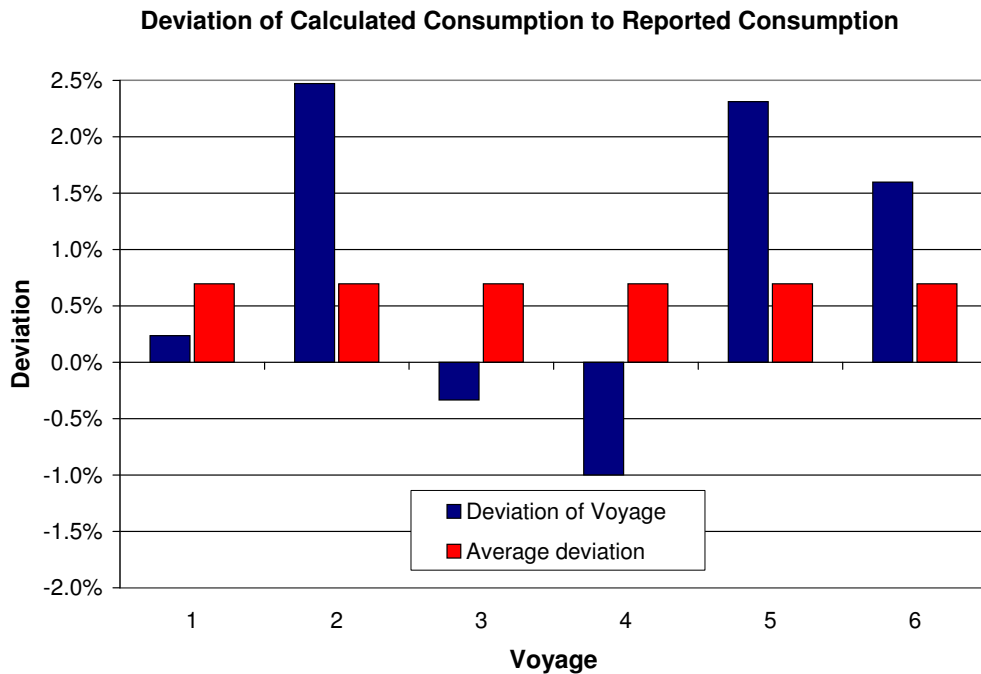
Figure 3.35. Deviation between calculated and reported consumption of complete voyages in per cent, positive deviation indicate higher calculated than reported consumption.

4 Optimization

Optimization in mathematical terms refers to solving a problem, in which an objective function $f(x)$ is minimized or maximized by systematical variation of variables. Constraints of the problem are integrated by limiting the input variables to allowed sets and output solutions to certain ranges X. Generally, the limits can be inequality and equality constraints, shown below as $g_i(x)$ and $h_j(x)$, respectively, which can be presented in short notation as [JUN2008]

$$
\begin{aligned}
\text{minimize} \quad & f(x) \\
\text{within} \quad & g_i(x) \leq 0 \qquad \text{for } i = 1, ..., p \\
\text{and} \quad & h_j(x) = 0 \qquad \text{for } j = 1, ..., m \\
& x \in X \subseteq \Re^n \qquad .
\end{aligned}
$$

The objective function $f(x)$ can be linear, uni- or multi-modal. Linear functions contain at least one optimum, which is normally located at the limit of the constraints if they are active. Unimodal functions contain one single optimum, while multi-modal functions can contain different minima or maxima or develop suboptimal minima or maxima. Sets of variables not violating the constraints are feasible solutions. The feasible solutions of an optimization form a set of solutions X, in which the optimal solution has to be determined. For the optimal solution applies

$$
\begin{aligned}
& x^* \in X, \quad \text{i.e. feasible solution} \\
& f(x^*) \leq f(x) \quad \forall x \in X \ .
\end{aligned}
$$

For non-linear problems only special cases can be solved analytically. Common methods for optimization of other non-linear cases are iterative or heuristic algorithms, for the latter e.g. genetic and evolutionary algorithms as well as particle swarm optimization can be used.

Problems described by two or more objective functions require multi-objective optimization, where a conflict of functions regarding the optimal solutions can occur, as one function impairs the optimization of the second. The process of optimization results in a range of feasible solutions, forming a border of optimal solutions depending on the objective functions, called *Pareto Frontier*. Solutions lying on this border are Pareto optimal solutions, i.e. it exists no solution that is best in regard to all objective functions and a trade-off between them has to be done [HIN2007].

Optimization in thermodynamics aims at the minimization of inefficiencies, which can be described with exergy destruction and exergy losses in the processes [BTM1996]. One step further, the thermoeconomic or exergoeconomic optimization incorporates the costs related to inefficiencies as well as to higher efficient equipment for minimized overall costs.

The multitude of internal and external effects in vessel operation that have to be taken into account complicate the definition of distinct target functions with clear constraints. For an optimization using the above presented mathematical methods, a detailed description of the systems and their behavior depending on system load and external effects have to be developed, including all relevant alternative configurations and components. This is considered impossible to be globally done, as real operational data are to be evaluated for application at existing vessel. For this reason, the optimization processes are mainly executed manually with direct comparison of results from distinct changes in operation and machinery.

4.1   Optimization in Energy Systems

In engineering of large energy systems, the reaching of an absolute optimum is not possible except for special cases, but an optimization in relation to the different objectives and external constraints may be achieved. These constraints, as mathematically described above, can be of constructional, operational, legal as well as economic nature. The clear definition of a system boundary is the first step in an optimization, including all subsystems that significantly affect the performance. For a complex system it can be beneficial to break it down into smaller subsystems, which are then optimized individually. Especially in these suboptimizations, setting of system boundaries can affect the results and hence requires particular attention [BTM1996].

Optimization can be applied to both optimization during design phase of an energy system as well as during operation of energy systems. While the overall approach can be considered comparable, degrees of freedom to choose between options are more limited in already operating systems, as usually main components are fixed and can not be exchanged with reasonable costs. In the presented work, optimization is limited to already operating systems and the inherent complications through inefficient but not economically exchangeable machinery.

For the given challenge of optimization of a vessel's efficiency in operation, the optimum may be determined as minimized energy input per achieved work of trans-

ported goods. The target function to be minimized may be the exergy or power consumption for a given transport work, which can be arbitrarily separated in propulsion power, auxiliary power and cargo care requirements. A refinement of the aim may lead to energy conversion at best point operation of machinery and optimum efficiency of consumers, potentially including different machinery arrangements. On consumer side this includes not only efficiency of the consumer in its work, but also the question if the consumer's work is required for the vessel operation has to be evaluated.
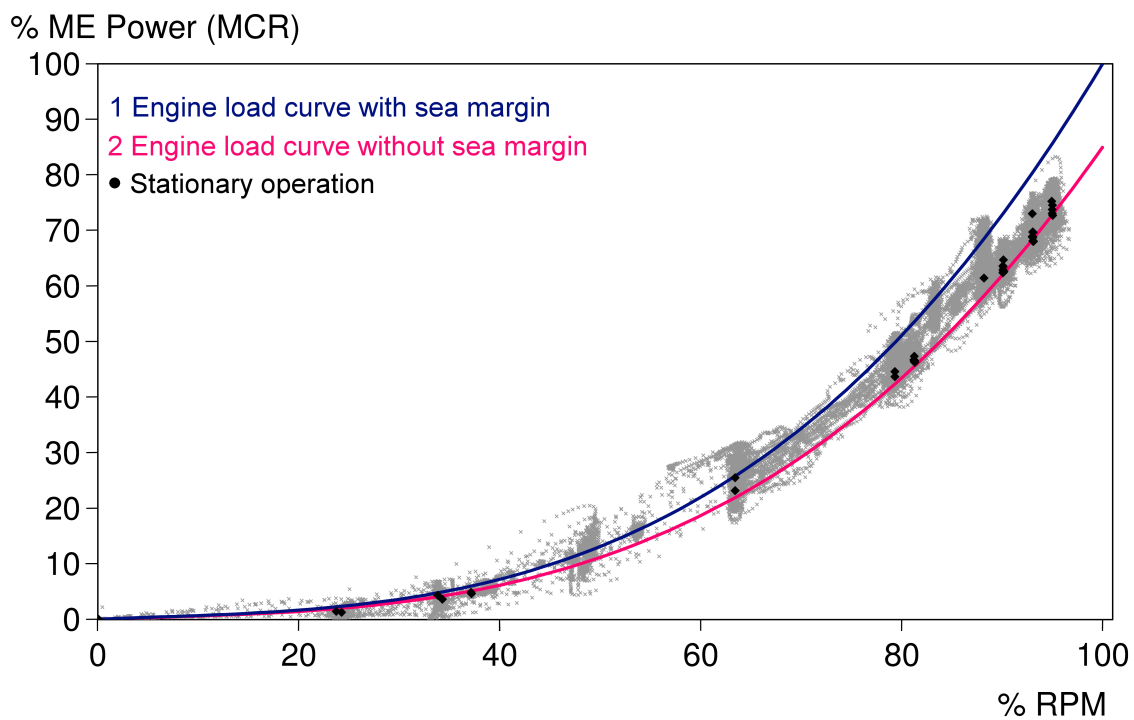
Figure 4.1. Propulsion diagram of main engine power over rotational speed, engine load curves and points of stationary operation.

The determination of the current performance is the first step in an optimization process of an energy system. At a large energy system, the energy and exergy balance can often not completely be covered by the available measurement systems and not all systems can be represented by transient, physical models. Stable, stationary operational points can be used to determine the current conditions of the systems and to compare these with reference values and baselines. Hence, an on-line performance analysis requires determination of stationary conditions of the energy system and of subsystems, as presented e.g. by Adamietz et al. [ALS1999] for power plants

and Omar [OMA2009] for ship diesel engines.

For a vessel's main engine even constant operation at open sea does not automatically mean stationary operation with exactly constant power and rotational speed. During normal operation, cyclic changes in power consumption of about 1-2% MCR are commonly found in measurement of high time resolution, at a frequency of 2-5 minutes. Therefore stationarity has to be defined as periods with least variance, which were here filtered based on variation of main engine power and rotational speed. The required power for a given rotational speed varies at a normal measured propulsion diagram with the changing resistance of the vessel, compare e.g. Fig. 3.4. In case of the test vessel, the variations are well between the engine load curves with and without sea margin. Reducing the scatter of all operations to only points of stationary operation shows a close following of the load curve without sea margin. This is presented in Fig. 4.1, where the points of stationary operations are marked as black dots.

An interesting result is that when removing these unstable operations, which are caused e.g. through accelerations, waves and wind, only minor differences from a given load line are observed. As the vessel displacement was not constant over the time but varied between 70 000 t and 100 000 t, the power variation through changes in displacement are small compared to weather and other influences.

Numerical methods offer chances to analyze scenarios and influencing factors with comparable small efforts. Not available or hard-to-acquire values describing the system behavior can be determined based on available data using physical or empirical models. Prior to actual modifications to machinery systems, different configurations can be analyzed without the need to alter the original system. By deploying identical influencing factors and conditions, the variants can be directly compared and their effects quantified. Numerical methods, on the other side, comprise risks that have to be kept in mind when analyzing results. Inaccurately measured or prepared input data will inevitably result in inaccurate output data. If simulation models are validated to accurately reproduce the physical behavior of the system, but the input data are not checked with the required diligence, the results of a simulation may be misleading without being noticed. In addition, boundary conditions of a modeled system can have significant influences. If relevant boundary conditions are not or inaccurately captured, the simulation results can not represent the reality. The advantages of numerical methods are outweighing the potential risks. As only simulation model allow for the analysis and direct comparison of a multitude of variants for optimization of a system, such evaluations of variants and optimization

would not be feasible with modifications at the real systems.

In the following, an example for optimization using the developed simulation described in Section 3.2 will be presented. For a holistic view, not only the mechanical power for propulsion and the related efficiencies in the main engine, but also the provision of the required electrical power has to be analyzed. The related exergy flows of the test vessel at a typical operation of 50% MCR of the main engine is presented in Fig. 4.2 as Sankey diagram [WÄR2008] [MAN2005b]. For illustration, the diagrams of main engine and auxiliary engine exergy flows are not printed to scale. Instead, their axes and the percentages of the exergy inflows are displayed. At 50% ME MCR, about 44.5% of the fuel's exergy are converted to mechanical
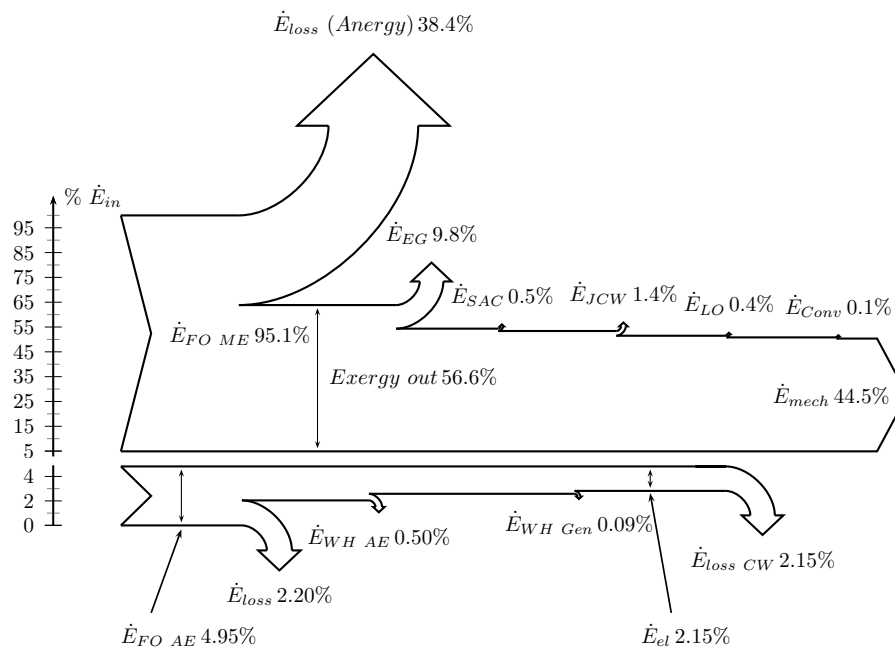
Figure 4.2. Sankey diagram of the vessel's exergy flows at 50% MCR of the main engine, diagrams of main engine (top) and auxiliary engine for electricity production (bottom) not to scale.

power, while the electrical power demand of the auxiliary systems are about 2.15%, requiring about 5% of the fuel's exergy for its generation. The electrical power demand of the vessels auxiliary systems can be considered independent of the main engine power with a relatively constant value, except for very low loads, compare Section 4.2 below. At higher main engine power the percentage of electrical power is therefore smaller, but comprises comparable saving potentials in terms of absolute

energy and exergy. This is demonstrated in Fig. 4.3, where a Sankey diagram for
the engine is shown for vessel operation at 75% ME MCR. Here, the electrical power
demand is about 1.49% of the fuel exergy, but it results in the consumption of 3.42%
of the fuel's exergy for power generation.
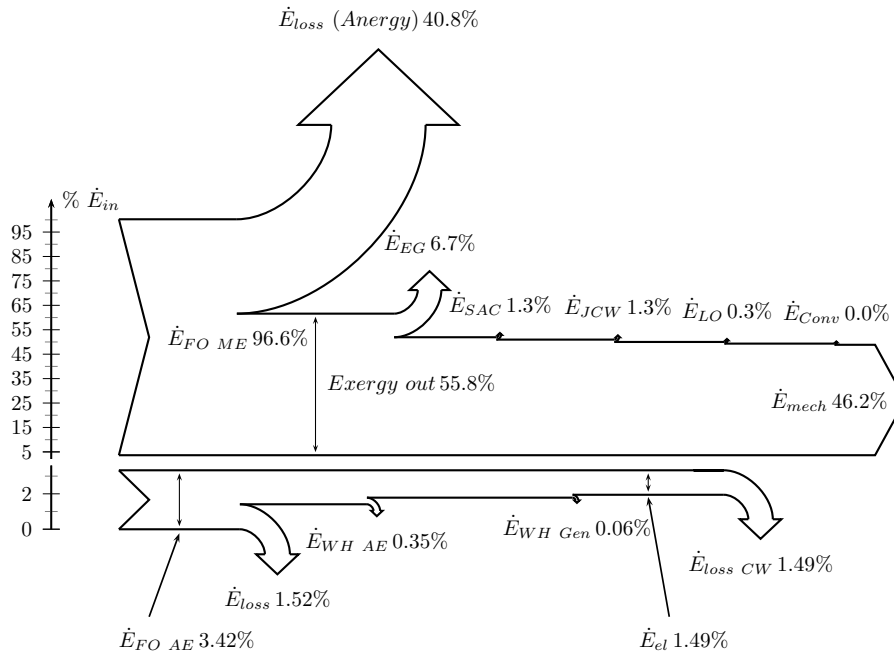
Figure 4.3. Sankey diagram of the vessel's exergy flows at 75% MCR of the main engine,
diagrams of main engine (top) and auxiliary engine for electricity production (bottom) not
to scale.

The mechanical power propels the vessel and contributes therefore directly to the
vessel's purpose of transporting goods. Unlike, the electrical power is not directly
contributing to the transport work but while it is being used, e.g. for electrical
motors and lighting, it is dissipating within the vessel and ultimately transferred
into cooling water and air. Therefore, for optimizing the vessel's exergetic efficiency
without restricting the transport work, the target function is the power consumption
of auxiliary systems for main engine operation. This can be described as minimiza-
tion of "parasitic" exergy consumption not directly required for the ship machineries'
main function, the propulsion.

4.2   Variation of the Machinery at given Operational Profile

The electric power consumption aboard the test vessel accounts for about 7-10% of the vessel's overall fuel consumption. Electric power can be considered as pure exergy, which indicates its value and the necessity of a sensible usage. For an optimization of the operation, the target function is therefore the minization of electric power consumption for a given transport demand. This transport demand can be defined as transported goods over a certain distance with a certain vessel speed, which defines a required propulsion power demand and cargo care within changing external influences.
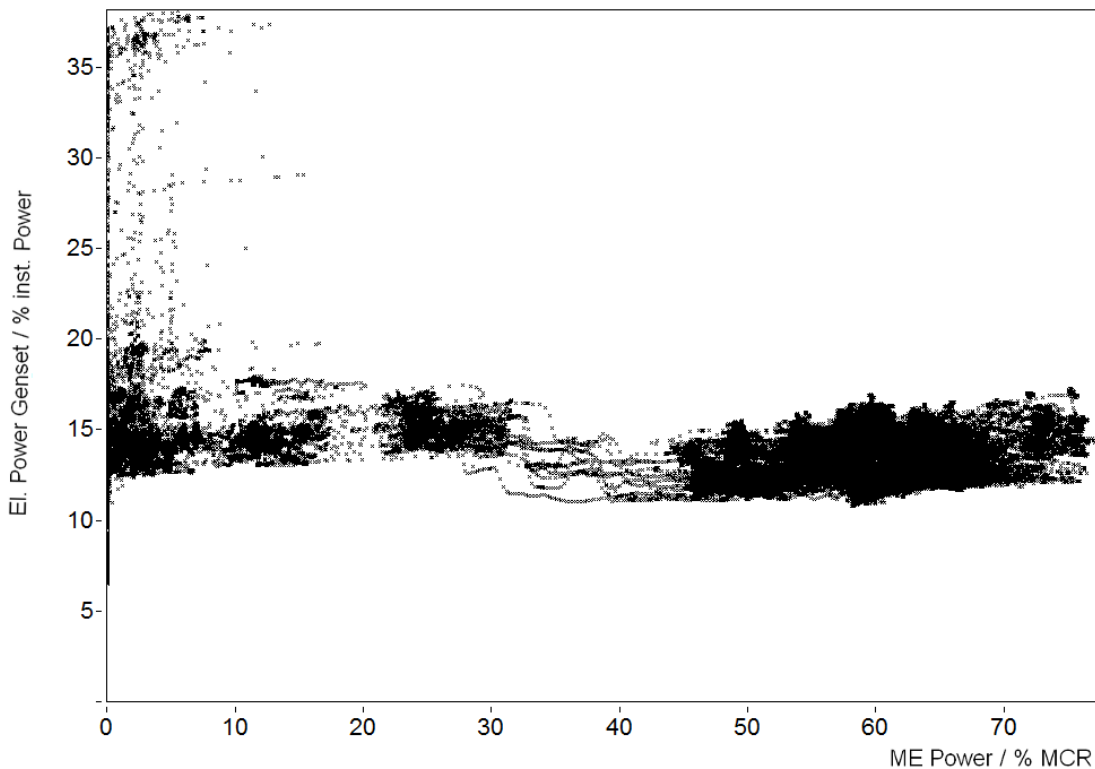
Figure 4.4. Consumed electrical power plotted over main engine power from onboard measurement over one month, each dot representing an averaged period of 10 s.

To determine the relation between main engine power and the required electrical power for vessel operation, a x-y plot of main engine power versus corresponding electrical power is evaluated. These data are presented in Fig. 4.4 as the black dots. Aside from a step in electrical power consumption between 30% and 35% main engine power, which will be explained below, no interrelation can be found, with a

constant power consumption of about 15% of the installed power. This low load in comparison to the installed power is explainable by the vessels reefer container carriage capability, which was not utilized during the measurement campaign. Having in mind that the largest consumers with high operation time aboard the vessel are auxiliaries for the main engine (compare Section 2.3), an efficient operation would be expected to have the auxiliaries operated depending on their demand. The step in power consumption at low main engine power is caused by operation of the auxiliary blowers, which provide scavenge air for the engine at low engine loads, when the turbo charger does not provide sufficient pressure.

The required amount of cooling water, lubrication, fuel oil and combustion air depend technically on the main engine power, whereas the constant electrical power consumption demonstrates that the equipment is operated at constant power, with their set point at maximum load. The target function in this case can then be defined as the minimization of power consumption at safe operation of the main engine with provision of required amount of cooling water and air.

Power for pumps and fans are defined by the operation pressure, which is required for overcoming the flow losses in the tubes, ducts, and armatures and systems [JUC1992], [SCH1986]. For pressure loss reduction, different possibilities exist. Pressure losses are induced by flow resistances, which are caused by friction in piping and the resulting velocity field in the flow, loss of momentum in bendings, and in orifices and valves. Pressure loss through pipe friction can be calculated by Eq. (4.1) [DGF2005]

$$\Delta p = (\lambda \cdot l/d) \cdot \rho \cdot v^2/2 \ . \tag{4.1}$$

The friction factor λ depends on the Reynolds number Re and the tube's surface roughness. λ can be calculated by equations of Nikuradse and Colebrook, which are also available as pre-calculated diagrams. The tube's length l and diameter d are factors for the geometry and density ρ defines the fluid. The importance of the fluid's velocity v is emphasized by its squared appearance in the equation.

The pressure drop can strongly be reduced by reduction of flow velocity, which depends on tube cross section area A and mass flow:

$$v = \frac{\dot{m}}{A \cdot \rho} \ , \tag{4.2}$$

in case of a circular tube

$$v = \frac{4 \cdot \dot{m}}{d^2 \cdot \pi \cdot \rho} \ . \tag{4.3}$$

Considering the surface roughness and fluid properties as invariable, the pressure drop can be reduced by reduction of the fluid's velocity, which is obtainable through increased tube sectional area or decreased mass flow. Optimization by improved piping in the vessel is part of a vessels constructional design process and therefore not further evaluated in this work. In contrary, reduction of mass flow is an operational measure that can be realized if the present vessel operation and external conditions allow for it, which will be further analyzed.

The potential of saving in power consumption through frequency control of cooling water pumps and engine room fans is evaluated in a first approach by a simple model of power consumption and affinity laws. From the vessel's Electric Load Analysis, the electric power consumption of pumps and fans are known. The required amount of cooling water and combustion and cooling air are determined to be as designed at engine maximum continuous rating (MCR), but to be linearly reduced to 50% of its design mass flow at 0% MCR. The 50% of mass flow can be considered a conservative value for saving potential estimation, incorporating minimum flow for prevention of fouling and potential additional cooling requirements in the engine room. Due to the affinity laws of pumps and fans with the third potency dependency of power consumption to volume flow (compare Section 2.3.3.3), the power consumption is reduced from 100% of design power at 100% MCR to 12.5% of design power at 0% MCR.

The operational profile of the vessel's main engine presented in Fig. 3.23 emphasizes the potential in main engine power depending auxiliaries. As the vessel is operated during the measurement almost half of the time between 40% and 60% MCR and never above 85% MCR, the auxiliary systems without load adaptation are running far from their design points and comprise therefore significant saving potentials.

In this evaluation, main cooling sea water pumps, low temperature cooling fresh water pumps, and jacket cooling fresh water pumps with a combined constant design power according to the Electric Load Analysis of about 435 kW are included, additionally the engine room vent fans with a combined power of 250 kW. In the calculations, these auxiliary systems' constant power consumption of 685 kW is subtracted from the current consumption and the main engine load depending power consumption of the systems as described above added instead. These calculated data are shown in Fig. 4.5 as pink dots, with a clear increase in power consumption with main engine load. The resulting savings as a function of main engine load can be found in the figure as gray line.

At 50% MCR, the power consumption of the selected auxiliaries is reduced by
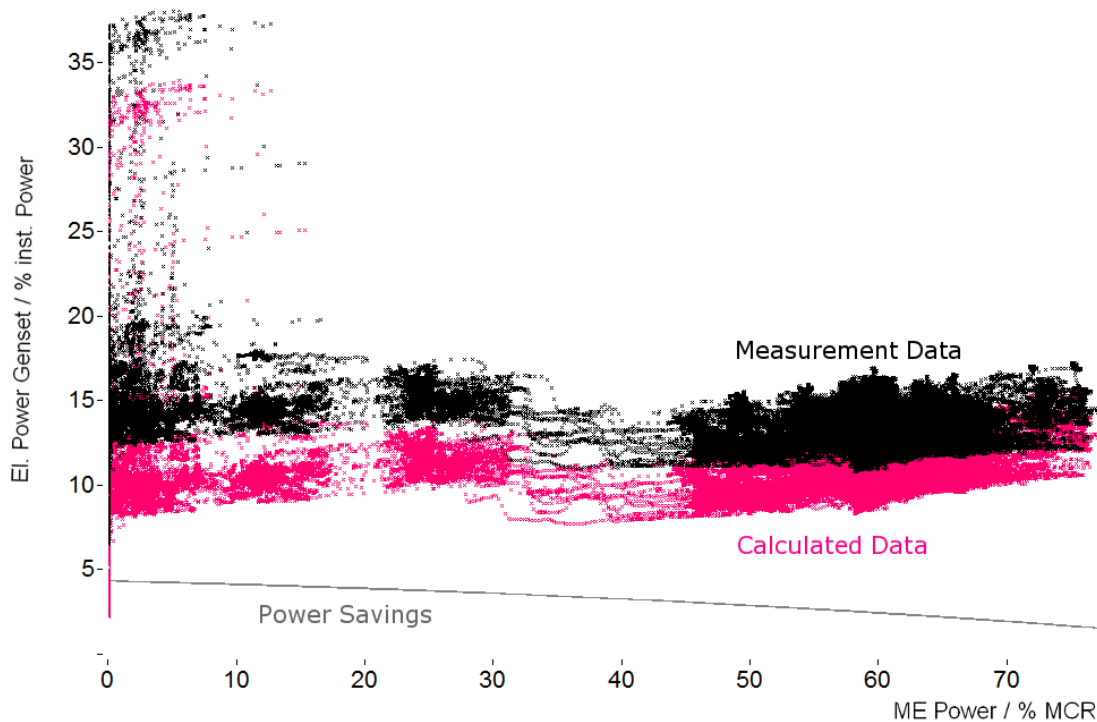
Figure 4.5. Consumed electrical power versus main engine power from onboard measurement (black dots) and with calculated reduced pumping power (pink dots) and resulting savings (grey line).

almost 400 kW, being 3% of the installed auxiliary power. The maximum can be found very close to 0% MCR of main engine with a calculated saving of more than 500 kW or 4% of the installed auxiliary power. A decrease of pumping efficiency through off-design operation and losses in frequency converters are in this evaluation not considered, but can - if quantified - be included without further efforts.

The cost of electricity aboard can be displayed as function of fuel oil prices and generation efficiency. Including generalized maintenance costs based on [W2007] and [EGE2010], this graph is shown in Fig. 4.6. Taking an average cost of 0.14 US $/kWh, the saving over the calculated month of operation shown above accounts to approximately 21000 US $. This points at the economical potential of fuel saving on board by optimized control of the machinery, which is strongly increasing with the use of expensive refined fuel oils for consumption in Emission Control Areas (ECA) and proposed additional surcharges for carbon dioxide emissions.
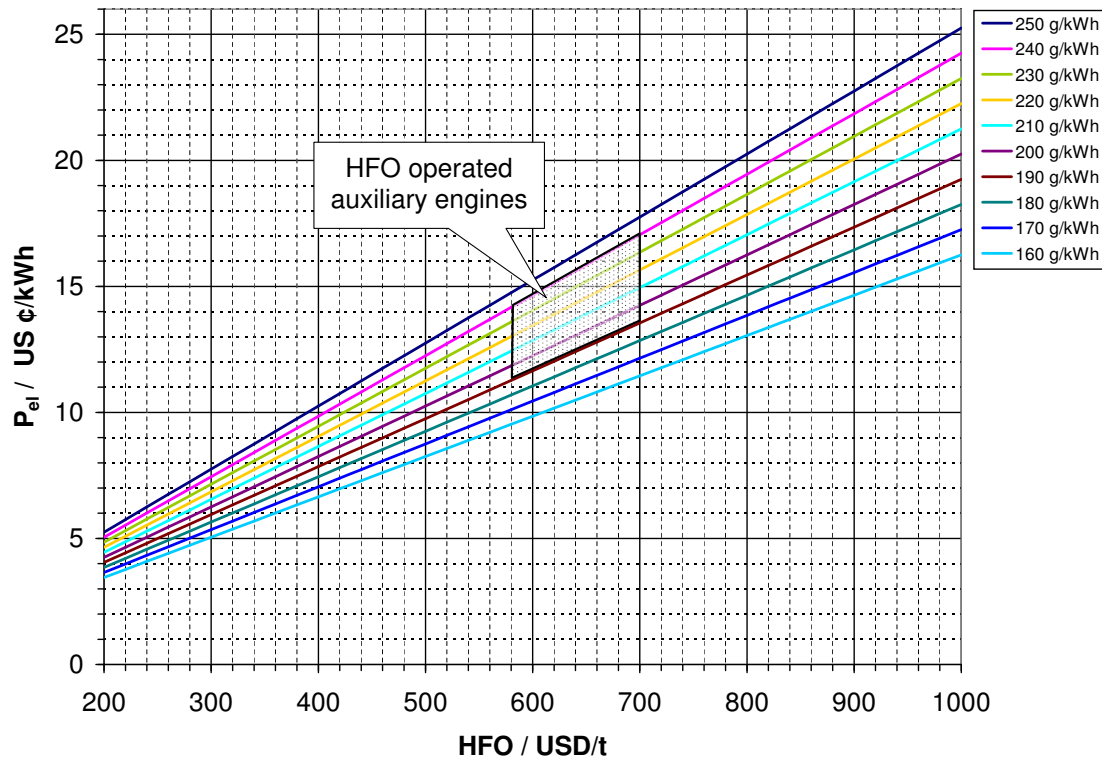
Figure 4.6. Cost of electricity production aboard depending on fuel oil prices and generating efficiency.

4.2.1   Savings through frequency controlled main seawater pumps

A second approach for power reduction can be found by evaluation of the design parameters for the cooling circuits described in Section 2.3.3.3. The systems are designed for providing the required cooling at 100% MCR of main engine in tropical waters of 32 °C. In Fig. 4.7 and Fig. 4.8, exemplary timelines of sea water temperatures for a trans-equatorial trade and a Europe-Far East trade, respectively, are displayed. Even in the seasons of the highest sea water temperatures, the average temperatures are only 20 °C and 28 °C and therefore significantly below design temperature. Savings through reduction in heat discharge due to lower main engine power than design case can be estimated for evaluations without simulations using timelines of main engine power from onboard longterm measurements as presented above. In contrast, more detailed evaluations with the combination of required cooling water for heat dissipation at prevailing sea water temperature of a given

journey has to be calculated by deploying a simulation model. This detailed evalua-
tion enables furthermore to incorporate the changing efficiency in energy conversion
within the engine, which results in changing amount of heat flows into cooling water
depending on engine load and ambient conditions.
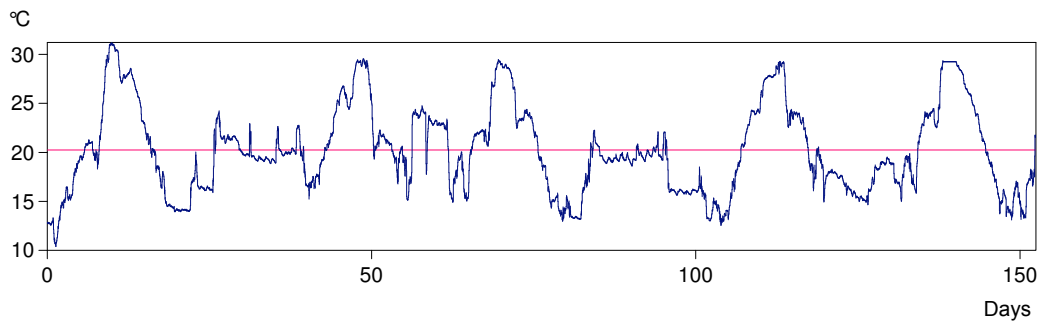
Figure 4.7. Sea water temperature over 160 days of trans-equatorial trade (spring to
autumn northern hemisphere, blue line) and average temperature of 20.3 °C (pink line).
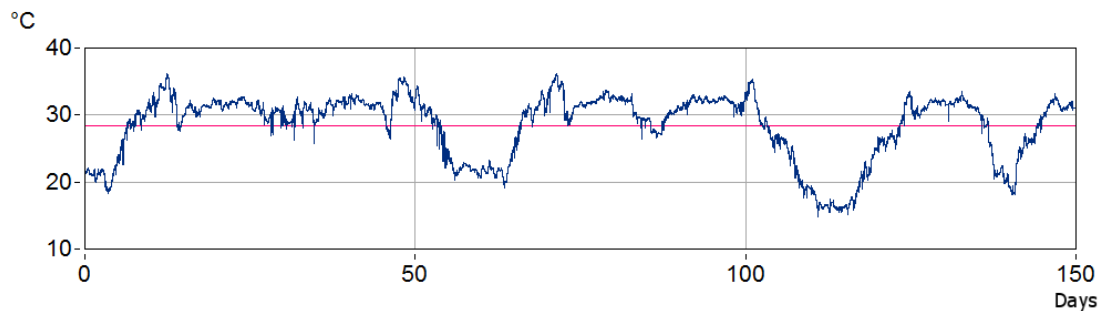
Figure 4.8. Sea water temperature over 150 days of Europe-Far East trade from July to
December.

The simulation models of the engines generate waste heat flows into cooling wa-
ter as output, compare Section 3.2.1.1. In a simulation this is used to calculate the
required mass flow of cooling sea water within restrictions through temperature and
flow limits. Due to the high corrosivity of sea water at elevated temperature, litera-
ture recommends to keep the cooling sea water temperature below 50 °C [MBA2006],
[HD1985]. Furthermore, low velocities in cooling water system caused by low mass
flow compared to nominal flow can cause fouling, colonization of crustacean and
sedimentation in the system, which has to be prevented. When keeping the output

temperature at a fixed set-point temperature, the mass flow in cooling water system would be reduced to very low flow rates at low inlet temperature and low heat inflow. This was taken into account by introduction of a minimum flow, which is recommended in literature to be kept at all times at least above 25% of nominal flow [NH2008]. Based on this, the lower limit in the presented evaluation was set to 35% (1000 m^3/h) of nominal flow in the system as a conservative value above the minimum flow.

In a pump circuit, the operating point is determined by the intersection of pump characteristics and the system characteristics. The test vessel's pump characteristics of the main sea water cooling circuit is presented in Fig. 4.9 based on manufacturers specifications and consultations [WOL2011]. The system as running on board of the vessel is shown as the top curve, with the design point flow of 2900 m^3/h at 1.8 bar provided by two pumps in parallel. The system characteristic is displayed as the pink curve. This characteristic of system pressure loss depending on volume flow, compare also Eq. (4.1), can be described by the parabola

$$H = a \cdot Q^2 + H_{stat} \quad , \tag{4.4}$$

being H the pump head to overcome the pressure loss, Q the volume flow, H_{stat} the static pump head of the system, and a the fitting parameter defined by the design point and the static pump head H_{stat}. Using the pump manufacturers specifications, the required pumping power for states along the system characteristic can be determined and implemented in the simulation. In the graphic, the pump characteristics at 75% and 50% nominal pump speed are additionally displayed for single pumps and two pumps in parallel.

The system characteristics show that the reduction in volume flow through switching off one pump would require throttling for adjustment of the pump characteristic to the system characteristic, as the single pump characteristics are not intersecting with the system characteristic. Instead, the maximum flow of one pump is reached on a higher pump head, which requires a throttling to the system pressure. The losses through throttling are estimated to be higher than the operation of the second pump in parallel. Therefore, the savings through speed control of both pumps in parallel is evaluated in the simulation.

The taken set of measurement data represents journeys from northern Europe to the Far East of 150 days from July to December. The time includes the months of highest sea water temperatures, which are presented in Fig. 4.10. Sea water temperatures reach up to 36 °C when passing Suez in summer, which is even above the

**Centrifugal Pump Operation with Variable Speed
and Cooling System's Characteristic Curve**
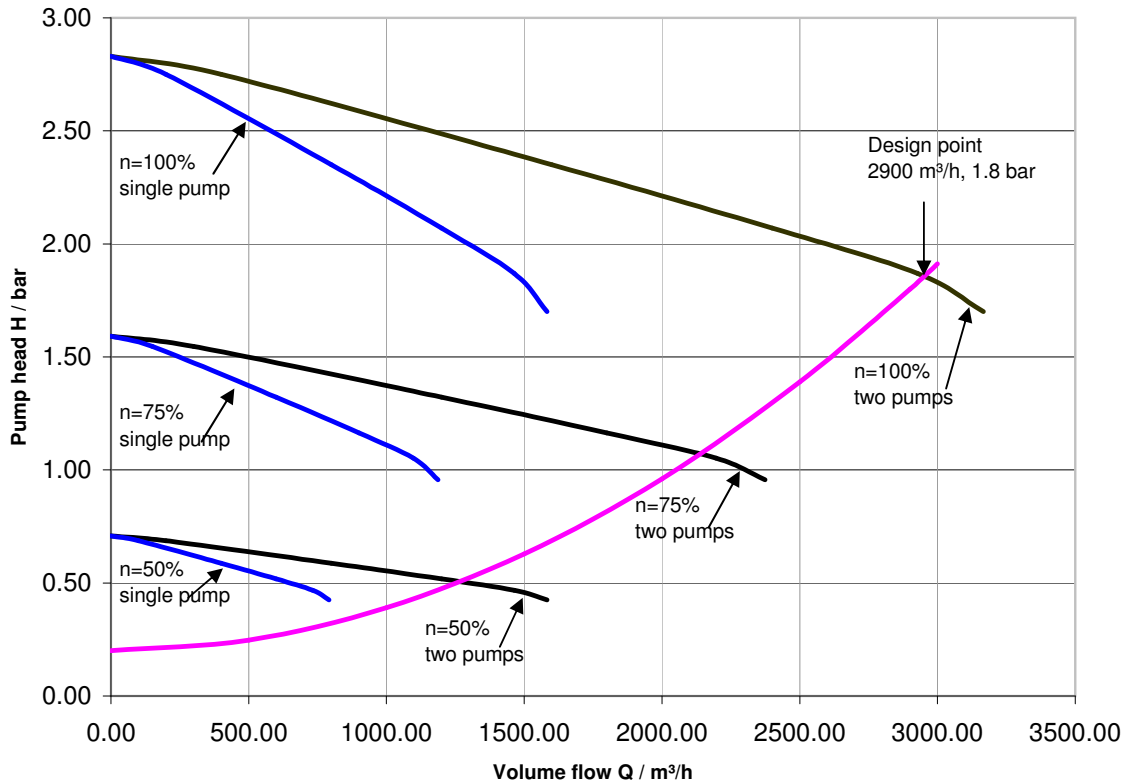
Figure 4.9. System characteristic and pump characteristic of the cooling system [WOL2011].

design criteria for tropical waters, compare above. Savings are therefore expected to be higher from December to July, when the sea water temperatures are lower in the oceans of the northern hemisphere. Additional heat sources to be accounted for in cooling water balance are auxiliary engines, steam condenser and fresh water generator condenser cooling. While the latter is considered negligible, the steam condenser is not taken into account but may be included in further evaluations. The steam condenser is built for condensing excess steam at 100% ME MCR in tropical waters, which is the operation of highest steam production and lowest heating demand. Due to the low engine power and low temperatures during the evaluated period, the amount of excess steam is expected to be neglible. Auxiliary engine waste heat flow

is estimated based on produced electrical power and taken into account as 1500 kW constant heat flow.
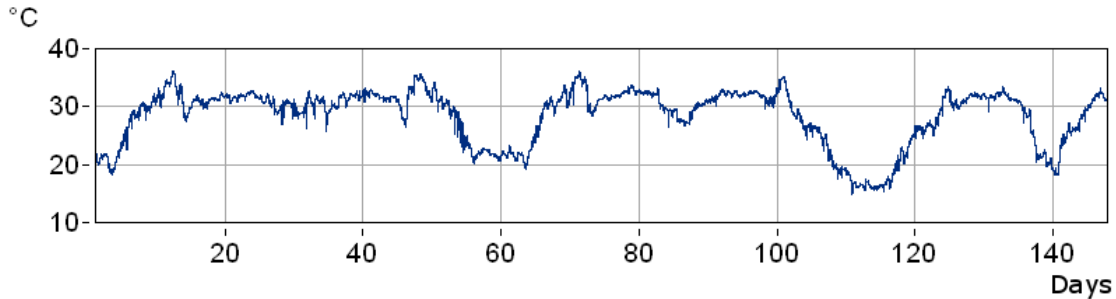
Figure 4.10. Sea water temperature on Europe Far-East trade over 150 days from July to December.

That the saving potential in cooling water exist even though the sea water temperatures reach higher temperatures than originally designed for is mainly caused by lower main engine power and therefore lower heat flow into the cooling system. In Fig. 4.11, the timeline of main engine power is presented. Main engine power during sea passages is mostly between 40% and 60% MCR, with regular peaks to 75% MCR and only three peaks of power up to 85% MCR.
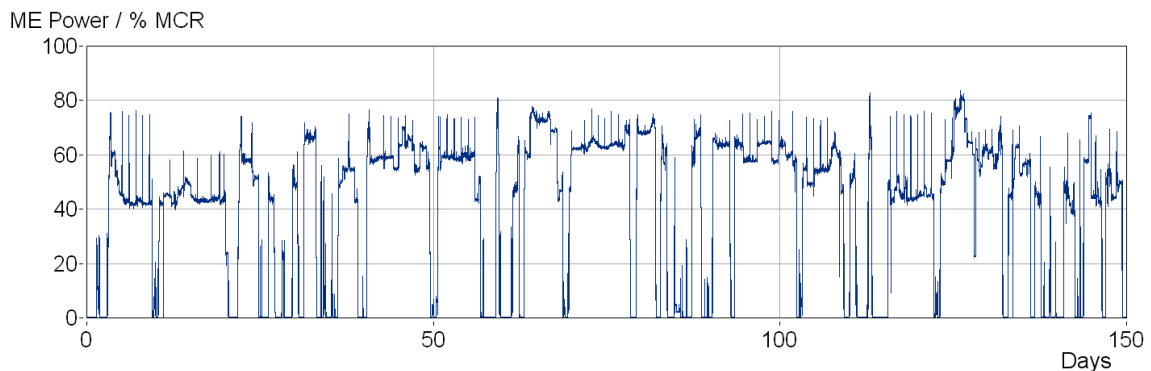
Figure 4.11. Main engine power on Europe Far-East trade over 150 days.

The installed cooling sea water pumps have an constant power of 91 kW each according to manufacturer data and Electric Load Analysis. During sea passage two pumps are running in parallel with combined 182 kW, while in port only one pump remains running. The required power of the installed pumps can be found in Fig.

4.12 as pink line. The power consumption of the simulated frequency controlled pumps as described above are displayed in the same graphic as blue line, with the minimum of 20 kW. Peaks of high main engine power are clearly visible as well periods of high sea water temperatures. Compared to the original pumps, the frequency controlled pumps require significantly less power, with an average power of 30 kW compared to 163 kW of the uncontrolled pumps as installed on board of the vessel. During the 150 days, the required volume flow doesn't exceed 2300m^3/h, or 100 kW pump power. This is considered low, as the water temperature reaches up to 36 °C and main engine power up to 83% MCR.
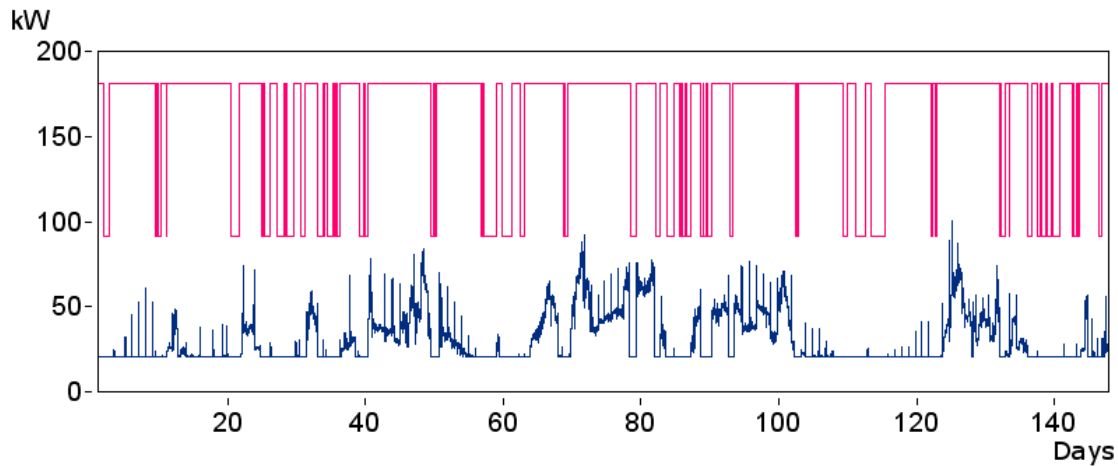
Figure 4.12. Electrical load of original sea water pumps (top, pink line) and simulated frequency controlled pumps (bottom, blue line) on Europe Far-East trade over 150 days from July to December.

The consumed electrical energy of originally installed pumps and frequency controlled pumps are determined with the simulation of the 150 days period from July to December. The results are presented in Table 4.1. Beside the consumed electric energy, the efficiency chain in power generation has to be taken into account. The generated electric power, which is an exergy flow, is provided by diesel generators. The associated exergy demand, expressed in terms of consumed fuel for electricity production, is determined based on Eq. (3.17). In this evaluation, an average specific fuel oil consumption of 215 g/kWh$_{el}$ and an average lower heating value of the fuel oil of 40.5 MJ/kg is taken for direct comparison of the variants.

The savings in fuel exergy are about 4411 GJ or 82% of the consumption of the original system. Considering costs for generated electricity of 0.14 US $/kWh based

Table 4.1. Consumed electrical energy in cooling sea water pumps as installed on board of the test vessel compared to simulated frequency controlled pumps.

	Average power		Consumed el. energy	Consumed fuel exergy
Original system	Sea passage:	182 kW	592 MWh	5395 GJ
	Port:	90 kW		
Freq. controlled pumps		30 kW	108 MWh	984 GJ

on a fuel oil price of 650 US $/t$_{\text{HFO}}$, compare Fig. 4.6, the savings in operating costs are 67760 US $. These savings in the simulated 150 days in Europe-Far East service have to be compared to the investment for retrofitting the required frequency converters. The investment is estimated by the pump manufacturer to about $35000 [WOL2011], but maintenance costs related to the frequency converters are unknown. These assumptions lead to an expected return on investment within 3 months.

The almost non-existence of frequency controlled pumps on board vessels raise questions about the reasons, as all studies show high savings [ALL2010], [NH2008], [JUC1992], [HD1985]. Ship owners so far show a reservation against frequency controlled pumps installed on board their vessels. Main reasons are expected to be [WOL2011]

- reliability: introduction of additional electronic components increase susceptibility to failure at a vital component (cooling system),

- grid interferences: induced problems at earlier models; according to manufacturers, grid feedback interferences are compensated with the latest technology,

- retrofitability: space limitations and implementation in existing automation systems may impede retrofitting in some vessels,

- maintenance: additional component to be maintained,

- fouling in cooling water systems: due to decreased flow velocities in the cooling water system, sedimentation and organic fouling may result; this is considered in the model with an minimum volume flow of 35%,

- non-standardized equipment: if the system is installed only on few vessels, crews are not acquainted to the system and require special training and spare parts.

These problems are expected to be overcome with improved reliability proved in onshore installations and growing numbers of installations on board.

4.2.2 Detection of "Hidden" Losses of Energy and Operational Improvements of Energy Efficiency

The acquired real operational data from board enable to pinpoint and improve even small details. An example for the combination of efficiency optimization in energy conversion and consumption in such a detail can be found in the power demand through small but constant losses. Beside the starting air for the engine, pressurized air is used for valve control, tools, and machinery and stored in pressure vessels. When unused, there are constant losses in the armatures of the tubing system for air distribution and at leaking components, which demands a frequent refill of the pressurized air storage. This refilling is done by air compressors, consuming at the test vessel about 110 kW in operation. In time lines of electrical power consumption, this demand for leakage air can be found as periodic peaks of the mentioned 110 kW, which are identifiable in Fig. 4.13 as highest peaks every 80 minutes. The smaller peaks in between are cause by periodic machinery operation not further investigated.
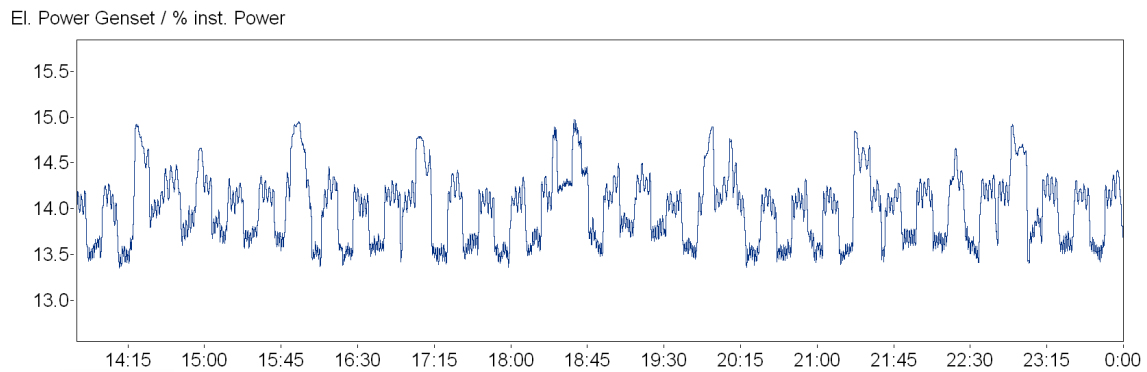
Figure 4.13. Detail of electrical power consumption with prominent frequent peaks.

The efficiency of the compressed air system is therefore depending on the air compressor's efficiency and, even more, depending on the leakages in the compressed air system. For optimization of the operation, leakages should be regularly identified and repaired. Additionally, it can be investigated if the exchange of pneumatic valves to electric valves is economically feasible. For this, savings in electric energy,

air compressor maintenance and even generator and auxiliary engine maintenance have to be compared to the investment for electric valves.

An example for improvements in vessel efficiency through reevaluation of external constraints can be found in higher yield of waste heat recovery due to operation with low sulfur fuel oils. The sulfur content of the fuel oil is oxidized during combustion to the sulfur oxides SO, SO_2 and SO_3 (combined: SO_x), with the fragmentation depending on the combustion. In combination with water vapor of the exhaust gas, between 3% and 5% of the SO_3 form sulfuric acids [FIL2006], which elevate the dew point significantly. Condensation of sulfuric acids from exhaust gas cause low temperature corrosion on the waste heat boiler and funnel and is therefore to be prevented by keeping the lowest temperature on waste heat boiler tubes and funnel above about 160 °C [BRO1988]. The sulfuric acid dew point, which sets the achievable lowest temperature on the waste heat boiler tubes and therefore the recoverable waste heat from exhaust gas, decreases when the sulfur content in the fuel oli is reduced. Current initiatives of legislations are to establish new (Sulfur) Emission Controlled Areas (ECAs) worldwide and tighten existing ECAs (compare Section 2.2.2). Vessels will be required to burn only low sulfur fuel oils as their routes are within an ECA, if they do not retrofit exhaust gas scrubber systems. These vessels comprise the potential to reduce the economizer water inlet temperature, which is the lowest temperature in the exhaust gas waste heat recovery boiler, and that way increase the recoverable heat. The lowering of the minimum temperature from 160 °C to 120 °C would increase the available heat from exhaust gas significantly. For ideal gases at constant pressure, the difference between inlet and outlet temperature defines the heat flow $\dot{q}$ with the mean isobaric heat capacity c_p,

$$\dot{q} = c_p \cdot (T_{out} - T_{in}) \quad . \tag{4.5}$$

Depending on boiler characteristics and achievable heat transfer coefficient, the increase in temperature difference can be estimated to increase the recoverable heat about 30% for a typical exhaust gas temperature at boiler inlet of 300 °C. This higher yield from exhaust gas can be used in a waste heat recovery system for substitution of running diesel generator, in case of diesel-electric machinery or of an installed power take-in (PTI) on the shaft, the generated power can be used to partly unload the main engine and increase therefore the efficiency in propulsion.

4.3   Exergoeconomic Target Function

Beside the thermodynamic optimization, which aims at maximizing the efficiency of processes, exergoeconomic optimization deals with the minimization of costs [BTM1996]. In exergoeconomics, two objective functions are included, which are typically of opposing character. Operational costs are bound to thermodynamic efficiency and related to exergy destruction and losses, while capital costs are related to the machinery and exchange of components, which typically increase for higher efficient components.

Tsatsaronis describes an approach for quantification of avoidable and unavoidable exergy destruction and corresponding investment costs [TP2002], dealing with the dilemma of exergoeconomics that increasing efficiency is usually associated with increasing investment costs and thus the component of lowest specific fuel expense *and* lowest specific investment cost has to be identified for achieving the lowest cost of product exergy. The components of a thermal system are evaluated and accounted for separately, for which capital cost curves depending on component efficiency are used. An example calculation for a cogeneration system can be found in [TP2002].

This concept of exergoeconomic optimization is based on market research for all components to be included in the evaluation, for achieving the cost curves and enabling the quantification of avoidable and unavoidable exergy destruction and their related costs. For optimization of vessels the connection of heat generators and heat consumers in heat exchanger networks as described by [BTM1996] and [MIC1995] promises savings in operation. In this optimization, matching of cooling demands with heating demands are accomplished using the pinch point method. Exergy demand may be lowered, as oil fired boilers provide steam while at the same time waste heat is dissipated into the environment through exhaust gas and cooling water.

Aim is the minimization of exergy use per distance. In the optimization of the auxiliary systems, propulsion power may be taken constant or predefined for exclusion of logistics with vessel load and optimal speed and hydrodynamics with weather, trim and hull condition influences. Such a generic requirement profile enables the comparison in exergy use per distance by different machinery concepts like main engine size with or without power take-in/take out and waste heat recovery, auxiliary system with speed controlled machinery, and choice of fuel with e.g. heavy fuel oil (HFO) compared to diesel oil (MDO) and liquefied gases (LNG). By means of the exergoeconomy, the exergy destruction can be directly compared to the related costs

of the different concepts and systems.

The presented onboard data acquisition in combination with simulation provides real operational data as input into an exergoeconomic evaluation and optimization process. Exergy destruction and exergy losses can be quantified for the varying requirements, including the external effects and operational constraints. At the current stage, the required data base of the various components and their capital costs in relation to the efficiency is not available. As this work is focused on the efficiency evaluation using simulation technology and real operational data, it is only indicated that further work may be invested into an in-depth exergoeconomic optimization of vessels.

5 Onboard Energy Efficiency Monitoring Tool

The following chapter describes the prototype installation of an onboard system based on the developed methodology as described in Ch. 3.

5.1 Motivation for Onboard Tool

The presented evaluations of energy consumption so far are carried out in retrospect on shore. These evaluations enable to identify potentials in machinery and operations, but for the latter only in terms of machinery control and general recommendations without the direct influence of the seafarers' operation of the vessel. The ships crew is an important factor for energy saving onboard [CAZ2009], and their awareness for energy efficient ship operation can be considered crucial for successful implementation of consumption reduction programs.

Onboard, the safe operation of the vessel is the crew's primary aim, while improving the operation for energy efficiency is done within the crews competence, interest in the topic and remaining time beside all other duties. The depicts the need for onboard tools for enhancing the knowledge about energy efficiency aboard and possible improvements, creating an awareness for energy efficiency and providing the information without costing additional time but supporting the crew in their duties aboard.

An important step for creating awareness is the provision of information about the current energy consumption of the systems for decision support, being at least main engine and auxiliary engines for electrical power consumption, and the recent history. In conjunction, the information enables the crew to recognize changes in operation of the vessel and the resulting influences on the efficiency in real time.

5.2 Energy Efficiency Monitoring Tool

The developed *Energy Efficiency Monitoring Tool* is based on the simulation models for energy converting systems onboard as described in Ch. 3 as the core data analysis. The aim is to provide an overview of the consumed electrical and mechanical power and the related efficiencies in energy conversion with the least possible input data from machinery. The actual connection to the crew, the graphical user

interface (GUI), is intended to be intuitively operable, with both current value and time line of the operational data available at a glance, as well as a display of the status of important parameters. This is achieved by introducing traffic signal symbols at distinct parameters, with a underlying logic evaluating the current value with predefined reference values. The traffic lights indicate the crew potential improvements in operational efficiency as a decision support, without patronizing the crew's operation.
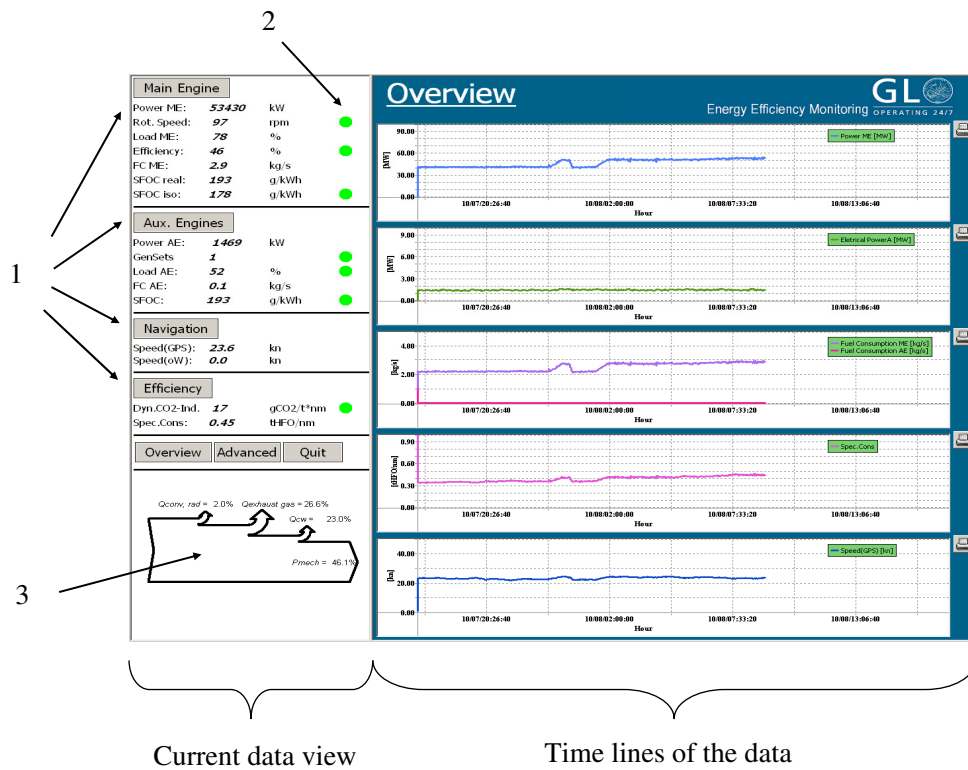
Figure 5.1. Pilot onboard tool display, 1: subsections for detailed view, 2: traffic lights for quick notification, 3: Sankey diagram of energy flow.

The functionality and layout of the GUI was developed in cooperation with experienced officers and engineers for achieving a functionality that supports the crew without requiring special attention during vessel operation or training beforehand.

The user interface of the EEMT is shown in Fig. 5.1. The display is divided into two different frames for display of current data and time lines. The current data and the Sankey diagram (3) for visualization of the energy flows in the main engine, located below in the left frame, are shown permanently. Time lines, being available

for all evaluated data, are presented in different groups of consumers and topics, accessible by mouse click at the respective header in the current data frame (1). The detailed views are available for main engine performance, auxiliary engines, navigation (speed history), and vessel efficiency (specific consumption, CO_2-indicator, fuel consumption). This limits the number of time lines displayed at the screen but allows for detailed views as needed by the user.

5.3   Onboard Data Provision

The provision of the operational data is an important task for the onboard tool. Two scenarios for data collection are further analyzed, which are presented in the following paragraphs.

The *Ideal World scenario* incorporates the availability of the required data channels within the vessels' automation system and an interface to the onboard tool. Modern automation systems include most required data for vessel operation from machinery, navigation and environment, which are provided to the control panels at the bridge and the engine control room via bus systems. By interconnecting the onboard tool with the vessel automation bus, the necessary input data can be provided without further installations of measuring devices on the machinery as described in Section 3.4.2.2, or at least be reduced to the few data which are not available. This is potentially possible on most modern vessels, but strongly discouraged by the automation manufacturers by using proprietary bus systems. Further more, as the automation system is highly relevant for operational safety, class rules restrict the interception of data. For newbuildings with bus connection already implemented during planning as well as vessels with upgraded automation systems enabling the data collection from the bus, this scenario enables a quick installation of the onboard tool.

In other cases, the *Real World Scenario* has to be applied, with the data collection at machinery and navigational systems as described in Section 3.4.2.2. As the data signals have to be collected at the respective machinery or instrument and hard-wired to data collection and onboard tool, it requires significantly more efforts for installation.

5.4   Layout of the Onboard Tool

The validation of approach and functionality of the *Energy Efficiency Monitoring Tool* is done on board of the postpanmax container vessel already equipped with the required measurement equipment. The test tool is programmed in C++, with the simulation model exported from SimulationX into C code and implemented as library, including a fixed-step solver. The test tool is structured in four units for the tasks data provision, data handling, model simulation, and GUI. The unit Input Data provides the tool with the required data, which are acquired from CAN bus. CAN bus was chosen, as it allows a high degree of flexibility for the data acquisition onboard the vessel, not limiting to certain manufacturers or measurement equipment. The unit Data Manager distributes the data to simulation, GUI and data storage, while the GUI unit provides the user interface. This segregated approach allows for a quick adaptation to different requirements and upgrades, as every unit can be adapted or exchanged separately. Data channels in the GUI, which are directly acquired from machinery are also directly presented in the GUI without being looped through the simulation model. The developed software can be considered as a demonstration tool, without the required longterm stability and professionalism of the user interface. Prior to commercial application of this system, these tasks have to be solved.

5.5   Test of the Onboard Tool

The already existing measurement data acquisition structure on board of the postpanmax test vessel is used as a basis for the test tool of the *Energy Efficiency Monitoring Tool.* The simulation model of the energy converting components, as described in Section 3.2 and also used for efficiency evaluation in the measurement campaign, is converted into a C code and implemented as the core module. There, the fuel consumption, efficiencies and resulting heat flows are calculated and provided to the data manager for storage and presentation in the GUI.

At the test vessel, all data are collected in the data acquisition unit located in the engine control room. Due to limited resources, the tool was installed at the data acquisition cabinet without further integration into bridge or control room. A picture of the test installation during sea passage is presented in Fig. 5.2.

After this proof of overall concept, the next consequential step is a long-term installation. This second test and demonstration of the onboard tool was successfully

Figure 5.2. EEMT test installation in the engine control room of the postpanmax container vessel.

performed on a multi-purpose vessel in trans-continental trade. At this demonstration, the system had been permanently installed at the bridge for information and decision support of the captain and officers on duty. The system was installed beside the map table, not interfering with normal work but in clear view. This enables the crew a quick check of the system and the current energetic status at a glance. A picture of the running system on the bridge can be found in Fig. 5.4.

This longterm demonstration successfully proved the concept of the onboard tool and the real-time applicability of the simulation for data analysis on board. The system ran continuously for more than half a year, except for occasional restarts due to signal losses from CAN-bus, within the normal operation of the vessel and was used by the crew.

Figure 5.3. Picture of the EEMT screen during sea passage, red traffic lights indicating high ship resistance and low auxiliary engine load.
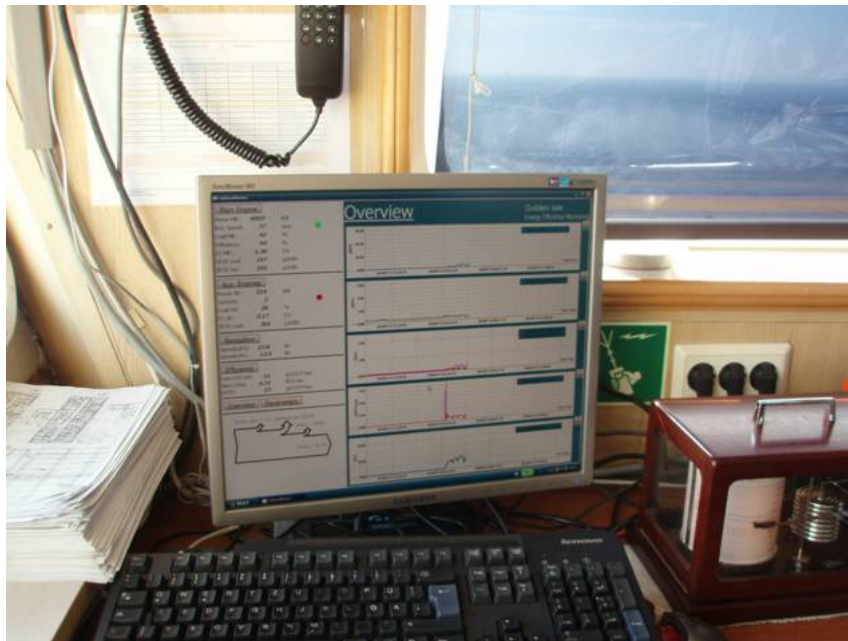
Figure 5.4. Installation of the demonstrator tool onboard of a multi-purpose vessel.

6 Conclusions and Outlook

The increasing costs for fuel oil and tightening regulations for ship emissions require an in-depth analysis of saving potentials in vessel operations through improved energy efficiency. The main drivers for improvements in more efficient vessel operation are identified, showing significant demand for optimization. Current efficiency evaluations of ship owners and operators are analyzed and the history of vessel efficiency leading to the current state of the art is presented.

As a starting point results of previous research projects are analyzed to evaluate the progress in technology and identify optimization potentials in current shipping. Main levers for efficiency optimization are identified and improvements on machinery level through new technology and vessel operation suggested. Technologies of shore-based industries not yet commonly applied in shipping are evaluated regarding their saving potentials on board, using real operational data of vessels instead of theoretical design criteria.

In the presented work a methodology for holistic acquisition and evaluation of efficiency in energy conversion on board of vessels is developed. Based on onboard measurements for capturing actual operational data in real time and data evaluation using simulation technology, the system evaluates the current energy conversion and efficiency of the vessel. Simulation of machinery components, both energy providers and consumers, are based on system characteristics and can be used in real-time on board as well as in retrospect and for planning ashore. The exergy flows and exergetic losses of the systems are analyzed.

Beside power consumption, the actual fuel consumption of a vessel under varying external influences and operational modes is an important indicator. Due to the complex fuel system and high mechanical and thermal loads on these systems on board of vessels, high precision measurement gauges directly at the engines are seldom applied. As an alternative, the developed simulation can provide the real time fuel flow based on system characteristics and measured delivered engine power. This method proved to accurately simulate the fuel consumption with an average deviation of 0.70% at a standard deviation of 1.46% based on reported consumption of vessel logbook, which can be considered within the accuracy of current reporting schemes.

The method was successfully applied to vessels in operation. Operational data of

more than two years were acquired and evaluated, detecting prior unnoticed wastes of energy and suggesting improvements. Retrofit measures with higher efficient machinery were evaluated regarding the actual saving potentials in current operations of the vessels, the exergy demand and achievable return of investment.

With an easily perceivable display of the vessel's energetic status with related recent history and data collection and storage, a tool for supporting crew and shore-based operators with required information for making profound decisions is developed.

The onboard system for engine monitoring and energy flow analysis may be improved through the inclusion of additional engine parameters from the engine control system, feeding into a detailed process cycle calculation and enabling a more detailed analysis of the energy flows within the engine. Online supervision of auxiliary systems and large consumers would allow for optimized operation, as deviations from optimum operation may be detected and indicated for immediate mitigating actions of the crew.

Based on the monitoring combined with an optimization calculation in real time a decision support system for the onboard use can be developed. Decision support may be given by comparing the current situation with optimum operation under prevailing internal and external effects on vessel operation. This could include not only the main energy converters, main engine and auxiliary engines, but also main consumers of electrical and thermal energy for optimized overall efficiency and minimized exergetic losses. Transferred ashore, the operational data may be reprocessed to performance indicators for the vessel operators to pinpoint inefficient machinery and vessel operation.

Bibliography

[ALS1999]   ADAMIETZ, M. ; LINNEMANN, C.; SCHRÖDER, J.: On-Line-Prozeß-güteüberwachung eines 880-MW-Steinkohlekraftwerks. *In: VGB KraftwerksTechnik* (1999) no. 8, pp. 41-47.

[ALL2010]   Allweiler: *Stena Hollandica: Energy boosting efficiency.* URL http://www.allweiler.no/Default.aspx?ID3551, accessed 2010-12-28.

[AM1980]   ALTE, R.; MATTHIESSEN, H.: *Schiffbau kurzgefaßt.* Hamburg: 2. Aufl. Ed. Schiffahrts-Verl. ”Hansa”, 1980.

[AQU2010]   Aquametro: *Aquametro AG, Basel, Switzerland.* URL http://www.aquametro.com/english/home_e.html, accessed 2010-08-16

[BAE1987]   BAEHR, H.: Die Exergie von Kohle und Heizöl. *In: BWK* 39 (1987) no. 1/2, pp. 42-45

[BK2009]   BAEHR, H. D.; KABELAC, S.: *Thermodynamik.* Berlin, Heidelberg: 14. Ed. Springer-Verlag, 2009.

[BTM1996]   BEJAN, A. ; TSATSARONIS, G.; MORAN, M. J.: *Thermal design and optimization.* New York [u.a.]: Wiley, 1996.

[BER2000]   BERTRAM, V.: *Practical ship hydrodynamics.* Oxford: Butterworth-Heinemann, 2000.

[BMT2008]   BMT SeaTech: *BMT SeaTech web site.* URL www.bmtseatech.co.uk, accessed 2008-05-15.

[BOE1970]   BOESE, P.: *Eine einfache Methode zur Berechnung der Widerstands-erhöhung eines Schiffes im Seegang.* Hamburg: Inst. für Schiffbau der Univ. Hamburg, 1970.

[BON2002]   BONFIG, K. W.: *Technische Durchflussmessung.* Essen: 3. Aufl. Ed. Vulkan-Verl, 2002.

[BRO1988]   BROSZEIT, R.: *Wärmetechnische Untersuchung von Zweidruck-Ab-gaskesselanlagen für Schiffsdieselmotoren.* Düsseldorf: Als Ms. gedr. Ed. VDI-Verl, 1988.

[BCE+2009]   BUHAUG, Ø. et al.: *Second IMO GHG study 2009.* London, UK: International Maritime Organization (IMO), 2009.

[BUN2012]   Bunkerworld: *Bunkerworld web site.*
             URL www.bunkerworld.com, accessed 2012-05-25.

[BG1998]   BUSCH, S.; GEISLER, O.: *Untersuchungen zur Prognose des elek-trischen Leistungsbedarfes auf Schiffen mit Hilfe künstlicher neu-ronaler Netze.* Aachen: Shaker, 1998.

[CAZ2009]   CAZZULO, R. P.: *Controlling costs while maintaining performance in the face of weak markets.* Shanghai: 2009.

[CGM+2006]   CE Delft; Germanischer Lloyd; Marintek; Det Norske Veritas: *Green-house Gas Emissions for Shipping and Implementation of the Marine Sulphur Directive.* CE Delft, 2006.

[CWW2009]   CORBETT, J. J. ; WANG, H.; WINEBRAKE, J. J.: The effectiveness and costs of speed reductions on emissions from international ship-ping. *In: Transportation and Environment* 14 (2009) no. 8, pp. 593-598.

[CRI2009]   CRIST, P.: *Greenhouse gas emissions reduction potential from inter-national shipping.* Paris: Joint Transport Research Centre, 2009.

[DAN2011]   Danaos Searoutes: *Danaos Searoutes web site.*
             URL www.searoutes.gr, accessed 2011-04-10.

[DEC2011]   Decision3: *Decision3 web site.*
             URL www.decision3.com, accessed 2011-05-16.

[DIN1976]   DIN: *DIN 1940 Hubkolbenmotoren: Begriffe, Formelzeichen, Ein-heiten.* Beuth, 1976.

[DIN2000]   DIN: *DIN 51900 Bestimmung des Brennwertes mit dem Bombenka-lorimeter und Berechnung des Heizwertes.* Beuth, 2000.

[DGF2005] DUBBEL, H. ; GROTE, K.; FELDHUSEN, J.: *Taschenbuch für den Maschinenbau.* Berlin [u.a.]: 21. neubearb. und erw. Aufl. Ed. Springer, 2005.

[EGE2010] EGEBERG, L. E.: *Total cost of ownership of Marine Propulsion Engines.* Hamburg: CIMAC Circle 2010, International Council on Combustion Engines (CIMAC), 2010.

[ENI2009] Eniram: *Eniram web site.*
URL www.eniram.fi, accessed 2009-04-03.

[FIL2006] FILOUNEK, A.: *Schutz von Ofenwänden vor Schädigung durch Kondensate.* Freiberg : Techn. Univ., Bergakad, 2006, Online-Ressource.

[FRI2004] FRITZSON, P.: *Principles of object-oriented modeling and simulation with Modelica 2.1.* Piscataway, NJ: IEEE Press [u.a.], 2004.

[FUT2012] FutureShip: *FutureShip web site.*
URL www.futureship.net, accessed 2012-05-15.

[GER1986] Germanischer Lloyd: *Ergebnisse des Forschungs- und Entwicklungsvorhabens "Schiff der Zukunft".* Hamburg: Eckardt und Messtorff, 1986.

[GER2010] Germanischer Lloyd: *Rules for Classification and Construction, I Ship Technology, 1 Seagoing Ships, 2 Machinery Installations.* Ed. 2010. Ed. Germanischer Lloyd, 2010.

[GOL2005] GOLLOCH, R.: *Downsizing bei Verbrennungsmotoren.* Berlin [u.a.]: Springer, 2005.

[GRE2009] Green Ship of the Future: *8500 TEU Container Ship Green Ship of the Future Concept Study.* Odense Steel Shipyard Ltd., 2009.

[HF2010] HANSEN, H.; FREUND, M.: *Assistance Tools for Operational Fuel Efficiency. 9th International Conference on Computer and IT Applications in the Maritime Industries (COMPIT'10).* Hamburg : Techn. Univ. Hamburg-Harburg, 2010.

[HIN2007] HINNENTHAL, J.: *Robust Pareto - optimum routing of ships utilizing deterministic and ensemble weather forecasts.* Techn. Univ., Diss–Berlin, 2007.

[HD1985]   HOCHHAUS, K.; DROSTE, W.: Reduzierung des elektrischen Energiebedarf auf Handelsschiffen. *In: HANSA* no. 121, 1985.

[HB2009]   HOCHKIRCH, K.; BERTRAM, V.: *Slow Steaming Bulbous Bow Optimization for a Large Containership.* Hamburg: TuTech, 2009.

[HYU2008]   Hyundai Heavy Industries: *Hyundai Heavy Industries web site.*
                URL www.hyundai-elec.com, accessed 2008-02-12.

[HYU2009]   Hyunday Heavy Industries: *Tech. Information Transmission Form Doc. No.: K24109/KCM/0898.*
                URL   http://www.infomarine.gr/attachments/026_Tech.
                %20Information   %20HHI-TI-0898-HiMSEN%20guideline%20-
                %20Fuel%20oil%20control.pdf, accessed 2010-12-28.

[IEA2010]   IEA: *World Energy Outlook 2010.* International Energy Agency, 2010.

[IMC2010]   IMC Messsysteme GmbH: *Famos.*
                URL www.imcfamos.de, accessed 2010-12-28.

[IMO2004]   IMO: *Resolution A.963(23) - IMO Policies and Practices Related to the Reduction of Greenhouse Gas Emissions from Ships.* London: International Maritime Organization, 2004.

[IMO2005]   IMO: *MEPC 54/4/2: Prevention of air pollution from ships - The potential of emissions trading to reduce carbon dioxide emissions from ships.* London: International Maritime Organization, 2005.

[IMO2009a]   IMO: *MEPC 1/Circ. 681: Interim Guidelines on the Method of Calculation of the Energy Efficiency Design Index for New Ships.* London: International Maritime Organization, 2009.

[IMO2009b]   IMO: *MEPC 1/Circ. 684: Guidelines for Voluntary Use of the Ship Energy Efficiency Operational Indicator.* London: International Maritime Organization, 2009.

[IMO2010a]   IMO: *MEPC 1/Circ. 723: Information on North American Emission Control Area (ECA) Under Marpol Annex VI.* London: International Maritime Organization, 2010.

[IMO2010b]   IMO: *MEPC 61/WP.10 Reduction of GHG Emissions from Ships
              - Report of the Working Group on Energy Efficiency Measures for
              Ships.* London: International Maritime Organization, 2010.

[IMO2011]   IMO: *MEPC 62/6/4 Consideration and adoption of amendments to
              mandatory instruments - Calculation of parameters for determination
              of EEDI reference values.* London: International Maritime Organiza-
              tion, 2011.

[ISO1996]   ISO 8217:1996: *Petroleum products – Fuels (class F) – Specifications
              of marine fuels.* International Organisation for Standardization, 1996.

[ISO2002a]   ISO 15016:2002: *Ships and marine technology - Guidelines for the
              assessment of speed and power performance by analysis of speed trial
              data.* ISO, 2002.

[ISO2002b]   ISO 15550:2002: *Internal combustion engines - Determination and
              method for the measurement of engine power - General requirements.*
              International Organisation for Standardization, 2002.

[ISO2002c]   ISO 3046-1:2002: *Reciprocating internal combustion engines - Per-
              formance - Part 1: Declarations of power, fuel and lubricating oil
              consumptions, and test methods - Additional requirements for engines
              for general use.* International Organisation for Standardization, 2002.

[ISO2005]   ISO 8217:2005: *Petroleum products - Fuels (class F) - Specifications
              of marine fuels.* International Organisation for Standardization, 2005.

[ITI2010]   ITI GmbH: *SimulationX.*
              URL www.iti.de, www.SimulationX.com, accessed 2010-12-28.

[JUC1992]   JUCHNIEWICZ, L.: *Dynamisches Verhalten der Kühlkreise von Diesel-
              motoren bei Gleitfrequenz und bei Einsatz drehzahlgeregelter Pumpen.*
              Düsseldorf: VDI-Verl, 1992.

[JUN2008]   JUNGNICKEL, D.: *Optimierungsmethoden.* Berlin [u.a.]: 2. Aufl. Ed.
              Springer, 2008.

[KAB2006]   KABELAC, S.: *VDI-Wärmeatlas.* Berlin [u.a.]: 10., bearb. und erw.
              Aufl. Ed. Springer, 2006.

[KAE2004]   KAEHLER, N.: *Full Scale Measurements Container Feeder.* Hamburg:
              Germanischer Lloyd AG, 2004.

[KDK+2012]   KHOR, Y. S. ; DØHLIE, K. A. ; KONOVESSIS, D. ; XIAO, Q.: *Optimum
              Speed Analysis for Large Containerships. 11th International Confer-
              ence on Computer and IT Applications in the Maritime Industries,
              COMPIT '12.* Hamburg : Techn. Univ. Hamburg-Harburg, 2012, pp.
              121-131.

[KON2012]   Kongsberg: *Kongsberg Maritime web site.*
              URL www.km.kongsberg.com, accessed 2012-05-15.

[KRA2011]   Kral: *Kral AG, Lustenau, Austria.*
              URL http://www.kral.at/en/_home/, accessed 2011-09-27.

[KYM2012]   Kyma: *Kyma web site.*
              URL www.kyma.no, accessed 2012-05-15.

[LAC1963]   LACKENBY, H.: The effect of shallow water on ship speed. *In: Ship-
              builder and Marine Engineer* 70 (1963) pp. 446-450.

[LEH2007]   LEHMANN, H.: Energiesparende Fahrweise bei der Deutschen Bahn.
              In: Elektrische Bahnen (2007) no. 105, pp. 397-402.

[LEM2012]   LEMAG: *LEMAG web site.*
              URL www.lemag.de, accessed 2012-05-15.

[MAN2005a]   MAN: *Thermo Efficiency System (TES).*
              URL http://www.manbw.com/files/news/filesof5055/P3339161.pdf,
              2005.

[MAN2005b]   MAN: *MAN B&W L27/38 Marine Project Guide.*   MAN B&W
              www.mandiesel.com, 2005.

[MAN2006]   MAN: *Basic Principles of Ship Propulsion.*
              URL http://www.mandiesel.de/article_005405.html, 2006.

[MAN2009]   MAN: *MAN B&W S60MC-C7 Project Guide.* MAN B&W
              URL www.mandiesel.com, 2009.

[MAN2010]   MAN: *Operation on Low-Sulphur Fuels.*
              URL http://www.mandieselturbo.com/files/news/filesof15012/5510-
              0075-00ppr_low.pdf, accessed 2010-12-30.

[MAN2011]   MAN: *CEAS-ERD: Engine Room Dimensioning of 7S60MC-C7.*
              URL http://www.mandieselturbo.com/ceas/index.html, accessed
              2011-10.

[MAR2012]   Marorka: *Marorka web site.*
              URL www.marorka.com, accessed 2012-05-15.

[MBA2006]   MEIER-PETER, H. ; BERNHARDT, F.; ACKERMANN, G.: *Handbuch
              Schiffsbetriebstechnik.* Hamburg: 1. Aufl. Ed. Seehafen Verl, 2006.

[MR2005]   MENZEL, W.; ROSTOCK, C.: *Langzeitmessung auf Schiffen.* In:
              Schiffbautechnische Gesellschaft e.V. (Ed.): *Jahrbuch der Schiff-
              bautechnischen Gesellschaft 2005.* Springer Verlag Berlin, 2005, pp.
              197-207.

[MH2007]   MEWIS, F.; HOLLENBACH, U.: Hydrodynamische Maßnahmen zur
              Verringerung des Energieverbrauches im Schiffsbetrieb. *In: Hansa* 144
              (2007) no. 5, pp. 49-58.

[MIC2008]   MICAD Marine: *MICAD Marine web site.*
              URL www.micadmarine.com, accessed 2008-02-12.

[MIC1995]   MICHALEK, K.: *Wärmenetze.* In: FRATZSCHER, Wolfgang (Ed.): *Ab-
              fallenergienutzung : technische, wirtschaftliche und soziale Aspekte
              / Interdisziplinäre Arbeitsgruppe Optionen Zukünftiger Industrieller
              Produktionssysteme.* Berlin : Akad.-Verl., 1995, pp. 158-188.

[MOD2012]   Modelica Association: *Modelica Association web page.*
              URL www.modelica.org, accessed 2012-05-15.

[MT2007]   MOLLENHAUER, K.; TSCHÖKE, H.: *Handbuch Dieselmotoren.* Berlin
              [u.a.]: 3. Ed. Springer, 2007.

[MOO1965]   MOORE, G. E.: Cramming more components onto integrated circuits.
              In: Electronics Magazine 38 (1965) no. 8, pp. 4.

[MOT2006]   Motor Ship: Teekay targets operational efficiency. *In: Motor Ship* (2006) no. 2, pp. 10-11.

[MUN2011]   MUNDT, T.: *MEPC 62 adopts Energy Efficiency Design Index.* Hamburg: GL Exchange Forum September 2011, 2011.

[N.N1971]   N.N.: Temperature corrections for density of petroleum products. *In: Journal of Chemistry and Technology of Fuels and Oils* Vol. 7 (1971) no. 9, pp. 712-716.

[NAP2010]   NAPA: *NAPA web site.*
URL www.napa.fi, accessed 2010-01-05.

[NG1988]   NAPP, M.; GEISLER, O.:   *Verfahren zur Prognose der elektrischen Energieverteilung an Bord von Schiffen.* Diss.- Arbeitsbereich Wärmekraftanlagen und Schiffsmaschinen, Techn. Univ. Hamburg-Harburg, 1988.

[NH2008]   NORDMYR, J.; HAIKKOLA, P.: *Energy- and cost savings with frequency control of electrically driven cooling water pumps in ship installations with several engines.* Helsinki, Finland: Wärtsilä, 2008.

[OEH2008]   OEHME, F.:   *Energetische Analyse eines Containerschiffs mit Kühlcontainerstellplätzen mit Hilfe eines Simulationsmodells.* Hamburg, TUHH, Institut Elektrische Energiesysteme und Automation, 2008.

[OMA2009]   OMAR, A.: *Opportunities and limits of performance monitoring for ship's diesel engines.* Hamburg: 2nd Optimising Ship Maintenance Conference, 2009.

[POS1994]   POSTEL, D.: *Beitrag zur Auslegung von Blockheizkraftwerken mit heissgekühlten Dieselmotoren.* Hannover, Universität Hannover, Dissertation, 1994.

[PRO2009]   Propulsion Dynamics: *Propulsion Dynamics web site.*
URL www.propulsiondynamics.com, accessed 2009-09-29.

[RUL2005]   RULFS, K.:   *Schiffsmotorenanlagen.* Hamburg: TUHH Institut Wärmekraftanlagen und Schiffsmaschinen, 2005.

[SAM2007]   SAMES, P. C.: *Which ship speeds offer greates economic benefits?*.
            London: Lloyds List Events: 9th Global Liner Shipping Conference,
            2007.

[SCH1986]   SCHAEFKE, B.: *Beitrag zur dynamischen Simulation von Kühlkreisen
            mit drehzahlvariablen Pumpenantrieben.* Düsseldorf: Als Ms. gedr.
            Ed. VDI-Verl, 1986.

[SCH2007]   Schiff & Hafen: Zuverlässige Bestimmung der Wellenleistung. *In:
            Schiff & Hafen* (2007) no. 5, pp. 50-51.

[SPE2002]   SPEIGHT, J. G.: *Handbook of petroleum product analysis.* Hoboken,
            NJ: Wiley-Interscience, 2002.

[SWA2010]   SWAIN, G. W.: *The importance of ship hull coatings and maintenance
            as drivers for environmental sustainability.* London: Ship Design and
            Operation for Environmental Sustainability, RINA, 2010.

[TKB+1993] TOWNSIN, R. L. ; KWON, Y. J. ; BAREE, M.; KIM, D.: *Estimating
            the influence of weather on ship performance.* Royal Institute of Naval
            Architects (RINA), 1993.

[TP2002]   TSATSARONIS, G.; PARK, M.: On avoidable and unavoidable exergy
            destructions and investment costs in thermal systems. *In: Energy
            Conversion and Management* 43 (2002) pp. 1259-1270.

[UNC2010]   UNCTAD: *Review of Maritime Transport.* United Nations Conference
            on Trade and Development (UNCTAD), 2010.

[UTH2009]   UTH, M.: *Integration einer Kreisprozess-Simulation in das Energie-
            Monitoring System eines Großcontainerschiffs.* Diplomarbeit TU
            Hamburg-Harburg, 2009.

[VAF2011]   VAF: *VAF Fluid-Technik GmbH, Lichtenau, Germany.*
            URL http://www.vaf-fluidtechnik.de/, accessed 2011-09-27.

[VB1970]   VIBE, I. I.; BUNK, W.: *Brennverlauf und Kreisprozeß von Verbren-
            nungsmotoren.* Berlin: Verl. Technik, 1970.

[VOE2006]   VOERMANS, A. A.: Propulsion improvement - fuel saving by means
            of upgrading ship propulsion. *In: Scandinavian shipping gazette* 18
            (2006) pp. 78-83.

[VS1998]   VOSS, G.; SANFTLEBEN, D.: Rechnergestützte energiesparende
              Fahrweise im Regelbetrieb. *In: Eisenbahntechnische Rundschau*
              (1998) no. 47, pp. 25-31.

[WÄR2008]   Wärtsilä: *WinGTD-General Technical Data software.* Bremerhaven:
              LOGO Datensysteme GmbH, 2008.

[WGS2008]   Wgsimon: *Transistor counts for integrated circuits plotted against
              their dates of introduction.*
              URL http://commons.wikimedia.org/wiki/User:Wgsimon. Published
              under GNU Free Documentation License, accessed 2010-03-10.

[WIK2010]   Wikipedia: *Moore's Law.*
              URL http://en.wikipedia.org/wiki/Moore%27s_law, accessed 2010-
              03-10.

[W2007]   WILD, Y.: *Kühlcontainern im Seetransport - Energieverbrauch und
              Einsparmöglichkeiten.* Hamburg: Presentation at DKV Meeting,
              2007.

[WIL2007a]   WILD, Y.: *Einsatz von Absorptionskälteanlagen für die Klima-
              tisierung von Seeschiffen.* Hannover: Deutsche Kälte-Klima-Tagung,
              DKV, 2007.

[WIL2007b]   WILD, Y.: Absorptionskälteanlagen: neue Wege in der Schiffsklima-
              technik. *In: Jahrbuch der Schiffbautechnischen Gesellschaft* (2007)
              no. 101, pp. 31-36.

[WS2005]   WISCHHUSEN, S.; SCHMITZ, G.: *Dynamische Simulation zur
              wirtschaftlichen Bewertung von komplexen Energiesystemen.* Göttin-
              gen: 1. Ed. Cuvillier, 2005.

[WOL2011]   WOLF, S.: *Umsetzung energieeffizienter Technologien an Bord
              von Seeschiffen.* Koblenz, Universität Koblenz-Landau, Fachbereich
              Mathematik / Naturwissenschaften, Master Thesis, 2011.

[WOS1970]   WOSCHNI, G.: Die Berechnung der Wandwärmeverluste und der ther-
              mischen Belastung der Bauteile von Dieselmotoren. *In: MTZ Mo-
              tortechnische Zeitschrift* 31 (1970) pp. 491-499

List of Figures

Curriculum Vitae

Name:	Malte Freund
Year of birth:	1982
Place of birth:	Hannover

Education:

2001	Abitur (high school diploma) in Hannover
10.2001-03.2007	Mechanical engineering at the University of Hannover, major fields: energy technology and chemical engineering, degree: Dipl.-Ing. (diploma)
04.2006-10.2006	Research project at the National Institute of Standards and Technology in Boulder, Colorado, U.S.A.

Employments:

09.2003-04.2005	Student assistant at the University of Hannover, Institute for Thermodynamics Supervisor: Professor Dr.-Ing. habil. Andrea Luke
09.2004-03.2005	Student assistant at the University of Hannover, Institute for Turbomachinery and Fluid Dynamics Supervisor: Professor Dr.-Ing. Jörg Seume
05.2007-04.2010	PhD Program of Germanischer Lloyd: Project Engineer at Germanischer Lloyd Engineering Services, Hamburg, Research Assistant at the University of the Federal Armed Forces Hamburg, Institute for Thermodynamics Supervisor: Professor Dr.-Ing. habil. Stephan Kabelac
since 07.2010	Project Engineer at Germanischer Lloyd/FutureShip Engineering Services. Energy Efficiency Monitoring and Evaluation, Maritime Environmental Consulting